

Title	Development of tumour imaging and therapy strategies utilising unengineered bacteria
Authors	Stanton, Richard Michael
Publication date	2015
Original Citation	Stanton, R. M. 2015. Development of tumour imaging and therapy strategies utilising unengineered bacteria. PhD Thesis, University College Cork.
Type of publication	Doctoral thesis
Rights	© 2015, Richard M Stanton. - <a href="http://creativecommons.org/licenses/by-nc-nd/3.0/">http://creativecommons.org/licenses/by-nc-nd/3.0/</a>
Download date	2024-03-29 07:08:56
Item downloaded from	<a href="https://hdl.handle.net/10468/2876">https://hdl.handle.net/10468/2876</a>

*Ollscoil na hÉireann, Corcaigh*  
**THE NATIONAL UNIVERSITY OF IRELAND, CORK**

*Coláiste na hOllscoile,*  
*Corcaigh*  
UNIVERSITY COLLEGE CORK

Cork Cancer Research Centre



Development of tumour imaging and therapy strategies utilising  
unengineered bacteria.

*Thesis presented by*  
**Richard Michael Stanton BSc, MSc**

*Under the supervision of*

**Dr Mark Tangney**

*for the degree of*

**Doctor of Philosophy**

October 2015

*Head of department*

**Prof. David Sheehan**

# Table of Contents

Abstract .....	9
Declaration .....	11
Abbreviations .....	12
Acknowledgements .....	15
Chapter 1: Introduction .....	16
Abstract .....	17
Introduction .....	18
<i>In vivo</i> Imaging .....	21
Optical Imaging.....	21
Bioluminescence Imaging (BLI).....	22
Fluorescence Imaging .....	26
Instrumentation for OI.....	27
Engineering bacteria to express reporter genes.....	28
Dual bioluminescent/fluorescent labelling of microorganisms.....	30
Applications of OI Reporter Genes.....	31
OI alternative approaches - Bacterial-specific probes .....	32
Alternative modalities to OI.....	35
Photoacoustic Imaging .....	35
Positron Emission Tomography (PET) .....	35
Magnetic Resonance Imaging .....	36

Bacterial-Mediated Tumour Therapy .....	38
Exploiting endogenous bacterial activity for imaging .....	43
Bacterial Directed Enzyme Prodrug Therapy .....	44
Advantages of BDEPT as a therapeutic strategy .....	49
Bacterial therapeutic gene expression technology .....	51
Combined imaging and therapy .....	52
Conclusions and future perspectives .....	55
References .....	57
Chapter 2: Development of a novel probe-based strategy for <i>in vivo</i> imaging of non-GM bacteria.....	71
Abstract .....	72
Study Aim .....	74
Introduction .....	75
Materials and methods .....	79
<i>Bacterial strains.</i> .....	79
<i>Detection of NfsB by western blotting.</i> .....	79
<i>Animals and tumour induction.</i> .....	80
<i>Ethics statement.</i> .....	80
<i>Bacterial administration to mice.</i> .....	80
<i>Bacterial recovery from mice.</i> .....	81
<i>Preparation of CytoCy5S.</i> .....	81
<i>Image acquisition and formation.</i> .....	81

<i>Effect of CytoCy5S on bacterial viability assay.</i> .....	82
<i>Conversion of CytoCy5S by intracellular L. welshimeri.</i> .....	82
<i>Imaging of intramuscular bacteria using CytoCy5S as a fluorescent probe.</i> ....	83
<i>In vivo tracking of S. Typhimurium infection.</i> .....	83
<i>Non-invasive imaging of tumour colonising bacteria.</i> .....	83
<i>Statistical analysis.</i> .....	84
Results .....	85
<i>In vitro</i> monitoring of CytoCy5S activation by bacteria.....	85
NfsB nitroreductase activity is primarily responsible for CytoCy5S activation....	90
The effect of CytoCy5S on bacterial cell viability <i>in vitro</i> and <i>in vivo</i> . ....	92
Route of CytoCy5S administration for <i>in vivo</i> experiments. ....	94
<i>In vivo</i> fluorescence from bacterial activated CytoCy5S reflects bacterial numbers .....	96
<i>In vivo</i> imaging of <i>S. Typhimurium</i> infection in mice .....	98
<i>In vivo</i> imaging of tumour targeting <i>E. coli</i> .....	100
Discussion. ....	104
References .....	108
Chapter 3: Development of a novel, nitroreductase activated, luminescent probe ..	112
Abstract .....	113
Study Aim .....	114
Introduction. ....	115
Materials and Methods .....	118

<i>Chemical materials and synthesis.</i> .....	118
<i>Kinetics of NCL reaction with NTR by fluorescence.</i> .....	118
<i>Bioluminescent imaging of NTR with NCL in enzyme assay.</i> .....	118
<i>Bacterial strains, plasmids and culture conditions.</i> .....	119
<i>Bioluminescent imaging of NTR activity by NCL in E. coli.</i> .....	119
<i>Bioluminescent imaging of bacteria reduced NCL in a luciferase producing cancer cell line.</i> .....	120
<i>Ethics statement.</i> .....	120
<i>Bacterial administration and imaging of bacterial nitroreductase in mice.</i> ....	120
<i>Mice and tumour induction.</i> .....	121
<i>Imaging of nitroreductase in a mouse model of subcutaneous cancer.</i> .....	121
<i>Statistical analysis.</i> .....	121
Results .....	122
Probe design .....	122
Bioreductive activation of NCL in cell-free assays .....	126
Imaging of NTR activity in <i>E. coli</i> .....	129
Effect of NCL on bacteria cell viability .....	133
<i>In vitro</i> light production from bacteria activated NCL with 4T1 cells as the source of luciferase .....	135
Route of NCL administration for <i>in vivo</i> experiments .....	137
Luminescence from NCL outlasts D-luciferin <i>in vivo</i> . .....	137
<i>In vivo</i> comparison of NCL with CytoCy5S .....	140

Imaging of bacterial NTR <i>in vivo</i> in a mouse model of intramuscular infection.	142
Imaging of bacterial NTR activity in a mouse model of <i>Salmonella</i> infection ...	144
Imaging of NTR activity in subcutaneous xenograft model of cancer .....	146
Discussion .....	148
References .....	150
Chapter 4: Exploitation of endogenous bacterial enzymes for cancer therapy. ....	155
Abstract .....	156
Study Aim .....	157
Introduction .....	158
Materials and methods .....	161
<i>Bacteria and cell lines.</i> .....	161
<i>Drugs.</i> .....	161
<i>Cell cytotoxicity assay.</i> .....	161
<i>Bacterial plating assay.</i> .....	162
<i>Bacterial lysis and heat inactivation.</i> .....	162
<i>Bacterial prodrug susceptibility assay.</i> .....	162
<i>HPLC and Mass spectrometry analysis:</i> .....	162
<i>Murine experiments.</i> .....	163
<i>Animals and Tumour Induction:</i> .....	163
<i>Bacterial and drug administration:</i> .....	163
<i>Image acquisition and formation.</i> .....	164

<i>Cytospins</i> .....	164
<i>Statistical analysis</i> .....	164
Results .....	165
Effect of prodrugs on bacterial cell survival <i>in vitro</i> .....	165
Validation of prodrug co-activation by High Performance Liquid Chromatography (HPLC) .....	168
<i>E. coli</i> is capable of activating a range of prodrugs and inducing cancer cell killing. ....	170
Tumour colonising <i>E. coli</i> Nissle activates CB1954 and elicits a therapeutic effect <i>in vivo</i> . ....	172
<i>In vivo</i> optical imaging of NTR activity during CB1954 tumour therapy using CytoCy5S. ....	174
A cocktail of prodrugs can be activated by bacteria <i>in vitro</i> . ....	176
<i>In vivo</i> tumour therapy utilising a cocktail of CB1954 and 5-FC prodrugs .....	178
Immune cell recruitment to the tumour following drug activation by tumour localised bacteria. ....	181
Discussion .....	184
References .....	187
Chapter 5: Discussion and future work .....	189
Discussion and future work .....	190
Conclusion .....	194
References .....	196



## **Abstract**

The ability of systemically administered bacteria to target and replicate to high numbers within solid tumours is well established. Tumour localising bacteria can be exploited as biological vehicles for the delivery of nucleic acid, protein or therapeutic payloads to tumour sites and present researchers with a highly targeted and safe vehicle for tumour imaging and cancer therapy. This work aimed to utilise bacteria to activate imaging probes or prodrugs specifically within target tissue in order to facilitate the development of novel imaging and therapeutic strategies. The vast majority of existing bacterial-mediated cancer therapy strategies rely on the use of bacteria that have been genetically modified (GM) to express genes of interest. While these approaches have been shown to be effective in a preclinical setting, GM presents extra regulatory hurdles in a clinical context. Also, many strains of bacteria are not genetically tractable and hence cannot currently be engineered to express genes of interest. For this reason, the development of imaging and therapeutic systems that utilise unengineered bacteria for the activation of probes or drugs represents a significant improvement on the current gold standard. Endogenously expressed bacterial enzymes that are not found in mammalian cells can be used for the targeted activation of imaging probes or prodrugs whose activation is only achieved in the presence of these enzymes. Exploitation of the intrinsic enzymatic activity of bacteria allows the use of a wider range of bacteria and presents a more clinically relevant system than those that are currently in use. The nitroreductase (NTR) enzymes, found only in bacteria, represent one such option.

Chapter 2 introduces the novel concept of utilising native bacterial NTRs for the targeted activation of the fluorophore CytoCy5S. Bacterial-mediated probe

activation allowed for non-invasive fluorescence imaging of *in vivo* bacteria in models of infection and cancer.

Chapter 3 extends the concept of using native bacterial enzymes to activate a novel luminescent, NTR activated probe. The use of luminescence based imaging improved the sensitivity of the system and provides researchers with a more accessible modality for preclinical imaging. It also represents an improvement over existing caged luciferin probe systems described to date.

Chapter 4 focuses on the employment of endogenous bacterial enzymes for use in a therapeutic setting. Native bacterial enzymatic activity (including NTR enzymes) was shown to be capable of activating multiple prodrugs, in isolation and in combination, and eliciting therapeutic responses in murine models of cancer.

Overall, the data presented in this thesis advance the fields of bacterial therapy and imaging and introduce novel strategies for disease diagnosis and treatment. These preclinical studies demonstrate potential for clinical translation in multiple fields of research and medicine.

## **Declaration**

I hereby declare that I am the sole author of this thesis.

I authorise University College Cork to lend and photocopy this thesis to other institutions or individuals for the purpose of scholarly research.

---

R. Michael Stanton

## Abbreviations

Amp	Ampicillin
ANOVA	Analysis of variance
ATCC	American Type Culture Collection
ATP	Adenosine triphosphate
BDEPT	Bacterial directed enzyme prodrug therapy
BLI	Bioluminescence imaging
CBR	Click beetle red
CB1954	5-(Aziridin-1-yl)-2,4-dinitrobenzamide
cfu	Colony forming units
DMEM	Dulbecco's Modified Eagle's Medium
DMSO	Dimethyl sulfoxide
Em	Erythromycin
EPFL	The École polytechnique fédérale de Lausanne
FMN	Flavin mononucleotide
g	Grams
GDEPT	Gene-directed enzyme prodrug therapy
GFP	Green fluorescent protein
GM	Genetically modified
h	Hour
GMP	Good manufacturing practice
HPLC	High-performance liquid chromatography
IP	Intraperitoneal
IT	Intratumoural
IV	Intravenous
IVIS	<i>In vivo</i> imaging system
KB	Kilobases
kDa	Kilodalton

kg	Kilogram
KO	Knock out
LB	Luria Bertani broth
LLC	Lewis lung carcinoma
luc	Luciferase
MS	Mass Spectrometer
ml	Millilitre
mM	Millimolar
MRI	Magnetic resonance imaging
NADH	Nicotinamide adenine dinucleotide
NCL	Nitroreductase caged luciferin
nm	Nanometre
ng	Nanogram
NTR	Nitroreductase
OD <sub>600</sub>	Optical density at 600 nanometres
OI	Optical imaging
PBS	Phosphate buffered saline
PET	Positron emission tomography
PVDF	Polyvinylidene difluoride
p/sec/cm <sup>2</sup> /sr	Photons emitted per second per cm <sup>2</sup> per steradian
QD	Quantum dot
ROI	Region of interest
SD	Standard deviation
SEM	Standard error of the mean
SDS-PAGE	Sodium dodecyl sulfate polyacrylamide gel electrophoresis
SPECT	Single-photon emission computed tomography
UV	Ultra violet
wt	Wild type
5-FC	5-fluorocytosine

μg	Microgram
μl	Microlitre
μm	Micrometre
μM	Micromolar
°C	Degrees Celsius

## Acknowledgements

Firstly, I would like to express my sincere gratitude to my supervisor Dr Mark Tangney, without whose support, guidance and knowledge I would not have been able to complete this thesis. I would also like to extend my most sincere thanks to Dr Shelly Cronin for all of the help she has given me over the years. Her talent as a scientist is an inspiration and I highly value her friendship and assistance throughout the thesis. I would like to thank Dr Panos Lehouritis for all of his help with the prodrug studies and particularly for the work he put in to the *in vitro* studies and screens in Chapter 4.

To Dr Kellie Dean I extend my gratitude for her unwavering support as the coordinator of the PhD Scholars Programme in Cancer Biology. Her organisation and guidance were so important throughout this PhD, as were her friendship, approachability and expertise. I would also like to offer my genuine thanks to all of the member of the Scholars programme and the Molecular Cell Biology programme who I now count amongst my closest friends and have the utmost respect for.

To Chloe, Morgan and all of the members of the CCRC (particularly the members of the Tangney group, past and present), I will be forever grateful for the support, encouragement, friendship and importantly, the welcome distractions when they were needed most. Thank you.

Finally, my greatest thanks go to my family. Their endless support, encouragement and genuine interest make it all worthwhile. It is to them that I dedicate this thesis.

# Chapter 1: Introduction

Sections of this chapter have been published as

Cronin, M., Stanton, R. M., Francis, K. P., & Tangney, M. (2012). **Bacterial vectors for imaging and cancer gene therapy: a review.** *Cancer gene therapy*, 19(11), 731-740.

&

Lehouritis, P., Springer, C., & Tangney, M. (2013). **Bacterial-directed enzyme prodrug therapy.** *Journal of Controlled Release*, 170(1), 120-131.

## **Abstract**

The significant burden of resistance to conventional anticancer treatments in patients with advanced disease has prompted the need to explore alternative therapeutic strategies. The challenge for oncology researchers is to identify a therapy which is selective for tumours with limited toxicity to normal tissue. Bacteria have the unique potential to overcome traditional therapies' limitations by specifically targeting tumours. It has been shown that bacteria are naturally capable of homing to tumours when systemically administered, resulting in high levels of replication locally, either external to (non-invasive species) or within tumour cells (pathogens). Pre-clinical and clinical investigations involving bacterial vectors require relevant means of monitoring vector trafficking and levels over time, and development of bacterial-specific real-time imaging modalities are key for successful development of clinical bacterial gene delivery. This introduction discusses the currently available imaging technologies and therapies associated with bacteria and the progress to date exploiting these for monitoring of bacterial activity *in vivo*.

## **Introduction**

Although the potential anti-cancer effects of post-operatively acquired bacterial infection have been evident for over 120 years and the presence of bacteria in excised tumours has been noted for over 60 years [1], it is only in more recent times that the tumour-specific growth of bacteria has been considered for therapeutic purposes. While the precise mechanism(s) behind preferential bacterial tumour colonisation remain poorly understood, this phenomenon must relate to unique tumour attributes that separate them from healthy tissues. Factors such as the irregular/leaky blood supply; local immune suppression; inflammation and unique nutrient supply (e.g. purines) in tumours have been proposed to play a role [2]. Bacterial entry into the tumour environment is proposed to be facilitated by the leaky vasculature within the tumour, where systemically circulating bacteria effectively leak out of blood vessels that are supplying the tumour. Cancer cells are characterised by an aberrantly accelerated metabolism and proliferation leading to an imbalance of oxygen supply and consumption which is a major causative factor of tumour hypoxia [3]. The regions of low oxygen that exist within solid tumours enhances the growth of anaerobic and facultatively anaerobic bacteria. In addition, these areas of low oxygen and high interstitial pressure are considered to be an immunological sanctuary, where bacterial clearance mechanisms are greatly inhibited [4]. Necrotic regions are also rich in nutrients favoured by bacteria (e.g. purines) due to tumour cell turnover. However, tumour selective bacterial colonisation now appears to be both bacterial species and tumour origin independent, since aerobic bacteria are also capable of colonising tumours, and even small tumours lacking an anaerobic centre are colonised (Figure 1).

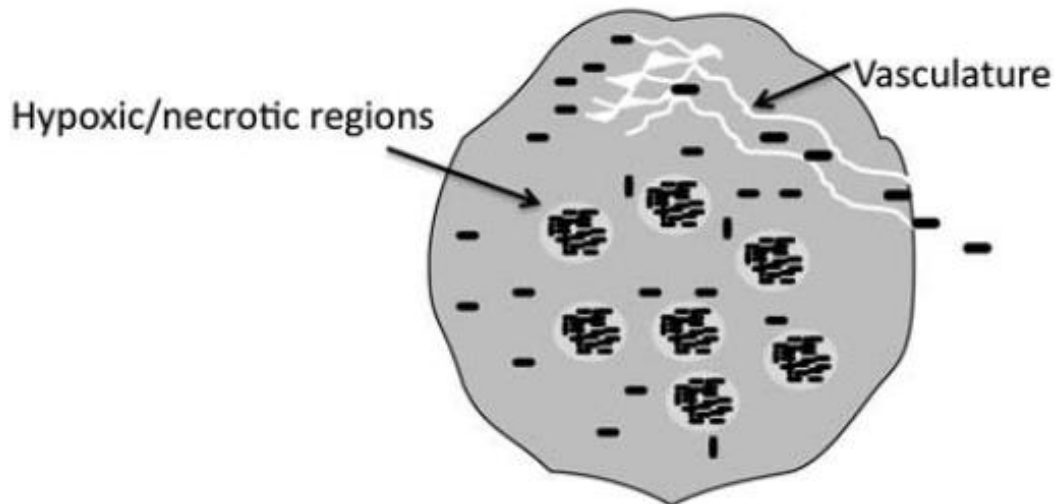


**Figure 1. Tumour characteristics associated with bacterial colonisation.** (1) Leaky microvasculature: Bacteria circulating systemically through the vasculature come into contact with the tumour; (2) Lack of immune clearance: The inability of the immune system to mediate clearance of bacteria from immune-privileged tumour sites allows for uninhibited bacterial growth within the tumour. (3) Hypoxic microenvironment: Hypoxic/necrotic areas within tumour provide the necessary microenvironment for anaerobic bacterial proliferation, unavailable elsewhere in the body. (4) Abundant nutrients: Areas of necrosis also provide nutrients to promote bacterial growth.

Invasive bacteria can internalise and replicate within tumour cells, while non-invasive bacteria grow externally to tumour cells, within the tumour micro-environment [5]. The tumour selective growth of bacteria, as well as the relative ease with which certain species of bacteria can be genetically modified, has made them an attractive vehicle for the delivery of reporter genes, therapeutic genes or inhibitory RNA to a tumour for ameliorative or potentially diagnostic purposes. Protocols for the genetic modification of bacterial genomes and the transformation of plasmid DNA containing genes of interest into bacteria are becoming established for an increasing range of species. This allows for the creation of bacteria that i) directly express therapeutic genes, and/or ii) efficiently internalise into tumour cells with subsequent therapeutic nucleic acid release for tumour cell expression (“bactofection”). The same bacterium can be engineered to co-express a reporter gene(s) that can be used for *in vivo* imaging of bacterial localisation and spread. Genetic manipulation of bacteria can also be used to create mutants with aberrant nutritional needs or that are attenuated and therefore non-pathogenic.

Bactofection of mammalian cells applies to both active invasion of non-phagocytic mammalian cells (e.g. tumour cells), and also ‘passive’ uptake by phagocytic immune cells (DNA vaccination). Vaccination strategies involving bactofection of antigen presenting cells (APC) with defined tumour antigen genes using replication deficient mutants of *Salmonella enterica* Typhimurium and other strains have shown significant promise both preclinically and in clinical trials [6, 7]. After oral intake, such bacterial vector cells are phagocytosed by monocytes in the intestine, which differentiate and migrate to lymph nodes and the spleen. Subsequently, the attenuated strains (unable to replicate in hosts) lyse and release plasmid into the cytoplasm of monocytes, followed by expression of the desired

antigen and presentation to the immune system. This delivery platform has shown success in several preclinical tumour models employing various tumour antigens [8].

### ***In vivo* Imaging**

The evolution of novel biological imaging techniques has played a major role in the development of modern medicine. Advances in the specificity and sensitivity of imaging devices has led to vast improvements in the diagnosis and treatment of disease as well as the development of drugs and the study of biological processes *in vivo*. The perpetual aim of *in vivo* imaging is to achieve increased sensitivity and resolution. A number of clinical molecular imaging strategies are available which are suited to preclinical studies of bacterial gene therapy, primarily Positron Emission Tomography (PET) and microPET. A more readily accessible technology available to standard research laboratories is Optical Imaging (OI) which is based on the detection and quantification of bioluminescent or fluorescent light from a subject, through use of a cooled charged coupled device (CCD) camera. The relevant merits and obstacles to these and other methodologies in the context of bacterial gene therapy of cancer are discussed hereafter.

### **Optical Imaging**

Optical imaging is a highly sensitive, nontoxic technique based on the detection of visible light, produced by luciferase enzyme-catalysed reactions (bioluminescence) or by excitation of fluorescent molecules, using sensitive photon detectors. Although

the light emitted may be dim, it is detectable externally using sensitive photon detectors such as those based on cooled, or intensified CCD cameras, mounted within light-tight specimen chambers. The development of bioluminescent/fluorescent microorganisms allows for the real-time non-invasive detection of bacteria within intact living animals. As light passes through a range of tissue types it is possible to observe and quantify the spatial and temporal distribution of light production from within tumours or other tissue. Multiple time-point imaging of the same animal throughout an experiment allows the progression of bacterial colonisation to be followed with accuracy, reducing the number of animals required to yield statistically meaningful data.

### **Bioluminescence Imaging (BLI)**

Bioluminescence involves the release of light energy following a chemical reaction catalysed by a luciferase enzyme [9]. Luciferases generate visible light of a specific wavelength through the oxidation of their specific substrates. Unlike fluorescence, no external light source is necessary. Luciferase proteins have been isolated from a variety of insects, marine organisms and prokaryotes [10]. Some of the most common BLI systems employed for use in research are the luciferase derived from the North American firefly *Photinus pyralis* (FLuc), the sea pansy *Renilla* luciferase (RLuc), the marine copepod *Gaussia princeps* luciferase, (GLuc) and the bacterial luciferase gene cassette (*lux*) [8, 11-14].

Both RLuc and GLuc metabolise coelenterazine to produce visible light predominately in the blue-green spectrum which is not optimal for whole body imaging as light in this range is efficiently absorbed by living tissue [15]. Red-

shifted RLuc variants have been developed which improve penetration of light in biological matrices [16]. The most significant disadvantage to the *in vivo* application of these reporters is the poor half-life of coelenterazine in animal systems; however, variants with improved longevity in animals are being developed [17]. To date *GLuc* has been successfully expressed in *Mycobacterium smegmatis* and used in whole animal imaging modalities [18]. *S. Typhimurium* engineered to express a variant of *Rluc* gene (*RLuc8*), under the control of the *E. coli* arabinose operon promoter ( $P_{BAD}$ ) have been imaged in murine tumours, with the added advantage of demonstrating ‘remote control’ of bacterial gene expression [19].

Notwithstanding the above luciferase/substrate combinations, the bacterial-native *lux* system represents the mainstay of current *in vivo* bacterial OI (Figure 2) [20]. The *luxAB* genes isolated from *Vibrio harveyi* [21] and *Photobacterium luminescens* (formerly *Xenorhabdus luminescens*), amongst others, have since been combined with all genes required for enzyme and substrate transcribed from a single cassette *luxCDABE* [22]. This non-invasive imaging system allows for qualitative and quantitative analysis of the localisation of bioluminescent bacteria in small animal models. It is important to note that bioluminescence from *lux*- and *Luc*-expressing microorganisms is related to an organism's metabolic activity. This is due to the reliance of the luciferases on microbial metabolites, mainly FMNH<sub>2</sub> and ATP, respectively. This is exemplified by the decrease in luminescence that has been observed when many *lux*-expressing bacterial species, such as *Bifidobacterium* [13], enter stationary phase during *in vitro* growth [23-25]. Bioluminescent bacteria have been used extensively to study a diverse range of biological processes such as infection [26], quorum sensing [27] and gene expression [28]. However, the employment of luciferase or *lux* tagged bacterial strains as gene delivery vehicles for

the treatment of cancer is an emerging field [29, 30]. A powerful potential diagnostic approach involves the use of genetically modified light-emitting bacteria to visualize their colonisation of tumours, thereby revealing the location of tumours based on light emission.

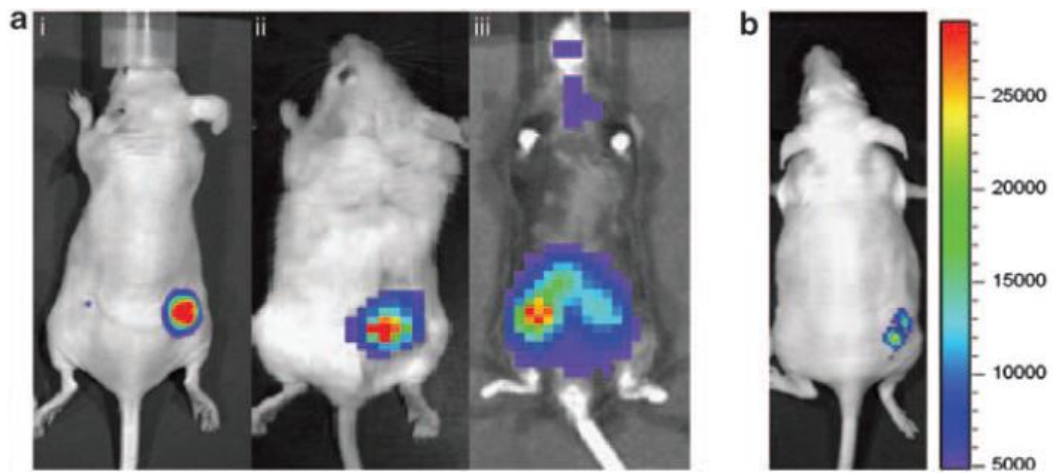


**Figure 2. Bioluminescence imaging (BLI) of bacterial vectors and gene delivery.** a) Bacterial vector bioluminescence. Lux-labelled (i) *E. coli* K12 MG1655 or (ii) *B. breve* UCC2003 were administered via tail vein to either athymic or BALB/c mice bearing subcutaneous FaDu hypopharyngeal carcinoma or CT26 colorectal carcinoma respectively. Lux signal was detected by 2D *in vivo* BLI specifically in tumours of mice 3–14 days post IV administration. 2D BLI is also useful for imaging DNA vaccine delivery using *Salmonella* as a vector in the gastrointestinal tract of mice. Trafficking of *S. Typhimurium* SL7207 in the initial 10h after gavage feeding was monitored using a bacterial lux expressing strain and BLI. A representative C57 BL/6 mouse gavage fed SL7207 is illustrated in (iii). A specific antitumour immune response was generated in a murine model of prostate cancer by oral administration of salmonellae containing a plasmid coding for murine prostate stem cell antigen (PSCA). b) Bacterial mediated transfer of plasmid DNA to tumour cells (bactofection) using *Listeria monocytogenes*. The ability to use *L. monocytogenes* to deliver genes to tumours *in vivo* was assessed using the eukaryotic cell-specific CMV promoter to express FLuc reporter gene.  $10^6$  *L. monocytogenes*/FLuc was intratumourally administered to athymic mice harbouring subcutaneous MCF-7 tumours. Mammalian cell expressed FLuc luminescence was observed specifically in tumours.

## Fluorescence Imaging

Another non-invasive imaging technique that has been successfully utilised to visualise bacterial vectors in cancer gene therapy is fluorescence imaging. In fluorescence imaging, an external light source excites a fluorophore [fluorescent protein (FP) or dye] and the transferred light energy is emitted at a different wavelength when the fluorophore returns back to its ground state. The excitation of the fluorophores by filtered light of a defined wavelength results in the emission of a fluorescent signal. This low energy, shifted wavelength light signal can be identified and quantified both *in vitro* and *in vivo* without the requirement for cell/animal sacrifice. The high level of autofluorescence and visible light absorption associated with *in vivo* imaging of fluorophores in the green spectrum greatly limits the tissue depth from which a clear fluorescent signal can be obtained [31, 32]. However, the development of near-infrared (NIR) probes has allowed for the *in vivo* analysis of fluorescence to become practical [33]. NIR probes reduce the level of background signal by increasing the signal-to-noise ratio and therefore facilitates fluorescent imaging at greater depths [34].

For a fluorescent marker to be successfully used for optical imaging it has to fulfil several criteria including suitable excitation and emission wavelengths, photostability, brightness and maturation speed [35-37]. Historically, the most commonly used fluorescent probe for the detection of bacterial vectors is the green fluorescent protein (GFP) or its derivatives. GFP is an isolate from the jellyfish *Aequorea victoria*. A number of studies have described imaging of GFP-expressing bacteria in live bacterial-infected animals [38-40]. Such studies use fluorescent imaging for monitoring the infection progression over time and illustrate the spatial–

temporal behaviour of the process. Bacteria expressing the GFP variants are sufficiently bright as to be clearly visible from outside the infected animal and the increasing levels recorded using a CCD camera. An auxotrophic strain of *S. Typhimurium* A1 expressing GFP which caused nuclear destruction *in vitro* and tumour inhibition and regression of xenografts has been visualized *in vivo* by whole-body imaging [39]. The sensitivity of GFP fluorescence, in conjunction with the *R. reniformis* luciferase (RUC), has been exploited to study *E. coli*, *S. Typhimurium* and *Vibrio cholera* colonisation of tumours in live animals [41]. The sensitivity of GFP imaging was also used to facilitate the identification of metastasised tumours where strong fluorescence demonstrates intratumoural growth of bacteria at primary and secondary tumour sites [42]. Fluorescence imaging is also valuable for fine-detail post-mortem histological study of bacterial localisation [43]. To date, almost all the published reports of fluorescent imaging for bacteria utilise GFP, despite its unsuitable excitation and emission wavelengths for tissue penetration. However, the relative explosion in the number of red-shifted FPs (and therefore more suitable for *in vivo* imaging) developed in recent years should see this exciting field begin to flourish.

### **Instrumentation for OI**

The minute amount of light emitted by optical reporters is detected using a CCD camera which is generally kept cooled to -90°C or below [44]. Depending on the imaging strategy, optical filters can select for both excitation and emission wavelengths as required. Although filters are primarily used for fluorescence

imaging, they can also distinguish between luminescent reporter signals and for determining the depth of a luminescent source within a subject. Both 2D and more recently 3D OI tomography instrumentation and software (e.g. IVIS Spectrum – Perkin Elmer; PhotonIMAGER - Biospace Lab) are available that provide quantitative information with improved spatial resolution [45]. An overview of currently available instrumentation is reviewed elsewhere [46]. Overall, the development of more affordable or more powerful instrumentation, in combination with other imaging methods such as X-ray and micro-CT is rapidly advancing the OI field [47].

### **Engineering bacteria to express reporter genes**

A caveat to the exploitation of bacterial reporter systems is the recalcitrance of certain species to genetic manipulation. The engineering technology currently available for tagging of different species has dictated what bacterial strains have been reported in the context of OI to date. The suitability of OI for bacterial studies is dependent on the ability to genetically modify the bacterial strain in question to stably carry and express the reporter gene (e.g. *lux* or a FP gene), and also the activity of the reporter system in that strain. Even in currently genetically tractable strains, the activity of the *lux* system varies dramatically between bacterial species [20]. Some considerations for improving bacterial reporter gene expression are discussed below.

*Stable gene expression:* The integration of reporter genes in a bacterial genome is preferable over episomal plasmid-based expression to ensure stable and homogenous expression levels. Importantly, this also provides the opportunity to remove the need

for antibiotic selection generally required to maintain plasmids which would be unavailable *in vivo*, and represents an important regulatory consideration in terms of clinical application. Alternative methods of maintaining episomal plasmids in the absence of antibiotic selection have also been developed. For example, strains of *E. coli* rendered metabolically dependent on diaminopimelic acid (DPI) have been generated, permitting maintenance of plasmids featuring DPI-producing genes as plasmid loss leads to bacterial cell death [48, 49]. Transposon [23, 50], transducing bacteriophages [19], temperature sensitive vectors [51] and bacteriophage integrase systems [52-54] have been developed to integrate genes into the chromosomes of selected bacteria. However, it is important to stress that the maintenance and expression of high levels of recombinant DNA may place an unwelcome metabolic burden on microorganisms. Indeed, a number of researchers have described attenuation in *lux*- and GFP-expressing strains [24, 55-57].

*Maximizing reporter expression:* Bacterial reporter gene expression is exquisitely dependent on transcriptional and translational signals. The choice of promoter is vital for optimizing reporter levels and should be assessed on an individual strain basis. The codon usage of the particular organism of interest is also an important consideration. The sequence of the *lux* genes is AT-rich (>69%) and as a result they are not always expressed efficiently in high-GC bacteria such as *Streptomyces coelicolor*. A synthetic *lux* operon lacking TTA codons was constructed and validated for *S. coelicolor* [58]. Furthermore, codon optimizing the firefly luciferase for *M. tuberculosis* resulted in a 30-fold increase in signal [54]. However, codon optimization may have unforeseen effects; the *lux* operon codon optimized for *M. tuberculosis* was found to be non-functional [54] reported to be as a result of secondary DNA structures which impede translation.

*Increasing cofactor availability:* For bacteria expressing the *lux* operon, it is possible that the availability of aldehyde and FMNH<sub>2</sub> are limiting factors. The insertion of an extra promoter in front of *luxCDE* to boost substrate synthesis resulted in a six-fold higher *lux* signal in *M. smegmatis* [54] and *S. aureus* [59]. In yeast, co-expression of *luxAB* together with an *frp* gene which encodes an NADPH–FMN oxidoreductase from *V. harveyi*, led to a 100-fold increase in luminescence [60]. This strategy has also been applied to bacteria and the *frp* from *V. harveyi* was cloned in reporter gene constructs for use in *S. aureus*. However, in this case, inclusion of *frp* was detrimental and resulted in no transformants [59] potentially due to the generation of superoxide (O<sub>2</sub><sup>•-</sup>) from the auto-oxidation of flavoproteins [59].

### **Dual bioluminescent/fluorescent labelling of microorganisms**

In genetically accessible strains of bacteria, the dual labelling of strains with both fluorescent and bioluminescent reporter genes combines the strengths of both systems and reduces the effect of individual cofactor requirements of fluorescent proteins and luciferases. Tagging strains with a luciferase in tandem with GFP has allowed the discrimination between microbial counts (by fluorescence) and metabolic activity (by bioluminescence) [61-63]. Furthermore, fluorescence labelling allows samples to be analysed by fluorescence microscopy and flow cytometry in addition to OI. Importantly, this means that more data can be gathered using fewer experimental animals while also bridging the gulf between the macroscopic and microscopic levels of resolution, that is, individual microorganisms at one end of the imaging spectrum and the detection of mass populations in specific niches in the living animal at the other [64].

## Applications of OI Reporter Genes

Early demonstrations of the tumour targeting capabilities of *lux* expressing bacteria not only provided clear evidence for selective *in vivo* growth and replication of bacteria within tumours, but also importantly showed that whole body imaging of animals colonised by bioluminescent bacteria could be a useful method in the study of bacterial gene therapy of cancer. A model organism, *E. coli* K12 MG1655, has been demonstrated to specifically colonise a wide array of tumour xenografts, including metastases, following IV administration [48, 49]. This has also been supported by findings with other bacterial species such as bifidobacteria [13]. The use of co-imaging techniques to simultaneously visualise luciferase and *lux* signals *in vivo* has been used to great effect to demonstrate the clustered growth pattern of *lux* expressing bacteria in different tumour models [43]. The administration of *lux*-tagged commensal bacteria to mice harbouring luciferase tagged tumours facilitates the generation of 3D diffuse optical tomography displaying the exact distribution of the bacteria within the tumour mass, in relation to viable tumour regions and vascular supply [through computed tomography (CT) imaging]. While non-invasive bacteria such as *B. breve* and *E. coli* MG1655 are not amenable to strategies requiring transfection of tumour cells, their ability to selectively grow within the tumour microenvironment makes them ideal candidates for ‘cellular therapy’ of cancer, i.e. bacterial production of therapeutics within the tumour stroma.

## **OI alternative approaches - Bacterial-specific probes**

Gene-based reporter technology is not applicable to all bacterial strains. The development of a suitable genetic reporter construct can involve substantial resource commitments, and differences in subsequent reporter gene expression between strains hinders applications. Therefore a number of groups have explored alternative strategies using synthetic probes in combination with OI to image bacteria *in vivo* [65]. Identification of substrates or metabolites specific to bacteria and not mammalian cells permits exploitation for imaging through addition of an imaging moiety.

*Near-infrared probes:* The use of an injectable NIR probe consisting of a bacterial affinity group conjugated to an NIR dye is recently demonstrating success [66, 67]. Maltodextrin-based optical imaging probes have been shown to successfully detect small numbers of bacteria *in vivo* with very high specificity and selectivity due to the fact that maltodextrin transporter is unique to bacteria [68]. A further advantage to this strategy is that the lumen of intestinal tissues and the skin are not permeable to glucose oligomers, and therefore MDPs delivered systemically should not be internalized by the resident bacterial microflora. Similarly, bis-zinc(II)-dicolylamide ligands have high affinity for the anionic phospholipids and other molecules residing in bacteria [67]. Xenolight RediJect probe sold by Perkin Elmer is a NIR fluorescent agent for *in vivo* detection of bacteria targeting the anionic phospholipids of bacterial cell membranes. The potential to adapt these technologies to image bacteria colonising tumours is exciting; however this approach may only be applicable to subcutaneous surface tumours. Imaging of bacteria in deeper tissues with higher

background fluorescence requires colonisation numbers of  $10^8$  or more in a defined space.

*Quantum Dots:* In recent years, quantum dots (QDs) have received some attention as probes for OI, especially in cancer research. QDs are small fluorescent nanocrystals made of inorganic semiconductor materials. They are extremely photostable following excitation by an exogenous light source and possess wide excitation and narrow emission spectra. Their emission wavelength depends on their size and they can be manufactured to suit the requirement. However, for bacterial gene therapy applications the size of the QD can inhibit binding of the probe to its target on the bacterial surface [69]. Although autofluorescence is decreased with NIR emission wavelengths, tissue absorption and scattering still impede the amount of excitation light that reaches the fluorophore. To address this ‘self-illuminating’ QDs have been developed which couple QDs with the *Renilla* luciferase [70]. By completely eliminating the need for excitation light, this very elegant approach could be refined by combining different luciferases with QDs of different wavelengths [64].

*Caged luciferin probes:* An emerging form of bioluminescence imaging that employs the use of activatable luminescent probes referred to as “caged luciferin probes” represent a variant of the standard luciferase-luciferin system that is most commonly utilised for BLI. These caged probes allow for more targeted production of the luminescent signal and hence increased ability to determine the spatial localisation of the light signal. The caged probe consists of D-luciferin conjugated to a caging moiety that can be removed by target cells (such as bacteria) to liberate D-luciferin which, in the presence of luciferase, leads to photon generation and emission of a quantifiable light signal [71]. Such a probe has been used to detect luciferase expressing bacteria *in vivo* in models of infection and tumour colonisation

[72]. This probe was designed to be uncaged by bacterial nitroreductase (NTR) enzymes leading to the production of a luminescent signal at the site of infection.

Overall, such strategies represent an exciting avenue for imaging bacteria within all tissue types which is ideally suited to cancer gene therapy-related applications.

## **Alternative modalities to OI**

### **Photoacoustic Imaging**

Photoacoustic imaging (PAI), also known as optoacoustic imaging is an imaging modality based on the photoacoustic effect. Excitation of a target molecule or tissue is achieved using pulsed lasers. The absorbed energy from the pulsed laser is converted to heat, thereby causing the excited molecule or tissue to transiently expand. This thermal expansion results in the emission of ultrasonic waves which can be detected by ultrasonic transducers before conversion to a 2D or 3D image. While BLI, FLI and PAI all rely on optical excitation of a target molecule, the detection of a sound wave is unique to PAI and is in contrast to BLI or FLI which both rely on detection of emitted light from the excited molecule for image acquisition and signal dissemination. While many endogenous molecules such as haemoglobin produce an intrinsic photoacoustic signal, the modality can also be exploited to detect photoacoustic signals from specific exogenous contrast agents [73, 74].

### **Positron Emission Tomography (PET)**

While fluorescent and luciferase based imaging is effective in small animal models, these imaging techniques have not, as yet, been adapted for routine clinical use. It is in this respect that PET is seen as a vital imaging modality in the translation of cancer gene therapy from the lab to the clinic [75]. PET exploits the emission of pairs of  $\gamma$ -rays from positron emitting radionuclides to create quantitative, 3D

images, of *in vivo* biological processes [76]. Molecular probes labelled with positron-emitting isotopes are used to detect biologically active molecules, as a result of the target-dependent sequestration of the systemically administered positron-emitting probes [77]. While one of the most commonly utilised PET probes fluorodeoxyglucose labelled with fluorine<sup>18</sup>, also known as [<sup>18</sup>F] FDG, has previously been used as a radiotracer to image bacteria *in vivo*, it is the use of thymidine kinase (TK) substrates that has been appropriated to greatest effect in bacterial gene therapy studies. These TK substrates become trapped within tumour cells that have been colonised by bacteria allowing for quantitation of intra-tumoural bacteria as well as visualisation of the tumour *in vivo*. Two substrates of the herpes simplex virus 1 TK (HSV-TK) reporter gene that have been reportedly used successfully to image tumour targeting bacteria are [<sup>124</sup>I] 2'-fluoro-1-β-D-arabinofuranosyl-5-iodo-uracil ([<sup>124</sup>I]FIAU) [78] and [<sup>18</sup>F]-2'-Fluoro-2' deoxy-1β-D-arabionofuranosyl-5-ethyl-uracil ([<sup>18</sup>F]FEAU) [79]. Using these radionuclides it had been possible to quantitatively confirm targeting of *E. coli* Nissle 1917 [79] and the *S. Typhimurium* [78] to tumour sites within mice.

### **Magnetic Resonance Imaging**

Magnetic resonance imaging (MRI) has a number of important advantages over other non-invasive imaging modalities, described in detail by Waerzeggers *et al* [80] but are summarised as follows; (i) it has relatively high three-dimensional spatial resolution when compared with PET (ii) it has very good sample penetration in multiple imaging planes, (iii) it has the ability to measure more than one physiological parameter using different radiofrequency pulse sequences, (iv) it has

no risk of ionizing radiation and (v) it is already widely used in the clinic [81]. A drawback is its low sensitivity: approximately micromolar concentrations of an imaging probe can be detected within a given voxel ( $10^{-3}$ – $10^{-5}$  mol/L) which is three to six orders of magnitude lower than the sensitivity of optical imaging for detection of fluorochromes *in vivo* [82].

Benoit *et al.* (2009) exploited the innate physiology of magnetotactic bacteria to target tumours in mice and provide positive contrast for visualization using MRI. The ability of *Magnetospirillum magneticum* AMB-1 to confer positive MRI contrast was determined both *in vitro* and *in vivo* [83]. The strain was administered to tumour bearing mice either intratumourally or intravenously and tumour targeting was confirmed using a multiple of approaches including  $^{64}\text{Cu}$ -labeled bacteria. Significantly *M. magneticum* with small magnetite particles generate T1-weighted positive contrast, enhancing *in vivo* visualization by MRI. Ferritins are ubiquitous iron storage proteins and recent studies have shown that human ferritin can be used as a reporter of gene expression for MRI [84]. Bacteria also encode three classes of ferritin-type molecules which Hill *et al.* (2011) have recently investigated for their potential as MRI reporter genes [85]. Tumour specific induction of bacterioferritin-expression in colonised murine tumours resulted in contrast changes within the bacteria-colonised tumours. However, such research on MR imaging genes is still in its infancy and with the exception of the previously discussed studies, its ability to complement bacterial gene therapy imaging is currently limited.

## Bacterial-Mediated Tumour Therapy

The attractiveness of bacteria as vectors for cancer gene therapy is evidenced by the growing number and range of studies that have employed bacteria as gene delivery vectors. To date, the genera of bacteria that have been exploited as vehicles for delivery to tumours include *Salmonella*, *Escherichia*, *Listeria*, *Clostridium* and *Bifidobacterium* [14, 38, 43, 86-91]. These bacteria can be delivered to the tumour via multiple routes such as intratumoural injection (IT), intravenous injection (IV) or in certain instances orally. Preclinical studies have shown the ability of different bacterial strains to locally produce therapeutic agents and mediate highly effective and specific therapeutic responses [5]. A wide range of gene therapy strategies exist, aiming at inducing malignant cell death either directly (e.g. using ‘suicide’ genes) or indirectly, such as cancer immunotherapy approaches based on killing tumour cells through intervention of various effector cells of the immune system [6]. Invasive bacteria can enter cancer cells and deposit genes within them for host cell expression. In the case of non-invasive bacteria, strains can be engineered to secrete therapeutic proteins locally within the tumour environment, external to tumour cells [91]. This approach is suitable for indirectly acting therapeutic strategies such as anti-angiogenesis and immune therapy (Figure 3).

Live bacteria were first associated with cancers almost two centuries ago when tumour regression was observed in patients who contracted gas gangrene [92] caused by *C. perfringens* [93]. Clostridia are obligate anaerobic bacteria which proliferate preferentially in regions of solid tumours resulting in tumour regression but also acute toxicity. The application of non-pathogenic *Clostridium* strains has generally not provided efficient clinical tumour therapy to date. For example, in

clinical studies, *C. butyricum* M-55 induced ‘liquefaction’ (oncolysis) of gliomas at the well oxygenated outer rim of tumours but lead to regrowth in all patients [94]. However, a recent study utilising an attenuated strain of *Clostridium*, *C. novyi*-NT, was shown to effectively lyse tumour cells in canine models and also in a single human patient. This encouraging result, while limited to a single patient, indicates the potential for the efficacious use of bacteria, and in particular *Clostridium*, in tumour therapy [95]. Unfortunately, the paucity of molecular tools for this genus has also hindered success at further adapting the species for gene delivery.

Genetically engineered strains of *Salmonella* have also been proposed for tumour selective therapy. In contrast to Clostridia, *Salmonella* are Gram-negative motile bacteria that have potential to grow in both oxygenated and hypoxic tumour areas. *S. Typhimurium* has been genetically engineered to produce a variety of therapeutic agents, with success in animal models, accomplishing relatively tumour-specific therapeutic gene expression, reviewed by Chorobik *et al.* [96]. Despite the preferential tumour colonisation following the administration of attenuated *Salmonella* to tumour-bearing animals normal tissues are also colonised transiently and to a lesser extent [91]. A safety-attenuated strain of *S. Typhimurium* designated VNP20029 has been examined in several clinical trials [97]. The pre-clinical success of *Salmonella* has not, however, translated into human studies, and clinical trials have demonstrated tumour colonisation in only a low proportion of patient tumours [98]. This is most likely as a result of the maximum tolerable dose exceeding the therapeutic dose, resulting in a poor therapeutic window. The only established, licenced cancer therapy employing bacteria is Bacillus Calmette-Guérin (BCG), an attenuated *Mycobacterium bovis* strain which was successfully used by Morales, Eidinger and Bruce in 1976 for the treatment of superficial bladder cancer [99]. BCG

has become the treatment of choice for high risk, superficial bladder cancer in most countries, with an increasing rate of treating approximately one million patients per year [100]. The BCG vaccine is a form of immunotherapy that stimulates a local immune response leading to a therapeutic response to the tumour.

While the benefits of using bacteria as vectors for cancer gene therapy are abundantly clear, there are some disadvantages associated with their use in cancer treatment. As with all vector strategies, balance between efficacy and safety is key. In terms of safety, despite the use of safety-attenuated bacterial strains in gene therapy studies employing pathogenic species, the possibility of inducing an immune-mediated toxic response in the host following bacterial administration remains a concern. Therefore, interest in prokaryote-based approaches to cancer therapy has re-emerged with the discovery of non-pathogenic strains that specifically and preferentially target solid tumours. This method has drawn further attention with the development of techniques to genetically modify the bacteria, thereby enabling the expression of anti-cancer therapeutic genes in these hosts [101]. Numerous publications provide convincing evidence that genera of bacteria including *Bifidobacterium* and *Escherichia* have potential in cancer therapy [43, 86, 87, 91, 102-105]. This vector class compares favourably with other vectors in terms of key attributes such as safety, ease of manipulation, and production. While non-pathogenic bacteria have yet to enter clinical trial in the context of tumour targeting vectors, existing knowledge strongly indicates their suitability as a vector system for clinical use.

The inconclusive outcomes to date from bacterial therapy strategies in Phase I/II clinical trials has hindered the progression of this concept [94, 106]. For gene therapy in general, a paucity of technologies to monitor events post vector

administration to patients represents a block in clinical progression [107]. Indeed, in response to the first gene therapy death, the NIH Recombinant DNA Advisory Committee (RAC) called for better assays to monitor gene delivery [108]. As the field of bacterial gene therapy develops, it is becoming clear that the ability to image bacteria *in vivo* following administration is essential. Therefore, in order to determine the location and spread of bacteria within the treated host, the bacteria must be amenable to one of the rapidly evolving modes of imaging that are available to researchers today. Unlike other vector strategies, humans feature a ‘background’ of indigenous bacteria (GIT, oral and genital cavities, skin), and therefore, high specificity for the vector of interest is required, be it from introduced reporter genes, or strain-specific probes.

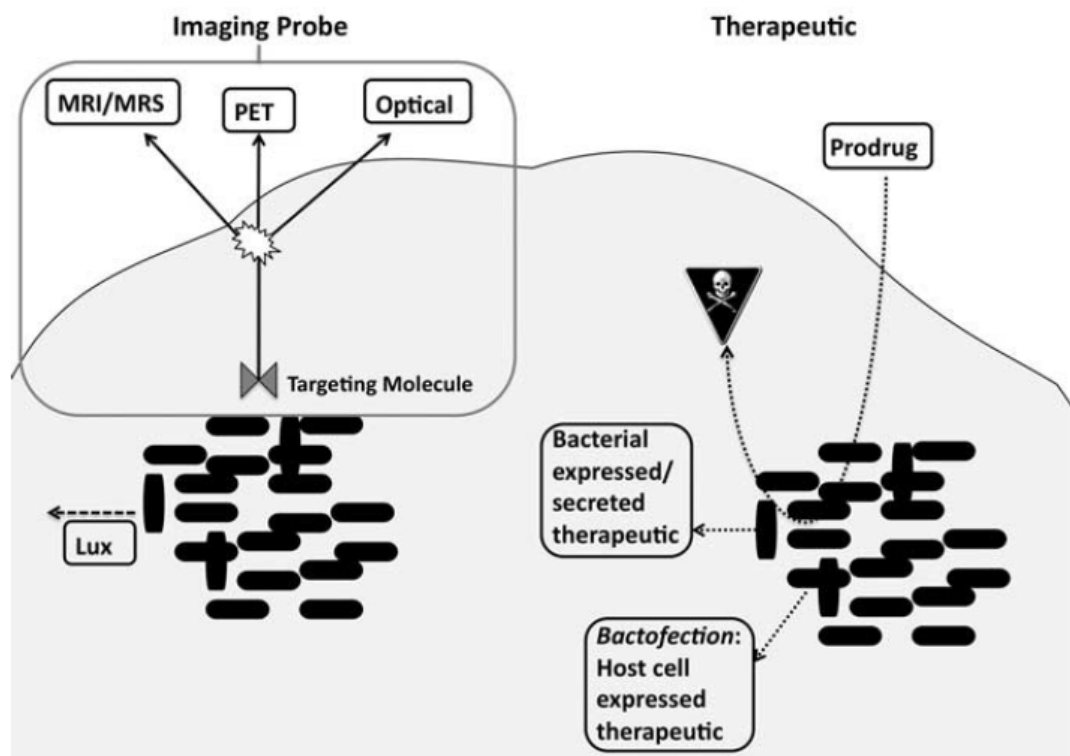


**Figure 3. Bacterial imaging and therapy.** Schematic illustrating strategies for *in vivo* bacterial imaging or tumour therapy.

## Exploiting endogenous bacterial activity for imaging

A major limitation currently exists regarding the availability of plasmids and tools for engineering of a wide range of bacterial genera (both Gram positive and Gram negative) to enable tagging with reporter genes. The development of imaging techniques and therapies that rely solely on the endogenous activities of bacteria present fewer regulatory hurdles than vectors featuring genetic modifications. The endogenous bacterial TK activity of several strains including *E. coli*, *C. novyi*, *S. aureus*, and *Enterococcus faecalis* has been exploited to monitor their location and tumour targeting activity [109]. The bacteria can be selectively imaged in experimentally-infected mice using exogenously administered [<sup>125</sup>I]FIAU, a nucleoside analogue substrate for microbial TK that is taken up by rapidly proliferating cancer cells at an accelerated rate compared to non-cancer cells [110]. The TK enzyme phosphorylates FIAU, leading to accumulation within the bacteria. Since FIAU is a poor substrate for mammalian TK, the radiotracer selectively labels bacteria. The bacteria can therefore be imaged *in situ* using PET or single photon emission computed tomography (SPECT) in conjunction with CT. Since radio-pharmaceutical based imaging provides a comprehensive 3D assessment of the whole tumour it correlates well with colonisation levels.

A strategy termed sequential reporter-enzyme luminescence has been described recently, which combines luciferase-expressing bacteria with a  $\beta$ -lactamase-cleavable substrate [111]. Bluco is a ‘caged’ luciferin, which is released by bacterial  $\beta$ -lactamase hydrolysis for reacting with luciferase [112]. Tumour targeting bacteria such as certain strains of *Salmonella* or *E. coli* [113] endogenously produce the enzyme  $\beta$ -lactamase which may be sufficient to cleave the  $\beta$ -lactam ring

in Bluco and liberate D-luciferin. Free D-luciferin could then be oxidised by FLuc to produce light for *in vivo* detection of tumours and metastasis. Successful use of Bluco for *in vivo* tumour visualisation could pave the way for therapies utilising endogenous bacterial enzymes to cleave pro-drugs specifically within tumours thereby avoiding concerns associated with genetically modified organisms.

### **Bacterial Directed Enzyme Prodrug Therapy**

An exciting approach to increasing the efficacy of a bacterial vector and reducing its therapeutic dosage has been to use BDEPT. This involves ‘arming’ bacteria with a gene coding for a prodrug converting enzyme (that has no human homologue, or/and has more favourable enzyme kinetics than any human isozyme) and using them to deliver the enzyme to the locality of the tumour. BDEPT is a two-step therapy (Figure 4). In the first step, the armed vector is administered to the patient and targets specifically to the site of the tumour where the enzyme is expressed. In the second step, once the levels of enzyme expression are optimal, a prodrug is administered and is converted to a cytotoxic drug by the expressed enzyme strictly at the tumour site. This results in tumour-selective cytotoxicity.

BDEPT has a number of homologous therapeutic strategies: Antibody Directed Enzyme Prodrug Therapy (ADEPT) was first conceived more than 20 years ago [114] [115] [116]. It involves targeting tumour antigens extracellularly with a monoclonal antibody that is chemically conjugated to a purified prodrug converting enzyme. A number of ADEPT systems are under investigation [117] some of which have advanced to clinical trials [118]. Viral Directed Enzyme Prodrug Therapy (VDEPT) [119-121] has shown promise in pre-clinical [122] and clinical trials [123].

Other similar therapies include Polymer Directed Enzyme Prodrug Therapy (PDEPT) [124], Ligand Directed Enzyme Prodrug Therapy [125], Melanocyte Directed Enzyme Prodrug Therapy (MDEPT) [126] and Prodrug Monotherapy [127]. The broad term Gene Directed Enzyme Prodrug Therapy (GDEPT) covers all strategies which involve tumour cell gene expression of prodrug converting enzymes (for a review on the background and principles of both GDEPT and its prodrugs see [128] and [129]). One of the most described GDEPT systems has been the Herpes Simplex Virus thymidine kinase (HSV-tk)/nucleoside analogue combination and dates back to the 80's [130]. Delivery of the gene coding for HSV-tk *in vivo* has been achieved using many vectors e.g.; retroviruses [131], adenoviruses [132] and liposomes [133].

The Cytosine Deaminase enzyme (CD) is found in many bacteria and fungi but not in mammalian cells. It catalyses the deamination of cytosine to uracil but can also convert the antifungal agent 5-fluorocytosine (5-FC) to the popular antitumour drug 5-fluorouracil (5-FU). The latter is further metabolised by mammalian enzymes to RNA and DNA synthesis inhibitors. Initial BDEPT studies utilized *Clostridium beijerinckii* NCIMB 805 and *E. coli* CD (*codA*). CD could be expressed from shuttle vectors designed to work in Gram-positive bacteria. CD activity was measured in both supernatant and cell lysates and was sufficient to inhibit the growth of an EMT6 murine carcinoma cell line *in vitro*. Subsequently, *Clostridium sporogenes* was used to deliver CD activity to WAG/Rij rats bearing rhabdomyosarcoma [134]. *Clostridium acetobutylicum* could also target and deliver active CD to similar tumours. To further increase the effectiveness of BDEPT with this vector, vascular collapse was induced by combretastatin A4 phosphate which resulted in increased CD activity in tumours versus normal tissue (presumably by increasing the hypoxic

area of the tumour and allowing for more consistent targeting of clostridia spores [135]). In therapy experiments Liu et al [136] demonstrated that *Clostridium sporogenes* expressing CD could deliver CD to tumours exclusively. Following intravenous administration of 5-FC, tumour regression was observed in experimental models. However, no follow up studies on this particular system have ever been published since.

At a similar period, CD expression was being investigated in *Bifidobacterium longum* [137]. Active CD delivery to tumours was confirmed with VNP20047 [138] and later with *Bifidobacterium breve* I538w [139]. In separate studies, intratumoural and intravenous injections of *B. longum* expressing CD in rats resulted in a preferential proliferation within hypoxic areas of the tumours and efficient conversion of 5-FC to 5-FU. Tumour cell death was evaluated histologically using the TUNEL assay and revealed that the majority of the tumour cells were apoptotic at or near the sites of bacterial colonisation. A significant tumour mass regression was also documented [140]. Similar levels of efficacy were shown with *Bifidobacterium infantis* in melanoma tumours [141]. To improve BDEPT with *B. longum* in conjunction with CD; an *E. coli* CD mutant (D314A) initially identified by Mahan and co-workers [142] was utilised. Growth studies *in vitro* showed that during log phase, *B. longum*-CD (D314A) was about 10 fold more potent than *B. longum* expressing wild type CD [143]. Increased potency was maintained in late log phase and stationary phase making *B. longum*-CD (D314A) a good candidate vector for pre-clinical studies.

Impressive BDEPT results have also been achieved by *Salmonella* expressing *E. coli* CD. King and co-workers [144] demonstrated in murine experimental tumours that *Salmonella* harbouring CD resulted in high colony

forming units (CFU) in tumours ( $1 \times 10^9$  over normal tissue  $1 \times 10^6$ ) following IV administration. An 88%-96% tumour regression was achieved in mice treated with *Salmonella* -CD and 5-FC as opposed to 38%-79% achieved with *Salmonella* -CD in the absence of the prodrug. 5-FC alone did not show any effect on the tumour. These results prompted a small clinical trial (pilot study) involving 3 patients with head and neck cancer. Intratumoural injections of *Salmonella* -CD resulted in persistence of bacteria in two of three patients for 15 days however at low levels ( $1 \times 10^5$  CFU/g of tumour). *Salmonella* -CD was able to convert 5-FC to 5-FU at the tumour site in both patients. No significant 5-FC conversions were measured elsewhere. Despite this, no tumour regression was observed in any patient and the trial was discontinued [106]. In relation to this, there was a study done to assess the efficacy of 5-FC conversion by CD in tumour bearing mice [145]. Mice were treated with *Salmonella* -CD and 5-FC and 5-FC to 5-FU conversion within the tumours was measured by  $^{19}\text{F}$ -MRS (magnetic resonance spectroscopy) and chromatography. Paradoxically, although all tumours in the groups had comparable enzyme expression levels and CD activity, some tumours failed to convert 5-FC to 5-FU and did not respond to treatment. Tumour bacterial colonisation levels as well as histological examination of tumour hypoxia were found to be similar in both treatment “responders” and “non-responders”. However, this study did not report tumour structural vascularity studies or show microscopy images of bacterial distribution within the tumours. Further research into this phenomenon should broaden our understanding of prodrug activation in tumours by bacteria and could aid BDEPT improvements in the future.

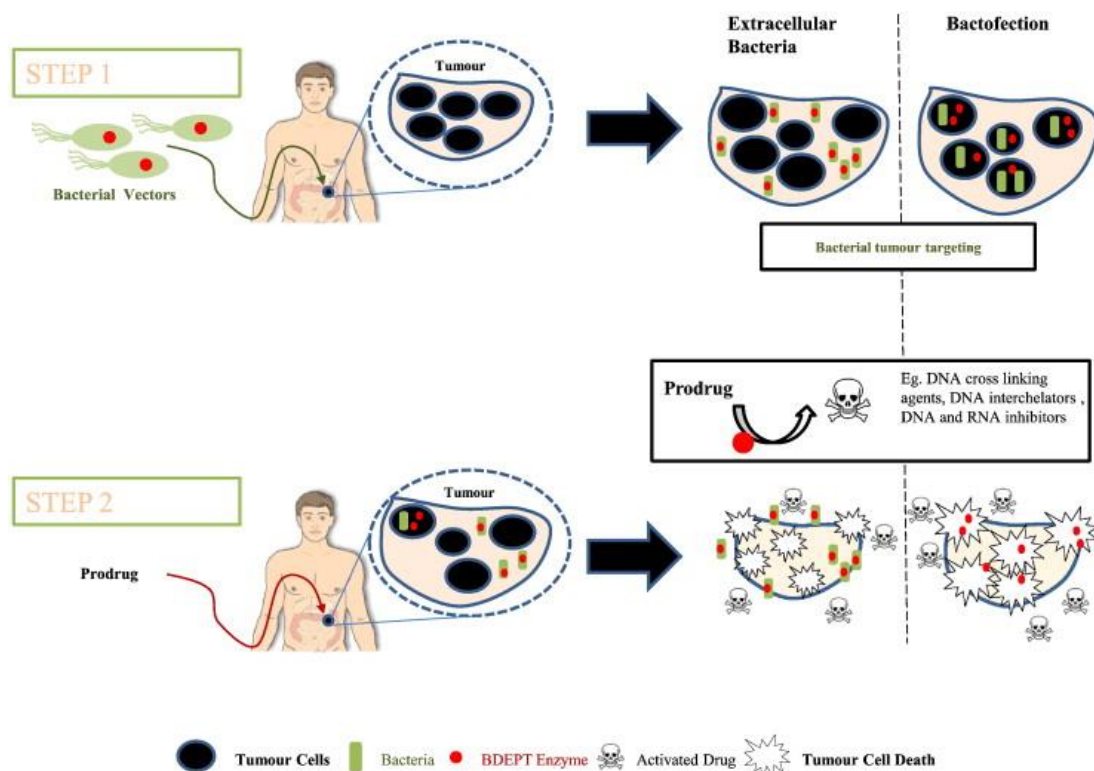


**Figure 4. BDEPT schematic.** In the first step of the therapy, bacteria carrying a BDEPT enzyme (e.g. CD) are administered to the patient and target to the site of the tumour where they establish extracellular colonies or directly invade the tumour cells and deliver the gene by bactofection. In the second step, a non-toxic prodrug is administered systemically and is converted to a cytotoxic agent (e.g. DNA cross linking agent) strictly at the tumour site by the expressed BDEPT enzyme. In addition to direct cytotoxicity, for both extracellular bacteria and bactofection strategies, the active drug is taken up by tumour cells in the vicinity (bystander cytotoxic effect) which leads to tumour regression. Taken from [146]

## **Advantages of BDEPT as a therapeutic strategy**

In BDEPT and other prodrug converting strategies, the drug is generated in situ following tumour targeting. This gives a number of advantages over conventional therapies. First, tumour selectivity is achieved as the prodrug is strictly converted within the tumour, reducing side effects in other organs. Second, an amplifying effect is achieved, which results from the ability of a single therapeutic enzyme molecule to activate many prodrug molecules. This results in high concentrations of active drug at the tumour site (which is higher than can be achieved with classical chemotherapy). Third, a bystander effect is accomplished. This is defined as the ability of bacterial cells expressing the enzyme to stimulate the killing of neighbouring tumour cells that do not express the enzyme. Therefore, bacteria can be clustered in colonies in the tumour stroma and do not need to invade cancer cells for successful eradication/regression of the tumour to occur. The bystander effect is integral to all prodrug-converting therapies and is key to their efficacy [129, 147].

BDEPT also has further benefits over its related therapies. For example, ADEPT is challenged by tumour antigen heterogeneity and antigen expression levels. VDEPT requires a productive viral infection for successful transgene expression that is dependent on both intracellular and extracellular proteins. Furthermore, retroviral genomic integration is not always stable and may result in spontaneous loss of the therapeutic gene. GDEPT may suffer from gene expression issues in general. A sufficient level of therapeutic gene/transgene expression is required for an effective prodrug conversion which is dependent on many molecular variables. In cases where the transgene is of bacterial origin, it is possible for its activity to be hampered by eukaryotic post-translational modifications, e.g N-linked

glycosylation of carboxypeptidase 2 [148]. In BDEPT, bacterial targeting relies on the physical rather than the biochemical nature of the tumour; non-pathogenic bacteria can be employed which are intrinsically nontoxic to the host; there exists a wealth of bacterial molecular biology technology with relatively few hurdles to bacterial gene expression; any possible transgene toxicity in human normal tissue (that could arise due to vector mistargeting) is avoided as the bacteria harbour the gene; serum components cannot inhibit the enzyme as it is protected by bacterial membranes and a cell wall; in the bacterial cell, there is a pool of cofactors such as NADH or NADPH available to therapeutic enzymes that require a reducing environment; and finally, bacteria, unlike viruses, can be scaled up for clinical use with relative ease.

One important difference between BDEPT and other bacterial therapies that employ constitutively toxic genes; (e.g. *Salmonella* expressing pro-apoptotic cytokine Fas ligand [149]) is that in BDEPT, toxicity is controlled and induced strictly following prodrug administration whereas the other types of bacterial therapies can be toxic following injection in the patient. Systemic toxicity can be induced rapidly, especially if the bacteria secrete the therapeutic protein. Furthermore, bacteria which carry therapeutic genes controlled by eukaryotic promoters can also pose problems if the vector mistargets to healthy cells, resulting in off target toxicity. Ideally, BDEPT could be integrated with imaging techniques in order for the clinician to be able to evaluate targeting and decide beforehand if it is appropriate to administer the prodrug.

## Bacterial therapeutic gene expression technology

There are a number of ways to express prodrug-converting enzymes in tumours with bacteria. One way involves cloning the gene of choice in a plasmid under a bacterial promoter (which can be inducible e.g.[150, 151]) that can direct high levels of protein expression. In our laboratory, the gene coding for CPG2 as well as other gene constructs have been expressed successfully in *Salmonella* strains using a cassette (found in commercially available plasmid pTrc99A) consisting of the hybrid trc promoter, the LacZ Shine Dalgarno sequence and the *E. coli* rrnB operon T1 terminator. Others have also used various commercially available plasmids for their work with Gram-negative vectors. However, Gram-negative expression systems don't work well in Gram-positive bacteria such as *Clostridia* or *Bifidobacteria* as they have different requirements. Therefore, researchers have developed their own shuttle vectors for use in *Bifidobacteria* [143] and *Clostridia* [152]. These shuttle vectors contain compatible origins of replication to the host's replication machinery as well as endogenous promoters in order to direct high gene expression levels. Further, researchers may also opt to optimise codon usage of foreign genes inserted into those plasmids to achieve better expression [153].

Alternatively, instead of artificial expression systems, plasmid free bacteria which express enzymes from their natural promoters can be used (e.g. Endogenous *E.coli* genes; cytosine deaminase (CD) *codA*, nitroreductase (NR) *nfsA* and *nfsB* and purine nucleoside phosphorylase (PNP) *deoD*). However when using this strategy, the gene expression level and enzymatic activity within the bacteria must be sufficient for an efficient prodrug conversion to occur in order for them to be 'effective agents'.

Finally, during therapy, we have observed that in the absence of antibiotic selection pressure, the plasmid may be lost also resulting in the loss of the therapeutic gene (see also Min [154]). Strategies to bypass this problem do exist. For strains where suitable genetic technology is available, gene constructs can be integrated into the bacterial genome, or an antibiotic resistance-free ‘balanced lethal system’ [155] could be employed [156], which is also clinically preferable.

Tumour cell transfection of the BDEPT gene represents an alternative approach, and involves cloning the gene of interest in a mammalian plasmid under a mammalian promoter like the cytomegalovirus promoter [157] and using bacteria as *in vivo* gene transduction agents, much like viral vectors, in order to transduce individual tumour cells. This method is termed bactofection and is becoming popular as means to deliver toxic genes to tumours [14]. It is also widely used in bacterial vaccination strategies against cancer [8] (this topic is beyond the scope of this article; see [158] and [159] for an extensive review). Its drawback is that in the case of any unforeseeable emergency it is impossible to shut down gene expression as transduced mammalian cells actively producing the therapeutic protein will not respond to antibiotics. It also suffers from similar issues as GDEPT (see above). Delivering transgenes inside tumour cells by bactofection makes this strategy a hybrid between BDEPT and GDEPT.

### **Combined imaging and therapy**

Magnetic resonance spectroscopy (MRS) complements MRI as a non-invasive means for the characterization of tissue. MRS has been used for quantitative non-invasive imaging of tumours expressing cytosine deaminase as a combined reporter

and therapeutic gene [160]. Stegman *et al.* (1999) exploited cDNA encoding for yeast cytosine deaminase in combination with the 5-fluorocytosine (5-FC) prodrug. The yCD-catalyzed conversion of 5-FC to the chemotherapeutic agent (5-FU) was quantified *in vivo* using  $^{19}\text{F}$  MRS. Similar prodrug therapy approaches using bacterial expressed CD exist in the literature [161] and its derivative TAPET-CD (which expresses the *E. coli* CD) have been investigated in Phase 1 clinical trials in cancer patients. Pre-clinical studies with the commensal *Bifidobacterium* have also been conducted. The “*Bifidobacterial Selective Targeting*” BEST [86, 162] strategy exploits *B. longum* 105-A containing pBLES100-S-eCD, a plasmid containing a CD under the control of the *hup* gene promoter of *B. longum* [137]. *B. longum* selectively produces CD in hypoxic mammary tumour tissues in rats, converts 5-FC into 5-FU *in vivo* [139, 140, 143]. This system could be significantly improved by combination with MR imaging technology.

Thymidine Kinase is another example of a gene therapy approach which combines both therapeutic and reporter activity simultaneously. The most commonly used *TK* for gene therapy studies is HSK-*TK* in combination with an acycloguanosine such as ganciclovir which has been tested in a series of pre-clinical and clinical trials in a wide range of cancer types [163, 164]. The potential exists to improve this study by combining it with multi-modality imaging techniques such as SPECT, PET or MRI. Combined application of the imaging modalities and imaging probes will maximise the diagnostic and therapeutic potential of bacterial gene therapy and achieve a targeted regime for cancer therapy with minimal off-target effects.

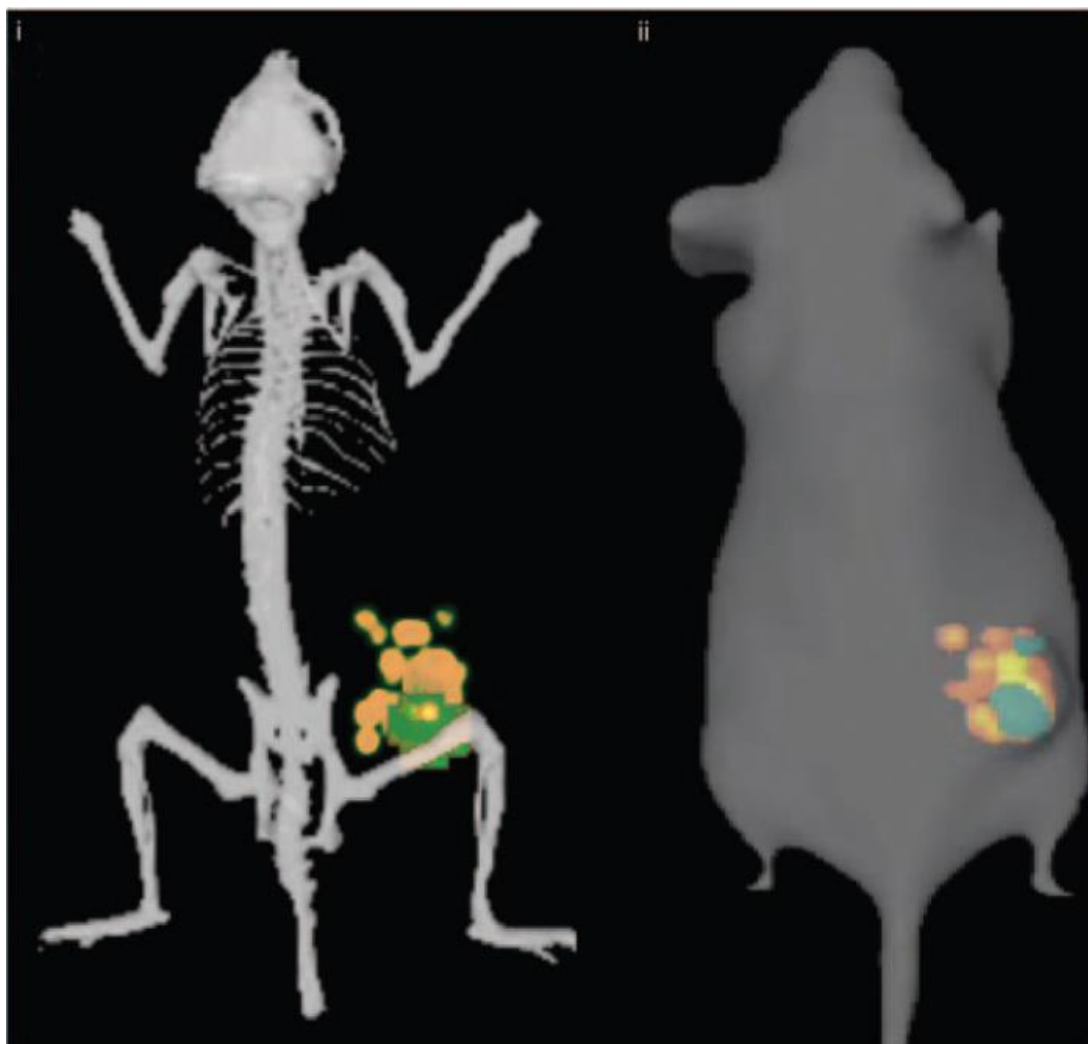


**Figure 5. Dual imaging of tumour and bacterial bioluminescence.** (i) 3D Bioluminescence co-registration. An athymic mouse bearing a subcutaneous FLuc expressing HCT116 tumour 7 days post IV administration of  $10^5$  *B. breve* UCC2003 pluxMC3. Tumour FLuc = orange, Bacterial lux = green. Both bacterial lux and tumour FLuc were imaged sequentially. An Atlas mouse skeleton is shown for spatial reference. (ii) A still from a movie illustrating tomographic detail of source signal distribution of *B. breve* pluxMC3 10 days post IV administration to mice bearing HCT116 FLuc (orange) expressing tumours. *B. breve* lux is observed in multiple disparate ‘clusters’ within the tumour.

## Conclusions and future perspectives

A growing number of studies have reported the successful targeting and treatment of murine tumours by bacteria. However, numerous challenges remain before these vectors can be routinely applied in the clinic, including identifying the targeting mechanism as well as addressing concerns regarding toxicity and genetic instability. The potential for the vector to cause toxicity in the host as well as the genetic instability of any exogenous genes will need to be addressed on an individual strain basis but may be circumvented through the use of non-pathogenic strains or exploiting endogenous genes for prodrug activation. The challenge of successful targeting of the bacterial vector to the tumour is a complex issue. The ideal application of the vector would target not only the primary tumour but also metastases at distal sites without affecting healthy tissue. In order to demonstrate this targeting, the ability to image the vector in patients is essential.

Each imaging modality has inherent strengths and weaknesses, with none fulfilling all purposes. Nuclear medicine imaging modalities such as PET are highly sensitive but suffer from poor spatial resolution [81]. MRI has the highest image resolution, but sensitivity is less than nuclear techniques [9]. FP detection has shown some success at preclinical levels however high background levels and poor tissue penetration of both excitation and emission waves restrict efficacy. BLI reporting systems display fewer drawbacks and autoluminescence is almost non-existent permitting much higher sensitivity and specificity than fluorescence *in vivo*. However, there are some obvious limitations to OI such as light scattering and spatial resolution which is depth dependent [165]. 3D optical tomography systems have improved the resolution and the increasing availability of defined bandwidth

filters for capturing photonic signals, and improvements in spectral unmixing algorithms to differentiate between signals with different emission spectra, opens up exciting new avenues for bacterial imaging *in vivo*. However the OI technology is currently limited to small animals or surface tumours.

The inherent disadvantages associated with each modality means none are perfectly suited to advance the concept of bacterial gene therapy of cancer alone. However, the potential to co-register optical-imaging data with other technologies such as MRI, PET or even SPECT, X-ray and CT is an exciting development. A variety of factors determine the choice of specific imaging system, some of them are the imaging requirements (single or repeated), the proposed use (animal or human) and spatial requirements (tissue depth). Combination imaging should allow each modality to bring its unique advantages to the fore, while providing complementary information. The ability to monitor bacterial colonisation dynamics by optical imaging or exploiting endogenous/exogenous genes in combination with an imaging technology while simultaneously recording the resultant changes in host physiology and anatomy using other imaging modalities, will considerably enhance our understanding of the complexities of this process *in vivo* and can be applied to multiple fields of research including the detection of infectious disease.

## References

1. Abelman, H., *Cancer as I see it*. New York Philosophical Library, New York, NY, 1951.
2. Yu, Y.A., Q. Zhang, and A.A. Szalay, *Establishment and characterization of conditions required for tumor colonization by intravenously delivered bacteria*. Biotechnol Bioeng, 2008. **100**(3): p. 567-78.
3. Harada, H., et al., *The Akt/mTOR pathway assures the synthesis of HIF-1 $\alpha$  protein in a glucose- and reoxygenation-dependent manner in irradiated tumors*. J Biol Chem, 2009. **284**(8): p. 5332-42.
4. Pawelek, J.M., K.B. Low, and D. Bermudes, *Bacteria as tumour-targeting vectors*. Lancet Oncol, 2003. **4**(9): p. 548-56.
5. Baban, C.K., et al., *Bacteria as vectors for gene therapy of cancer*. Bioeng Bugs, 2010. **1**(6): p. 385-94.
6. Tangney, M., et al., *Gene therapy for prostate cancer*. Postgrad Med, 2010. **122**(3): p. 166-80.
7. Ahmad, S., et al., *Prostate stem cell antigen DNA vaccination breaks tolerance to self-antigen and inhibits prostate cancer growth*. Mol Ther, 2009. **17**(6): p. 1101-8.
8. Ahmad, S., et al., *Induction of effective antitumor response after mucosal bacterial vector mediated DNA vaccination with endogenous prostate cancer specific antigen*. J Urol, 2011. **186**(2): p. 687-93.
9. Chuang, K. and T. Cheng, *Noninvasive Imaging of Reporter Gene Expression and Distribution In Vivo*. Fooyin J Health Sci, 2010. **2**(1): p. 1-11.
10. Michelini, E., et al., *Luminescent probes and visualization of bioluminescence*. Methods Mol Biol, 2009. **574**: p. 1-13.
11. Morrissey, D., G.C. O'Sullivan, and M. Tangney, *Tumour targeting with systemically administered bacteria*. Curr Gene Ther, 2010. **10**(1): p. 3-14.
12. Tangney, M. and C.G. Gahan, *Listeria monocytogenes as a vector for anti-cancer therapies*. Curr Gene Ther, 2010. **10**(1): p. 46-55.
13. Cronin, M., et al., *Orally administered bifidobacteria as vehicles for delivery of agents to systemic tumors*. Mol Ther, 2010. **18**(7): p. 1397-407.

14. van Pijkeren, J.P., et al., *A novel Listeria monocytogenes-based DNA delivery system for cancer gene therapy*. Hum Gene Ther, 2010. **21**(4): p. 405-16.
15. Prescher, J.A. and C.H. Contag, *Guided by the light: visualizing biomolecular processes in living animals with bioluminescence*. Curr Opin Chem Biol. **14**(1): p. 80-9.
16. Loening, A.M., A.M. Wu, and S.S. Gambhir, *Red-shifted Renilla reniformis luciferase variants for imaging in living subjects*. Nat Methods, 2007. **4**(8): p. 641-3.
17. Levi, J., et al., *Bisdeoxycoelenterazine derivatives for improvement of bioluminescence resonance energy transfer assays*. J Am Chem Soc, 2007. **129**(39): p. 11900-1.
18. Wiles, S., et al., *Alternative luciferase for monitoring bacterial cells under adverse conditions*. Applied and environmental microbiology, 2005. **71**(7): p. 3427-3432.
19. Nguyen, V.H., et al., *Genetically engineered Salmonella typhimurium as an imageable therapeutic probe for cancer*. Cancer Res, 2010. **70**(1): p. 18-23.
20. Gahan, C.G., *The bacterial lux reporter system: applications in bacterial localisation studies*. Curr Gene Ther, 2012. **12**(1): p. 12-9.
21. Belas, R., et al., *Bacterial bioluminescence: isolation and expression of the luciferase genes from Vibrio harveyi*. Science, 1982. **218**(4574): p. 791-3.
22. Riedel, C.U., et al., *Improved luciferase tagging system for Listeria monocytogenes allows real-time monitoring in vivo and in vitro*. Appl Environ Microbiol, 2007. **73**(9): p. 3091-4.
23. Francis, K.P., et al., *Visualizing pneumococcal infections in the lungs of live mice using bioluminescent Streptococcus pneumoniae transformed with a novel gram-positive lux transposon*. Infect Immun, 2001. **69**(5): p. 3350-8.
24. Hardy, J., et al., *Extracellular replication of Listeria monocytogenes in the murine gall bladder*. Science, 2004. **303**(5659): p. 851-3.
25. Wiles, S., et al., *Organ specificity, colonization and clearance dynamics in vivo following oral challenges with the murine pathogen Citrobacter rodentium*. Cell Microbiol, 2004. **6**(10): p. 963-72.
26. Davis, R.W.I.V., et al., *In Vivo Tracking of Streptococcal Infections of Subcutaneous Origin in a Murine Model*. Molecular Imaging and Biology, 2015: p. 1-9.

27. Nealson, K.H., *Autoinduction of bacterial luciferase. Occurrence, mechanism and significance.* Arch Microbiol, 1977. **112**(1): p. 73-9.
28. Bhaumik, S. and S. Gambhir, *Optical imaging of Renilla luciferase reporter gene expression in living mice.* Proceedings of the National Academy of Sciences, 2002. **99**(1): p. 377.
29. Baban, C.K., et al., *Bacteria as vectors for gene therapy of cancer.* BioEngineered Bugs, 2010. **1**(12).
30. Chen JQ, Z.Y., Wang W, Jiang SN, Li XY, *The engineered Salmonella typhimurium inhibits tumorigenesis in advanced glioma.* EXPERIMENTAL THERAPEUTICS AND TARGETED THERAPIES, 2015. **2015**:8: p. 2555—2563.
31. Min, J.J., V.H. Nguyen, and S.S. Gambhir, *Molecular Imaging of Biological Gene Delivery Vehicles for Targeted Cancer Therapy: Beyond Viral Vectors.* Nuclear Medicine and Molecular Imaging, 2010. **44**(1): p. 15-24.
32. Beckmann, N., et al., *In vivo mouse imaging and spectroscopy in drug discovery.* NMR in Biomedicine, 2007. **20**(3): p. 154-185.
33. Hilderbrand, S.A. and R. Weissleder, *Near-infrared fluorescence: application to in vivo molecular imaging.* Current Opinion in Chemical Biology, 2010. **14**(1): p. 71-79.
34. Bokobza, L., *Near infrared spectroscopy.* Journal of Near Infrared Spectroscopy, 1998. **6**: p. 3-18.
35. Zhao, M., et al., *Spatial-temporal imaging of bacterial infection and antibiotic response in intact animals.* Proc Natl Acad Sci U S A, 2001. **98**(17): p. 9814-8.
36. Mehta, S.R., et al., *Real-time in vivo green fluorescent protein imaging of a murine leishmaniasis model as a new tool for Leishmania vaccine and drug discovery.* Clin Vaccine Immunol, 2008. **15**(12): p. 1764-70.
37. Kong, Y., et al., *Application of optical imaging to study of extrapulmonary spread by tuberculosis.* Tuberculosis (Edinb), 2009. **89 Suppl 1**: p. S15-7.
38. Zhao, M., et al., *Tumor-targeting bacterial therapy with amino acid auxotrophs of GFP-expressing Salmonella typhimurium.* Proc Natl Acad Sci U S A, 2005. **102**(3): p. 755-60.

39. Hayashi, K., et al., *Cancer metastasis directly eradicated by targeted therapy with a modified Salmonella typhimurium*. J Cell Biochem, 2009. **106**(6): p. 992-8.
40. Miwa, S., et al., *Tumor-targeting Salmonella typhimurium A1-R prevents experimental human breast cancer bone metastasis in nude mice*. Oncotarget, 2014. **5**(16): p. 7119.
41. Yu, Y.A., et al., *Visualization of tumors and metastases in live animals with bacteria and vaccinia virus encoding light-emitting proteins*. Nat Biotechnol, 2004. **22**(3): p. 313-20.
42. Wang, Y.W., et al., *Renilla luciferase-Aequorea GFP (Ruc-GFP) fusion protein, a novel dual reporter for real-time imaging of gene expression in cell cultures and in live animals*. Molecular Genetics and Genomics, 2002. **268**(2): p. 160-168.
43. Cronin, M., et al., *High resolution in vivo bioluminescent imaging for the study of bacterial tumour targeting*. PLoS One, 2012. **7**(1): p. e30940.
44. Snoeks, T.J., C.W. Lowik, and E.L. Kaijzel, *'In vivo' optical approaches to angiogenesis imaging*. Angiogenesis, 2010. **13**(2): p. 135-47.
45. Zhang, Q., et al., *Quantitative bioluminescence tomography guided by diffuse optical tomography*. Opt Express, 2008. **16**(3): p. 1481-6.
46. Leblond, F., et al., *Pre-clinical whole-body fluorescence imaging: Review of instruments, methods and applications*. J Photochem Photobiol B, 2010. **98**(1): p. 77-94.
47. Tangney, M. and K.P. Francis, *In vivo optical imaging in gene & cell therapy*. Curr Gene Ther, 2012. **12**(1): p. 2-11.
48. Min, J.J., et al., *Noninvasive real-time imaging of tumors and metastases using tumor-targeting light-emitting Escherichia coli*. Molecular Imaging and Biology, 2008. **10**(1): p. 54-61.
49. Min, J.J., et al., *Quantitative bioluminescence imaging of tumor-targeting bacteria in living animals*. Nat Protoc, 2008. **3**(4): p. 629-36.
50. Winson, M.K., et al., *Engineering the luxCDABE genes from Photobacterium luminescens to provide a bioluminescent reporter for constitutive and promoter probe plasmids and mini-Tn5 constructs*. FEMS Microbiol Lett, 1998. **163**(2): p. 193-202.

51. Riedel, C.U., et al., *Construction of p16Slux, a novel vector for improved bioluminescent labeling of gram-negative bacteria*. Appl Environ Microbiol, 2007. **73**(21): p. 7092-5.
52. Bron, P.A., et al., *Novel luciferase reporter system for in vitro and organ-specific monitoring of differential gene expression in Listeria monocytogenes*. Appl Environ Microbiol, 2006. **72**(4): p. 2876-84.
53. Steinhuber, A., et al., *Bioluminescence imaging to study the promoter activity of hla of Staphylococcus aureus in vitro and in vivo*. Int J Med Microbiol, 2008. **298**(7-8): p. 599-605.
54. Andreu, N., et al., *Optimisation of bioluminescent reporters for use with mycobacteria*. PLoS One, 2010. **5**(5): p. e10777.
55. Rocchetta, H.L., et al., *Validation of a noninvasive, real-time imaging technology using bioluminescent Escherichia coli in the neutropenic mouse thigh model of infection*. Antimicrob Agents Chemother, 2001. **45**(1): p. 129-37.
56. Bumann, D., *Examination of Salmonella gene expression in an infected mammalian host using the green fluorescent protein and two-colour flow cytometry*. Mol Microbiol, 2002. **43**(5): p. 1269-83.
57. Sanz, P., et al., *Detection of Bacillus anthracis spore germination in vivo by bioluminescence imaging*. Infect Immun, 2008. **76**(3): p. 1036-47.
58. Craney, A., et al., *A synthetic luxCDABE gene cluster optimized for expression in high-GC bacteria*. Nucleic Acids Res, 2007. **35**(6): p. e46.
59. Mesak, L.R., G. Yim, and J. Davies, *Improved lux reporters for use in Staphylococcus aureus*. Plasmid, 2009. **61**(3): p. 182-7.
60. Gupta, R.K., et al., *Expression of the Photorhabdus luminescens lux genes (luxA, B, C, D, and E) in Saccharomyces cerevisiae*. FEMS Yeast Res, 2003. **4**(3): p. 305-13.
61. Unge, A., et al., *Simultaneous monitoring of cell number and metabolic activity of specific bacterial populations with a dual gfp-luxAB marker system*. Appl Environ Microbiol, 1999. **65**(2): p. 813-21.
62. Qazi, S.N., et al., *Development of gfp Vectors for Expression in Listeria monocytogenes and Other Low G+C Gram Positive Bacteria*. Microb Ecol, 2001. **41**(4): p. 301-309.

63. Tamagnini, I., et al., *Generation and comparison of bioluminescent and fluorescent Bacillus licheniformis*. Curr Microbiol, 2008. **57**(3): p. 245-50.
64. Andreu, N., A. Zelmer, and S. Wiles, *Noninvasive biophotonic imaging for studies of infectious disease*. FEMS Microbiol Rev, 2011. **35**(2): p. 360-94.
65. van Oosten, M., et al., *Targeted imaging of bacterial infections: advances, hurdles and hopes*. FEMS Microbiology Reviews, 2015.
66. Leevy, W.M., et al., *Optical imaging of bacterial infection in living mice using a fluorescent near-infrared molecular probe*. J Am Chem Soc, 2006. **128**(51): p. 16476-7.
67. Leevy, W.M., et al., *Noninvasive optical imaging of staphylococcus aureus bacterial infection in living mice using a Bis-dipicolylamine-Zinc(II) affinity group conjugated to a near-infrared fluorophore*. Bioconjug Chem, 2008. **19**(3): p. 686-92.
68. Ning, X., et al., *Maltodextrin-based imaging probes detect bacteria in vivo with high sensitivity and specificity*. Nat Mater, 2011. **10**(8): p. 602-7.
69. Leevy, W.M., et al., *Quantum dot probes for bacteria distinguish Escherichia coli mutants and permit in vivo imaging*. Chem Commun (Camb), 2008(20): p. 2331-3.
70. Loening, A.M., et al., *Consensus guided mutagenesis of Renilla luciferase yields enhanced stability and light output*. Protein Eng Des Sel, 2006. **19**(9): p. 391-400.
71. Porterfield, W.B., et al., *A "Caged" Luciferin for Imaging Cell-Cell Contacts*. Journal of the American Chemical Society, 2015. **137**(27): p. 8656-8659.
72. Vorobyeva, A.G., et al., *Development of a Bioluminescent Nitroreductase Probe for Preclinical Imaging*. PloS one, 2015. **10**(6).
73. Kim, H.-S., et al., *In vivo imaging of hemoglobin and melanin variations using photoacoustic tomography*. Journal of Nuclear Medicine, 2015. **56**(supplement 3): p. 1206.
74. Krumholz, A., et al., *Multicontrast photoacoustic in vivo imaging using near-infrared fluorescent proteins*. Scientific reports, 2014. **4**.
75. Tjuvajev, J.G., et al., *Imaging Adenoviral-mediated Herpes Virus Thymidine Kinase Gene Transfer and Expression In Vivo*. Cancer Research, 1999. **59**(20): p. 5186-5193.

76. Bengel, F.M., et al., *Cardiac Positron Emission Tomography*. Journal of the American College of Cardiology, 2009. **54**(1): p. 1-15.
77. Collins, S.A., et al., *PET Imaging for Gene & Cell Therapy*. Curr Gene Ther, 2012. **12**(1): p. 20-32.
78. Soghomonyan, S.A., et al., *Positron emission tomography (PET) imaging of tumor-localized Salmonella expressing HSV1-TK*. Cancer Gene Therapy, 2004. **12**(1): p. 101-108.
79. Brader, P., et al., *Escherichia coli Nissle 1917 facilitates tumor detection by positron emission tomography and optical imaging*. Clinical Cancer Research, 2008. **14**(8): p. 2295-2302.
80. Waerzeggers, Y., et al., *Methods to monitor gene therapy with molecular imaging*. Methods, 2009. **48**(2): p. 146-160.
81. Waerzeggers, Y., et al., *Methods to monitor gene therapy with molecular imaging*. Methods, 2009. **48**(2): p. 146-60.
82. Weissleder, R. and U. Mahmood, *Molecular imaging*. Radiology, 2001. **219**(2): p. 316-33.
83. Benoit, M.R., et al., *Visualizing implanted tumors in mice with magnetic resonance imaging using magnetotactic bacteria*. Clin Cancer Res, 2009. **15**(16): p. 5170-7.
84. Gossuin, Y., R.N. Muller, and P. Gillis, *Relaxation induced by ferritin: a better understanding for an improved MRI iron quantification*. NMR Biomed, 2004. **17**(7): p. 427-32.
85. Hill, P.J., et al., *Magnetic resonance imaging of tumors colonized with bacterial ferritin-expressing Escherichia coli*. PLoS One, 2011. **6**(10): p. e25409.
86. Fujimori, M., *[Anaerobic bacteria as a gene delivery system for breast cancer therapy]*. Nippon Rinsho, 2008. **66**(6): p. 1211-8.
87. Zhou, S., M. Zhang, and J. Wang, *Tumor-targeted delivery of TAT-Apoptin fusion gene using Escherichia coli Nissle 1917 to colorectal cancer*. Med Hypotheses, 2011. **76**(4): p. 533-4.
88. Tangney, M., J.P. van Pijkeren, and C.G. Gahan, *The use of Listeria monocytogenes as a DNA delivery vector for cancer gene therapy*. Bioeng Bugs, 2010. **1**(4): p. 284-7.

89. Walther, W., et al., *Novel Clostridium perfringens enterotoxin suicide gene therapy for selective treatment of claudin-3- and -4-overexpressing tumors*. Gene Ther, 2011.
90. Theys, J., et al., *Clostridium as a tumor-specific delivery system of therapeutic proteins*. Cancer Detect Prev, 2001. **25**(6): p. 548-57.
91. Tangney, M., *Gene therapy for cancer: dairy bacteria as delivery vectors*. Discov Med, 2010. **10**(52): p. 195-200.
92. Minton, N.P., *Clostridia in cancer therapy*. Nat Rev Microbiol, 2003. **1**(3): p. 237-42.
93. Hall, S.S., *A commotion in the blood : life, death, and the immune system*. 1997, London: Little, Brown, 1998. xiv,544p., [8]p. of plates.
94. Heppner, F. and J.R. Mose, *The liquefaction (oncolysis) of malignant gliomas by a non pathogenic Clostridium*. Acta Neurochir (Wien), 1978. **42**(1-2): p. 123-5.
95. Roberts, N.J., et al., *Intratumoral injection of Clostridium novyi-NT spores induces antitumor responses*. Science Translational Medicine, 2014. **6**(249): p. 249ra111-249ra111.
96. Chorobik, P. and J. Marcinkiewicz, *Therapeutic vaccines based on genetically modified Salmonella: a novel strategy in cancer immunotherapy*. Pol Arch Med Wewn, 2011. **121**(12): p. 461-6.
97. Cunningham, C. and J. Nemunaitis, *A phase I trial of genetically modified Salmonella typhimurium expressing cytosine deaminase (TAPET-CD, VNP20029) administered by intratumoral injection in combination with 5-fluorocytosine for patients with advanced or metastatic cancer. Protocol no: CL-017. Version: April 9, 2001*. Hum Gene Ther, 2001. **12**(12): p. 1594-6.
98. Toso, J.F., et al., *Phase I study of the intravenous administration of attenuated Salmonella typhimurium to patients with metastatic melanoma*. J Clin Oncol, 2002. **20**(1): p. 142-52.
99. Morales, A., D. Eidinger, and A.W. Bruce, *Intracavitary Bacillus Calmette-Guerin in the treatment of superficial bladder tumors*. J Urol, 1976. **116**(2): p. 180-3.
100. Sylvester, R.J., *Bacillus Calmette-Guerin treatment of non-muscle invasive bladder cancer*. Int J Urol, 2011. **18**(2): p. 113-20.

101. Patyar, S., et al., *Bacteria in cancer therapy: a novel experimental strategy*. J Biomed Sci, 2010. **17**(1): p. 21.
102. Cronin, M., et al., *Progress in genomics, metabolism and biotechnology of bifidobacteria*. Int J Food Microbiol, 2011. **149**(1): p. 4-18.
103. Zhu, L.P., et al., *Therapeutic efficacy of Bifidobacterium longum-mediated human granulocyte colony-stimulating factor and/or endostatin combined with cyclophosphamide in mouse-transplanted tumors*. Cancer Sci, 2009. **100**(10): p. 1986-90.
104. Tang, W., et al., *A novel Bifidobacterium infantis-mediated TK/GCV suicide gene therapy system exhibits antitumor activity in a rat model of bladder cancer*. J Exp Clin Cancer Res, 2009. **28**: p. 155.
105. Brader, P., et al., *Escherichia coli Nissle 1917 facilitates tumor detection by positron emission tomography and optical imaging*. Clin Cancer Res, 2008. **14**(8): p. 2295-302.
106. Nemunaitis, J., et al., *Pilot trial of genetically modified, attenuated Salmonella expressing the E. coli cytosine deaminase gene in refractory cancer patients*. Cancer Gene Ther, 2003. **10**(10): p. 737-44.
107. Tangney, M., *Editorial: in vivo imaging & gene therapy*. Curr Gene Ther, 2012. **12**(1): p. 1.
108. Hollon, T., *Researchers and regulators reflect on first gene therapy death*. Nat Med, 2000. **6**(1): p. 6.
109. Bettegowda, C., et al., *Imaging bacterial infections with radiolabeled 1-(2'-deoxy-2'-fluoro-beta-D-arabinofuranosyl)-5-iodouracil*. Proc Natl Acad Sci U S A, 2005. **102**(4): p. 1145-50.
110. Davis, S.L., et al., *Bacterial thymidine kinase as a non-invasive imaging reporter for Mycobacterium tuberculosis in live animals*. PLoS One, 2009. **4**(7): p. e6297.
111. Kong, Y., et al., *Whole-body imaging of infection using bioluminescence*. Curr Protoc Microbiol, 2011. **Chapter 2**: p. Unit 2C 4.
112. Yao, H., M.K. So, and J. Rao, *A bioluminogenic substrate for in vivo imaging of beta-lactamase activity*. Angew Chem Int Ed Engl, 2007. **46**(37): p. 7031-4.

113. Bradford, P.A., et al., *SHV-7, a novel cefotaxime-hydrolyzing beta-lactamase, identified in Escherichia coli isolates from hospitalized nursing home patients*. Antimicrobial agents and chemotherapy, 1995. **39**(4): p. 899-905.
114. Bagshawe, K.D., *Antibody directed enzymes revive anti-cancer prodrugs concept*. Br J Cancer, 1987. **56**(5): p. 531-2.
115. Bagshawe, K.D., et al., *A cytotoxic agent can be generated selectively at cancer sites*. Br J Cancer, 1988. **58**(6): p. 700-3.
116. Bagshawe, K.D., *Antibody-directed enzyme/prodrug therapy (ADEPT)*. Biochem Soc Trans, 1990. **18**(5): p. 750-2.
117. Tietze, L.F. and K. Schmuck, *Prodrugs for targeted tumor therapies: recent developments in ADEPT, GDEPT and PMT*. Curr Pharm Des, 2011. **17**(32): p. 3527-47.
118. Francis, R.J., et al., *A phase I trial of antibody directed enzyme prodrug therapy (ADEPT) in patients with advanced colorectal carcinoma or other CEA producing tumours*. Br J Cancer, 2002. **87**(6): p. 600-7.
119. Lukashev, A.N., et al., *Late expression of nitroreductase in an oncolytic adenovirus sensitizes colon cancer cells to the prodrug CB1954*. Hum Gene Ther, 2005. **16**(12): p. 1473-83.
120. Schepelmann, S. and C.J. Springer, *Viral vectors for gene-directed enzyme prodrug therapy*. Curr Gene Ther, 2006. **6**(6): p. 647-70.
121. Tychopoulos, M., et al., *A virus-directed enzyme prodrug therapy (VDEPT) strategy for lung cancer using a CYP2B6/NADPH-cytochrome P450 reductase fusion protein*. Cancer Gene Ther, 2005. **12**(5): p. 497-508.
122. Schepelmann, S., et al., *Suicide gene therapy of human colon carcinoma xenografts using an armed oncolytic adenovirus expressing carboxypeptidase G2*. Cancer Res, 2007. **67**(10): p. 4949-55.
123. Patel, P., et al., *A phase I/II clinical trial in localized prostate cancer of an adenovirus expressing nitroreductase with CB1954 [correction of CB1984]*. Mol Ther, 2009. **17**(7): p. 1292-9.
124. Satchi-Fainaro, R., et al., *PDEPT: polymer-directed enzyme prodrug therapy. 2. HEMA copolymer-beta-lactamase and HEMA copolymer-C-Dox as a model combination*. Bioconjug Chem, 2003. **14**(4): p. 797-804.

125. Spooner, R.A., et al., *A novel vascular endothelial growth factor-directed therapy that selectively activates cytotoxic prodrugs*. Br J Cancer, 2003. **88**(10): p. 1622-30.
126. Knaggs, S., et al., *New prodrugs derived from 6-aminodopamine and 4-aminophenol as candidates for melanocyte-directed enzyme prodrug therapy (MDEPT)*. Org Biomol Chem, 2005. **3**(21): p. 4002-10.
127. Tietze, L.F., et al., *Duocarmycin-based prodrugs for cancer prodrug monotherapy*. Bioorg Med Chem, 2008. **16**(12): p. 6312-8.
128. Springer, C.J. and I. Niculescu-Duvaz, *Prodrug-activating systems in suicide gene therapy*. J Clin Invest, 2000. **105**(9): p. 1161-7.
129. Niculescu-Duvaz, I., et al., *Gene-directed enzyme prodrug therapy*. Bioconjug Chem, 1998. **9**(1): p. 4-22.
130. Moolten, F.L., *Tumor chemosensitivity conferred by inserted herpes thymidine kinase genes: paradigm for a prospective cancer control strategy*. Cancer Res, 1986. **46**(10): p. 5276-81.
131. Finzi, L., et al., *Improved retroviral suicide gene transfer in colon cancer cell lines after cell synchronization with methotrexate*. J Exp Clin Cancer Res, 2011. **30**: p. 92.
132. Abate-Daga, D., et al., *Oncolytic adenoviruses armed with thymidine kinase can be traced by PET imaging and show potent antitumoural effects by ganciclovir dosing*. PLoS One, 2011. **6**(10): p. e26142.
133. Suzuki, S., et al., *Liposome-mediated gene therapy using HSV-TK/ganciclovir under the control of human PSA promoter in prostate cancer cells*. Urol Int, 2001. **67**(3): p. 216-23.
134. Nuyts, S., et al., *Increasing specificity of anti-tumor therapy: cytotoxic protein delivery by non-pathogenic clostridia under regulation of radio-induced promoters*. Anticancer Res, 2001. **21**(2A): p. 857-61.
135. Theys, J., et al., *Specific targeting of cytosine deaminase to solid tumors by engineered Clostridium acetobutylicum*. Cancer Gene Ther, 2001. **8**(4): p. 294-7.
136. Liu, S.C., et al., *Anticancer efficacy of systemically delivered anaerobic bacteria as gene therapy vectors targeting tumor hypoxia/necrosis*. Gene Ther, 2002. **9**(4): p. 291-6.

137. Nakamura, T., et al., *Cloned cytosine deaminase gene expression of Bifidobacterium longum and application to enzyme/pro-drug therapy of hypoxic solid tumors*. Biosci Biotechnol Biochem, 2002. **66**(11): p. 2362-6.
138. Mei, S., et al., *Optimization of tumor-targeted gene delivery by engineered attenuated Salmonella typhimurium*. Anticancer Res, 2002. **22**(6A): p. 3261-6.
139. Hidaka, A., et al., *Exogenous cytosine deaminase gene expression in Bifidobacterium breve I-53-8w for tumor-targeting enzyme/prodrug therapy*. Biosci Biotechnol Biochem, 2007. **71**(12): p. 2921-6.
140. Sasaki, T., et al., *Genetically engineered Bifidobacterium longum for tumor-targeting enzyme-prodrug therapy of autochthonous mammary tumors in rats*. Cancer Sci, 2006. **97**(7): p. 649-57.
141. Yi, C., et al., *Antitumor effect of cytosine deaminase/5-fluorocytosine suicide gene therapy system mediated by Bifidobacterium infantis on melanoma*. Acta Pharmacol Sin, 2005. **26**(5): p. 629-34.
142. Mahan, S.D., et al., *Alanine-scanning mutagenesis reveals a cytosine deaminase mutant with altered substrate preference*. Biochemistry, 2004. **43**(28): p. 8957-64.
143. Hamaji, Y., et al., *Strong enhancement of recombinant cytosine deaminase activity in Bifidobacterium longum for tumor-targeting enzyme/prodrug therapy*. Biosci Biotechnol Biochem, 2007. **71**(4): p. 874-83.
144. King, I., et al., *Tumor-targeted salmonella expressing Cytosine deaminase as an anticancer agent*. Hum Gene Ther, 2002. **13**(10): p. 1225-33.
145. Dubois, L., et al., *Efficacy of gene therapy-delivered cytosine deaminase is determined by enzymatic activity but not expression*. Br J Cancer, 2007. **96**(5): p. 758-61.
146. Lehouritis, P., C. Springer, and M. Tangney, *Bacterial-directed enzyme prodrug therapy*. J Control Release, 2013. **170**(1): p. 120-31.
147. Huber, B.E., et al., *Metabolism of 5-fluorocytosine to 5-fluorouracil in human colorectal tumor cells transduced with the cytosine deaminase gene: significant antitumor effects when only a small percentage of tumor cells express cytosine deaminase*. Proc Natl Acad Sci U S A, 1994. **91**(17): p. 8302-6.

148. Marais, R., et al., *A cell surface tethered enzyme improves efficiency in gene-directed enzyme prodrug therapy*. Nat Biotechnol, 1997. **15**(13): p. 1373-7.
149. Loeffler, M., et al., *Inhibition of tumor growth using salmonella expressing Fas ligand*. J Natl Cancer Inst, 2008. **100**(15): p. 1113-6.
150. Royo, J.L., et al., *In vivo gene regulation in Salmonella spp. by a salicylate-dependent control circuit*. Nat Methods, 2007. **4**(11): p. 937-42.
151. Loessner, H., et al., *Drug-inducible remote control of gene expression by probiotic Escherichia coli Nissle 1917 in intestine, tumor and gall bladder of mice*. Microbes Infect, 2009. **11**(14-15): p. 1097-105.
152. Minton, N.P., et al., *Chemotherapeutic tumour targeting using clostridial spores*. FEMS Microbiol Rev, 1995. **17**(3): p. 357-64.
153. Liu, S.C., et al., *Optimized clostridium-directed enzyme prodrug therapy improves the antitumor activity of the novel DNA cross-linking agent PR-104*. Cancer Res, 2008. **68**(19): p. 7995-8003.
154. Min, J.J., et al., *Noninvasive real-time imaging of tumors and metastases using tumor-targeting light-emitting Escherichia coli*. Mol Imaging Biol, 2008. **10**(1): p. 54-61.
155. Galan, J.E., K. Nakayama, and R. Curtiss, 3rd, *Cloning and characterization of the asd gene of Salmonella typhimurium: use in stable maintenance of recombinant plasmids in Salmonella vaccine strains*. Gene, 1990. **94**(1): p. 29-35.
156. Friedlos, F., et al., *Attenuated Salmonella targets prodrug activating enzyme carboxypeptidase G2 to mouse melanoma and human breast and colon carcinomas for effective suicide gene therapy*. Clin Cancer Res, 2008. **14**(13): p. 4259-66.
157. Fu, W., et al., *Synergistic antitumor efficacy of suicide/ePNP gene and 6-methylpurine 2'-deoxyriboside via Salmonella against murine tumors*. Cancer Gene Ther, 2008. **15**(7): p. 474-84.
158. Singh, R. and A. Wallecha, *Cancer immunotherapy using recombinant Listeria monocytogenes: transition from bench to clinic*. Hum Vaccin, 2011. **7**(5): p. 497-505.
159. Paterson, Y., P.D. Guirnalda, and L.M. Wood, *Listeria and Salmonella bacterial vectors of tumor-associated antigens for cancer immunotherapy*. Semin Immunol, 2010. **22**(3): p. 183-9.

160. Stegman, L.D., et al., *Noninvasive quantitation of cytosine deaminase transgene expression in human tumor xenografts with in vivo magnetic resonance spectroscopy*. Proc Natl Acad Sci U S A, 1999. **96**(17): p. 9821-6.
161. Fox, M.E., et al., *Anaerobic bacteria as a delivery system for cancer gene therapy: in vitro activation of 5-fluorocytosine by genetically engineered clostridia*. Gene therapy, 1996. **3**(2): p. 173-178.
162. Fujimori, M., *Genetically engineered bifidobacterium as a drug delivery system for systemic therapy of metastatic breast cancer patients*. Breast Cancer, 2006. **13**(1): p. 27-31.
163. Shen, Y. and J. Nemunaitis, *Herpes simplex virus 1 (HSV-1) for cancer treatment*. Cancer Gene Ther, 2006. **13**(11): p. 975-92.
164. Pawelek, J.M., K.B. Low, and D. Bermudes, *Tumor-targeted Salmonella as a novel anticancer vector*. Cancer Res, 1997. **57**(20): p. 4537-44.
165. Massoud, T.F., A. Singh, and S.S. Gambhir, *Noninvasive molecular neuroimaging using reporter genes: part I, principles revisited*. AJNR Am J Neuroradiol, 2008. **29**(2): p. 229-34.

## **Chapter 2: Development of a novel probe-based strategy for *in vivo* imaging of non-GM bacteria.**

Sections from this chapter have been published as

Stanton, M., Cronin, M., Lehouritis, P., & Tangney, M. (2015). ***In Vivo Bacterial Imaging without Engineering; A Novel Probe-Based Strategy Facilitated by Endogenous Nitroreductase Enzymes.*** *Current gene therapy*, 15(3), 277-288.

## Abstract

The viability and usefulness of bacteria as vectors for gene therapy is becoming increasingly recognised. This is primarily due to a number of intrinsic properties of bacteria such as their ability to carry large genetic or protein loads, their tumour targeting capabilities and the availability of well-established genetic engineering tools for a range of common lab strains. However, a number of issues relating to the use of bacteria as vectors for gene therapy need to be addressed in order for the field to progress. Amongst these is the need for the development of non-invasive detection/imaging systems for bacteria within a living host. The ability to track bacteria within a live host over time provides researchers developing bacteria as gene delivery vehicles and other disciplines with an invaluable tool. *In vivo* optical imaging has advanced preclinical research greatly, and typically involves engineering of bacteria with genetic expression constructs for luminescence (e.g. the lux operon) or fluorescent proteins (GFP etc.). This requirement for genetic modification can be restrictive, where engineering is not experimentally appropriate or technologically feasible (e.g. due to lack of suitable engineering tools). This chapter describes a novel strategy exploiting endogenous bacterial enzymatic activity to specifically activate an exogenously administered fluorescent imaging probe. The red shifted, quenched fluorophore CytoCy5S is reduced to a fluorescent form by bacterial-specific nitroreductase (NTR) enzymes. NTR enzymes are present in a wide range of bacterial genera and absent in mammalian systems, permitting highly specific detection of Gram-negative and Gram-positive bacteria *in vivo*. In this study, dose-responsive bacterial-specific signals were observed *in vitro* from all genera examined – *E. coli*, *Salmonella*, *Listeria*, *Bifidobacterium* and *Clostridium*

*difficile*. Examination of an NTR knockout (NTR KO) strain validated the enzyme specificity of the probe. *In vivo* whole-body imaging permitted specific, dose-responsive monitoring of bacteria over time in various infection models, and no toxicity to bacteria or host was observed. This study demonstrates the concept of exploiting innate NTR activity as a reporting strategy for wild-type bacteria using optical imaging, while the concept may also be extended to NTR-specific probes for use with other imaging modalities.

## Study Aim

The aim of this study was to develop a novel imaging strategy for the *in vivo* detection of non-genetically modified (GM) bacteria. Nitroreductases are a family of enzymes found in bacteria that are not present in mammalian cells and hence may be capable of the bacteria targeted reduction of the quenched fluorophore CytoCy5s leading to the emission of an imageable fluorescent signal *in vivo*. This fluorescent signal may then be used to detect the localization of non-GM bacteria within a live host.

## Introduction

Bacteria represent an attractive and viable alternative to viruses as gene therapy vectors. Bacteria are capable of carrying large genetic or protein loads and also possess a reservoir of enzymes and proteins that are not found in mammalian cells or tissue. These bacteria specific products can be exploited to confine activation of imaging probes or prodrugs to bacteria infected tissue and hence minimise off-target effects. GMP has been established for bacteria and the availability of invasive and non-invasive strains allows researchers to choose whether a payload is delivered externally or internally to target cells. This work aims to develop a non-invasive imaging system for the detection of live bacteria within a host in a number of infection settings. This system can be used to monitor multiple forms of bacteria such as Gram-positive and Gram-negative strains as well as invasive and commensal bacteria. The development of such a system is of interest and importance to the field of bacterial gene therapy as a whole but also to researchers from a number of other fields such as infectious disease and cancer.

The benefits provided to researchers in translational fields by the increasing availability of preclinical imaging technologies are multi-fold [1] [2], while at a clinical level, the European Centre for Disease Prevention and Control and the European Medicines Agency have recently highlighted the critical need to develop novel screening techniques and methods for the early detection of infectious diseases [3]. The accessibility of multiple preclinical imaging modalities such as micro Positron Emission Tomography ( $\mu$ PET), micro Magnetic Resonance Imaging ( $\mu$ MRI) and Optical Imaging (OI) has led to the development of an ever increasing array of probes and reporter systems to facilitate non-invasive imaging *in vivo* [4]. Preclinical imaging systems allow for longitudinal studies of small animals and

contribute to a considerable reduction in the number of animals required for studies. Optical imaging has become the most utilised preclinical *in vivo* imaging modality in academic and industrial research laboratories due to its relative cost-effectiveness, ease of use, and high-throughput potential [5] [6, 7].

Optical imaging is a non-invasive imaging technique that relies on the detection of either native light emitted by a molecule or of light emitted from a molecule following excitation by an exogenous light source such as a laser. The emitted light can be detected and quantified using specialised software. Optical imaging of bacterial luminescence afforded by the *lux* operon is currently the mainstay of preclinical *in vivo* imaging in this space. The *luxCDABE* operon isolated from *Vibrio harveyi* and other species has facilitated the generation of bioluminescent strains in different bacterial genera [8]. However, the degree of genetic tractability of a given bacterial strain limits its use, due to the large size of the operon (approaching 6 Kb) and the requirement for stably integrated constructs, ideally, to permit accurate longitudinal monitoring. Furthermore, light emission from *lux* varies dramatically between species due to variations in co-factor availability (FMNH<sub>2</sub> and molecular oxygen) [9], in addition to the level of expression afforded by different gene-expression systems (copy number and promoter variables). Eukaryotic luminescence genes have also been introduced to certain bacteria in an attempt to overcome such problems, such as beetle luciferases [10, 11]. Strains have also been engineered to express fluorescent proteins [12]. While genetic engineering tools for bacterial strains which are traditionally difficult to engineer are becoming available for some species, highly sophisticated technology permitting genomic integration of large heterologous sequences such as the *lux* operon are still unavailable for many species of interest. Furthermore, it is frequently not feasible to

engineer strains in studies involving mixed or undefined populations of bacteria (microbiome research etc.).

If the full potential of bacteria as vectors for gene therapy is to be exploited it is imperative that advances in the field of preclinical imaging are achieved to not only improve the technology and systems available, but also to develop novel imaging modalities and preclinical imaging systems that can be used to image un-engineered bacteria *in vivo*. Interest in the development of targeted or activatable probes in recent years has strongly contributed to many of the main advancements in preclinical imaging [13]. Since 2008, bacterial probes based on bis-dipicolylamine-Zinc(II) binding to bacterial anionic surfaces have been described, but these probes have not entered widespread use [14-16]. A novel fluorescent bacterial-specific probe has recently been described [17]. This strategy utilises a fluorescently-labelled sugar, maltodextrin, which specifically accumulates within bacteria, enabling focusing of the fluorescent signal following systemic administration of probe. It was hypothesised that exploitation of enzymatic activity unique to bacteria would permit identification of suitable substrate chemistry and therefore the downstream development of a wider range of probes. Endogenous bacterial enzymes that catalyse potentially suitable reactions have been described as evidenced by *in vitro* terminal assays [18], but to date, very few have been exploited with substrates for *in vivo* imaging. Kong *et. al* [19] have elegantly demonstrated the potential for use of endogenous bacterial enzymes for *in vivo* imaging of *Mycobacterium tuberculosis* infection with a system that exploits the intrinsic  $\beta$ -lactamase activity of *M. tuberculosis* to activate a  $\beta$ -lactam ring-containing fluorescent probe. However, expression of  $\beta$ -lactamases is confined to certain bacteria and the variety of  $\beta$ -lactamases found in Gram-positive and Gram-negative bacteria (reviewed in [20])

could make the production of a universally applicable probe for imaging of  $\beta$ -lactamase activity a difficult task. Therefore, the need to develop an imaging system based on probe activation by a widely expressed, endogenous bacterial enzyme that is not produced by mammalian cells still exists.

Nitroreductases are a family of bacterial enzymes that share the ability to reduce nitro functional groups and may be categorised as oxygen insensitive (type I) or oxygen sensitive (type II), and are widespread across the bacterial kingdom[21]. Nitroreductases are generally regarded as being unique to bacteria, (although have been described in species such as certain parasites), and therefore, their use for explicit reduction of NTR activatable drugs and imaging probes presents a highly viable method for targeted *in vivo* drug or probe activation. Isolation of NTR genes (in particular the *E. coli nfsB* gene) and engineering of gene delivery vectors (viruses) has permitted highly specific cancer therapeutic strategies—Gene Directed Enzyme Prodrug Therapy (GDEPT) [22]. In this context, NTR-based imaging probes have been under investigation as eukaryotic reporters [23] [24]. The cell permeable, quenched fluorophore CytoCy5S is a red-shifted cyanine fluorophore that is reduced to its fluorescent form by nitroreductase (NTR) enzymes. Recently, CytoCy5S has been demonstrated to be an effective reporter in eukaryotic settings, in the context of cancer cell lines and a virus engineered to express *nfsB*, and has been shown to be non-toxic to mammalian cells [25, 26]. We hypothesised that endogenous production of nitroreductases by bacteria might permit imaging of viable bacteria through reduction of CytoCy5S. By harnessing the intrinsic ability of bacteria to activate this near infra-red probe, the localisation of bacteria *in vivo* can be quickly and easily visualised by non-invasive optical imaging, and represents a novel *in vivo* bacterial imaging strategy, for a wide range of bacteria.

## Materials and methods

**Bacterial strains.** Bacterial cultures used for each experiment were in the late log growth phase unless otherwise stated. *E. coli* K-12 MG1655 containing the integrated p16*SluxABCDE* was grown aerobically at 37°C in LB medium containing 300 µg ml<sup>-1</sup> erythromycin (Em). The NTR KO strain, *E. coli* K-12 AB502NemA[27] and its parent strain AB1157 were a kind gift from Dr Antonio Valle (University of Cádiz, Cádiz, Spain) and were cultured at 37°C in LB medium supplemented with 20 µg ml<sup>-1</sup> streptomycin (AB1157) or 50 µg ml<sup>-1</sup> Kanamycin (AB502NemA). *Salmonella enterica* Typhimurium UK-1 containing the integrated p16*SluxABCDE* cassette was cultured aerobically at 37°C in LB medium supplemented with 300 µg ml<sup>-1</sup> Em. For anaerobic growth of *Bifidobacterium breve* and *infantis* 35624 and *Clostridium difficile* TL176 ribotype R014[28], bacteria were grown in static culture conditions in RCM medium (Oxoid) and in an anaerobic culture incubator (Don Whitley Scientific). *Lactococcus lactis* subspec. *cremoris* MG1363 was grown at 30°C in M17 medium (Oxoid) supplemented with 1% (w/v) glucose. *Listeria monocytogenes* EGD-e was cultured at 37°C in Brain Heart Infusion medium (Oxoid). For *in vitro* experiments wells contained 10<sup>7</sup> bacteria unless otherwise stated.

**Detection of NfsB by western blotting.** Bacteria in log growth phase were pelleted by centrifugation (3,000g for 15 min) and the pellets were frozen at -70°C overnight. Pellets were resuspended in lysis buffer (25mM Tris-Cl, 2mM EDTA, 15mg/mL<sup>-1</sup> lysozyme) at 37°C for 1 h before being briefly sonicated on ice. A Bradford assay standard curve was used to determine the protein concentration of total cell lysates. Equal levels of total protein were loaded in each lane of the gel. Proteins were

separated using the Novex NuPAGE SDS-PAGE Gel System (Invitrogen) and electroblotted onto PDVF membranes. Membranes were blocked using Odyssey blocking buffer (LI-COR) and probed with a polyclonal antibody to NfsB diluted 1:1000. Immune complexes were detected using an Odyssey infrared scanner (LI-COR).

***Animals and tumour induction.*** 6-8 week old female BALB/c mice weighing approximately 18-20 grams were kept as previously described [29]. For tumour induction, a 200  $\mu$ l suspension of  $5 \times 10^4$  4T1 cells in serum free Dulbecco's Modified Eagle's Medium (DMEM) culture medium or  $2 \times 10^5$  CT26 cells were injected subcutaneously into the flank of BALB/c mice. The viability of inoculated cells was determined using the Nucleocounter system (ChemoMetec). Tumour growth was monitored twice weekly and mice were randomly assigned to groups when the tumours reached approximately 100 mm<sup>3</sup> in volume as determined by caliper measurement.

***Ethics statement.*** All murine experiments were approved by the animal ethics committee of University College Cork (AERR #2010/003 and #2012/015).

***Bacterial administration to mice.*** Bacteria were grown overnight as described above. These bacteria were used to inoculate fresh growth medium containing the relevant antibiotic and allowed to grow until reaching OD<sub>600</sub> 0.6. Cultures were harvested by centrifugation (4000 x g for 10 min) and washed three times in phosphate buffered saline (PBS) before resuspension in one-tenth volume PBS. For tumour colonisation studies  $10^6$  bacteria were injected via the lateral tail vein (*E.*

*coli*) 1 week before imaging [30] or intratumourally (*B.breve*) 3 days before imaging . Mice used for intramuscular bacteria studies received a 50 µl injection of bacteria directly into the rear right or left quadriceps. These mice received  $10^7$  bacteria via intramuscular injection unless otherwise stated. For infection studies with *S. Typhimurium* UK-1, mice were injected via the tail vein with  $10^4$  bacteria and were monitored for progression of infection and localisation of bacteria within the liver and spleen before CytoCy5S administration.

***Bacterial recovery from mice.*** Following *in vivo* fluorescence imaging, tumours were resected aseptically and the tissue was homogenised by pushing through a 70 µm pore nylon filter into sterile PBS. The resultant cell suspension was then plated on selective agar following serial dilution in sterile PBS.

***Preparation of CytoCy5S.*** The fluorogenic, red-shifted substrate CytoCy5S (GE Healthcare) (excitation 628 nm/emission 638 nm) was dissolved in dimethyl sulfoxide to prepare a 1 mg/ml stock solution that was further diluted in PBS to a final working concentration of 10 µg/ml. Mice were injected with 100 ng CytoCy5S in a volume of 200 µl before *in vivo* imaging unless otherwise stated.

***Image acquisition and formation.*** *In vivo* bioluminescence and fluorescence imaging was carried out using the IVIS100 or IVIS Lumina II system (Perkin Elmer). At defined timepoints following injection of CytoCy5S mice were imaged for bioluminescence and regions of interest were quantified using LivingImage 3.2 or 4.3.1 software. For fluorescent image acquisition, mice were imaged for

excitation/emission 640 nm/660 nm. Representative images of mice show a randomly selected mouse from each group (minimum of n=3 in all cases).

***Effect of CytoCy5S on bacterial viability assay.*** *E. coli* K-12 MG1655 and *E. coli* K-12 AB502NemA were cultured aerobically and anaerobically overnight as described. Bacteria were then subcultured and divided into three groups (untreated, CytoCy5S treated and DMSO/PBS treated) in triplicate in fresh medium and grown until cultures reached OD<sub>600</sub> of 0.2. At this point, the CytoCy5S treated group was administered 100 ng CytoCy5S in an injection volume of 200 µl. The DMSO/PBS group received equal quantities of the diluent without CytoCy5S. At hourly timepoints, all cultures were subjected to serial dilution before plating on selective agar to determine cfu/ml values. Cultures were also tested for changes in OD<sub>600</sub> readings as well as bioluminescence and fluorescence.

***Conversion of CytoCy5S by intracellular L. welshimeri.*** RAW 264.7 cells were grown in 6 well plates until a monolayer of cells was formed. Cells were washed twice in DMEM before incubation with *L. welshimeri* (suspended in DMEM) at a multiplicity of infection of 1000:1 for 2 hours. Cells and bacteria were coincubated at 37°C. Following coincubation, the media was removed and the monolayer was washed twice with DMEM. Media containing 1% pen/strep antibiotics was then added to each well to kill extracellular bacteria. This incubation step was allowed to proceed for 1.5 h before the cell monolayer was washed and trypsinised. The resultant cell suspension was transferred to 1.5 ml tubes before imaging for fluorescence.

***Imaging of intramuscular bacteria using CytoCy5S as a fluorescent probe.***

BALB/c mice were anaesthetised and the fur on the rear limbs was removed. Mice were injected directly into the right quadriceps muscles at a depth of approximately 5 mm with 50  $\mu$ l of bacteria suspended in PBS. The number of bacteria injected ranged from  $5 \times 10^2$  to  $5 \times 10^7$ . Mice also received an intramuscular injection of 50  $\mu$ l sterile PBS in the left rear quadriceps. 1 h after bacterial injection, mice received an IP injection of 100 ng CytoCy5S. Mice were imaged for bioluminescence and fluorescence at regular intervals beginning immediately after probe injection.

***In vivo tracking of S. Typhimurium infection.*** BALB/c mice received an IV injection of  $10^4$  luminescent *Salmonella enterica* Typhimurium UK-1 suspended in PBS. Progression of infection was tracked by BLI until bacteria were localised to the liver and spleen approximately 3 days post bacteria injection. Mice then received an IP injection of CytoCy5S followed by fluorescence imaging 90 min post probe injection. Mice were culled and the livers and spleens removed for *ex vivo* luminescence and fluorescence imaging before homogenisation of the tissue to allow for creation of a single cell suspension and plating on selective agar to determine the presence and number of bacteria in each of the resected organs.

***Non-invasive imaging of tumour colonising bacteria.*** BALB/c mice bearing subcutaneous 4T1 or CT26 flank tumours were injected with bacteria intravenously (*E. coli*) or intratumourally (*B. breve*). Following tumour colonisation by bacteria (1 week post injection for *E. coli* or 3 days post injection for *B. breve*) mice received an intraperitoneal injection of CytoCy5S and were imaged for fluorescence at regular timepoints thereafter.

***Statistical analysis.*** All statistical analysis was carried out using GraphPad Prism® 5.0. Statistical differences were determined using a Two-tailed Student's t-test, Mann Whitney test or Two-way ANOVA with Bonferroni post-test where applicable. Statistical significance was defined at the 5% level.

## Results

### ***In vitro* monitoring of CytoCy5S activation by bacteria**

Bacteria were incubated with 50 ng of CytoCy5S (per well) *in vitro* and were IVIS imaged for fluorescence. A fluorescent signal that exceeded autofluorescence was evident in wells containing *E. coli* MG1655 (MG1655), *Salmonella enterica* Typhimurium UK-1, *Lactococcus lactis* MG1363 and *Listeria monocytogenes* EGD-e, *Clostridium difficile* and *Bifidobacterium infantis* 35624 immediately after probe addition (Figure 2). The signal increased over time and was maintained for over 2.5 h.

As can be seen in Figures 3a and 3b, the level of fluorescent signal obtained following probe incubation with bacteria is dependent on the number of bacteria per well as well as the concentration of CytoCy5S. CytoCy5S activation by MG1655 bacteria reaches saturation at 50 ng/ml of the probe (Figure 3b). Macrophage engulfed *L. welshimeri* have also been shown (Figure 4) to be capable of probe activation *in vitro*. Fluorescence from CytoCy5S activated by RAW 264.7 engulfed *L. welshimeri* was seen to be significantly (Student's t-test,  $p < 0.05$ ) greater than autofluorescence from probe alone or from RAW 264.7 cells coincubated with CytoCy5S in the absence of bacteria.

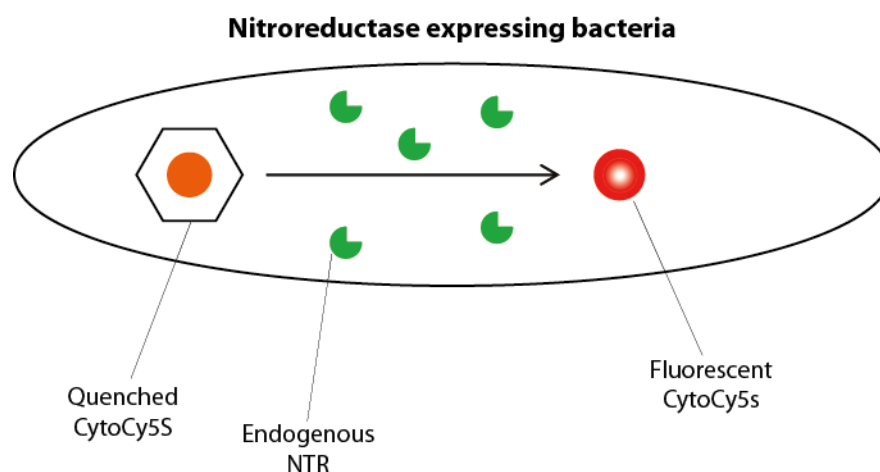


**Figure 1. Schematic representation of CytoCy5S reduction by bacterial nitroreductases.** The cell permeable, quenched fluorophore, CytoCy5S, enters bacteria cells where nitroreductase enzymes reduce the probe. Reduction leads to unquenching and a fluorescent signal is emitted from the probe upon excitation with an appropriate laser. The fluorescent probe is cell trapped and accumulates within bacteria.

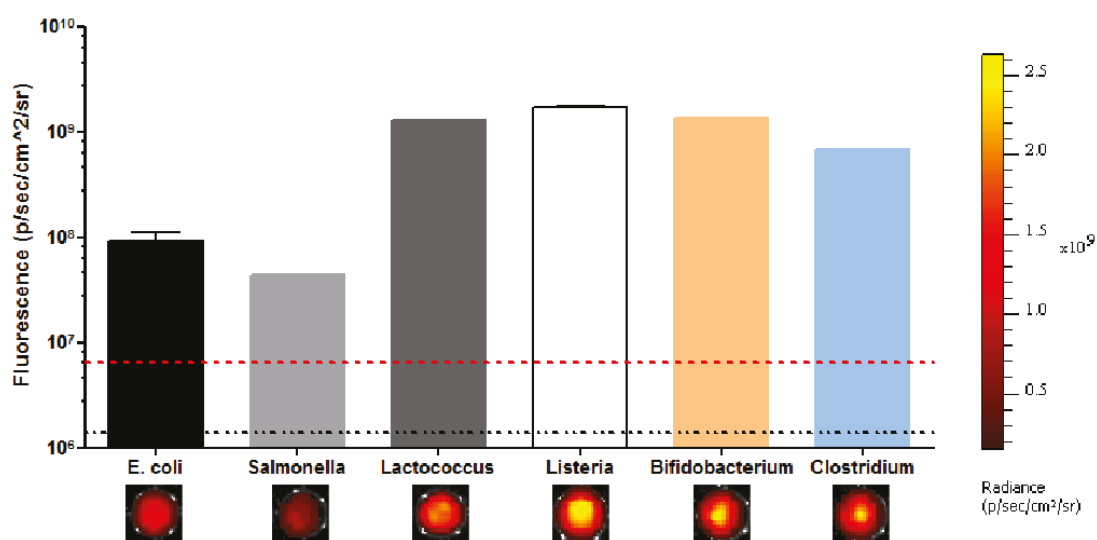


**Figure 2. *In vitro* analysis of CytoCy5S activation by bacteria.** Bar graph showing the change in fluorescence for a panel of bacteria 1 h post incubation with 50 ng/well CytoCy5S. Although a robust fluorescent signal is obtained following probe activation by all strains tested the level of activation varies between strains. No significant difference in fluorescence was observed between strains ( $p > 0.05$ ). The dotted red line represents fluorescence from probe in PBS and the dotted black line shows fluorescence from bacteria alone.  $n=3$  in all cases. Error bars represent SD.

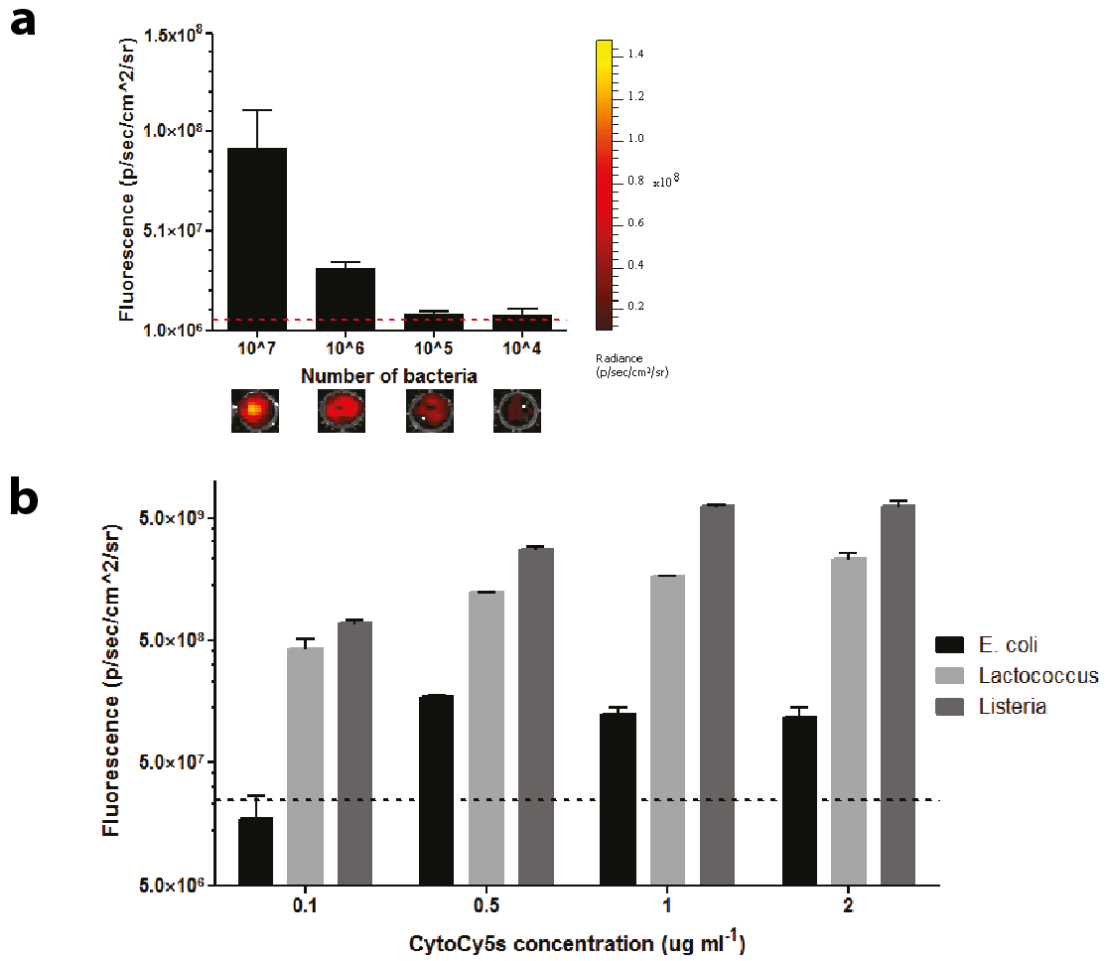


**Figure 3. Determination of the effect of bacterial cell numbers and CytoCy5S concentration on *in vitro* fluorescence.** a) Fluorescence from activated CytoCy5S increases with the number of *E. coli* MG1655 per well. The dotted line represents fluorescence from probe alone. b) Incubation of representative Gram-positive and Gram-negative bacteria with concentrations of CytoCy5S ranging from 10 ng/ml to 2 µg/ml. *E. coli* = MG1655, *Lactococcus* = *lactis* and *Listeria* = *welshimeri*. The dotted line represents fluorescence from probe alone. Error bars represent SD. n=3 in all cases.

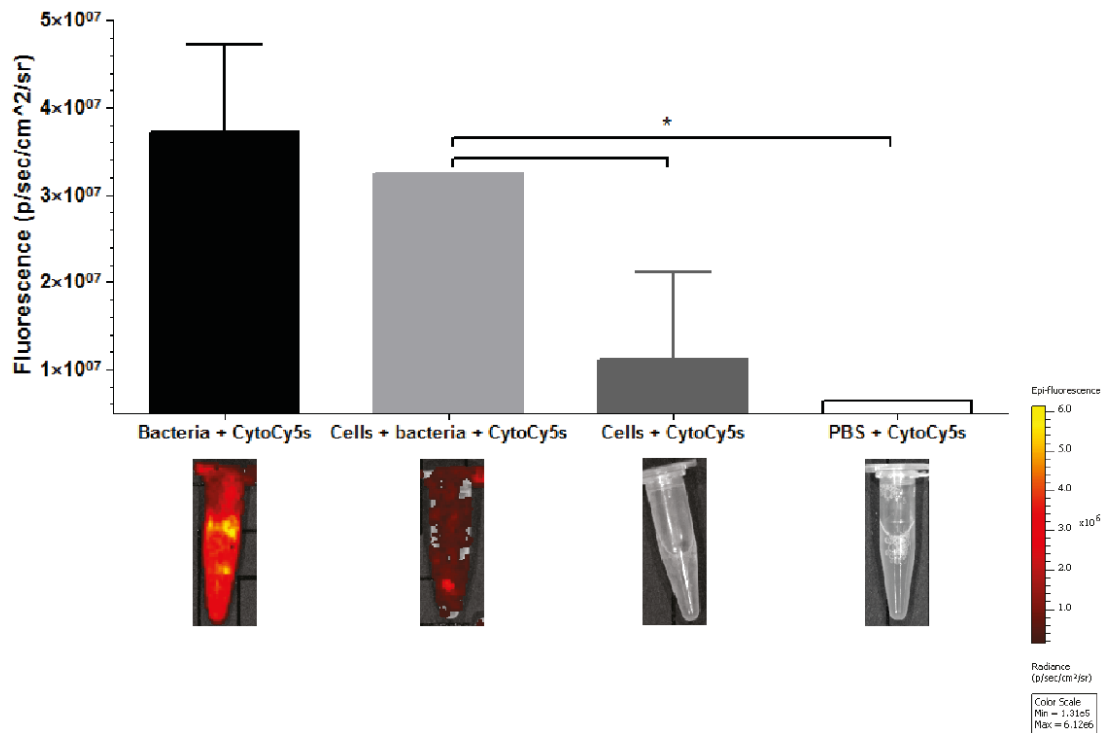


**Figure 4. *In vitro* CytoCy5S activation in by RAW 264.7 engulfed bacteria.** RAW 264.7 cell engulfed *L.welshimeri* are capable of activating CytoCy5S. Probe activation as determined by fluorescence is significantly greater than that seen when RAW 264.7 cells are coincubated with CytoCy5S in the absence of bacteria ( $p < 0.05$ ).  $n = 3$  in all cases. The dotted black line represents fluorescence from probe in PBS. Error bars represent standard deviation (SD).

### **NfsB nitroreductase activity is primarily responsible for CytoCy5S activation.**

Western blot analysis of NfsB expression levels in *E. coli* revealed that the protein is differentially expressed between strains (Figure 5a) . High levels of NfsB expression were observed in the *E. coli* AB1157 strain when compared with the NTR KO strain *E. coli* AB502NemA which is a derivative of AB1157 that has had *nfsB* knocked out as well as two of the other most enzymatically active *E. coli* nitroreductases (*nfsA*, *nemA*) [31, 32]. NfsB expression was rescued following transformation of bacteria with a plasmid expressing *nfsB* (Figure 5a). An increase in NfsB expression following pNfsB transformation was seen to correlate with an increase in fluorescence from bacteria incubated with CytoCy5S (Figure 5b). Although the fluorescent signal at 1 h from AB502NemA is significantly ( $P < 0.001$ ) less than AB1157 expressing the full NTR complement, a signal is still evident, indicating that multiple NTRs (other than NfsA, NfsB and NemA) are capable of CytoCy5S activation.

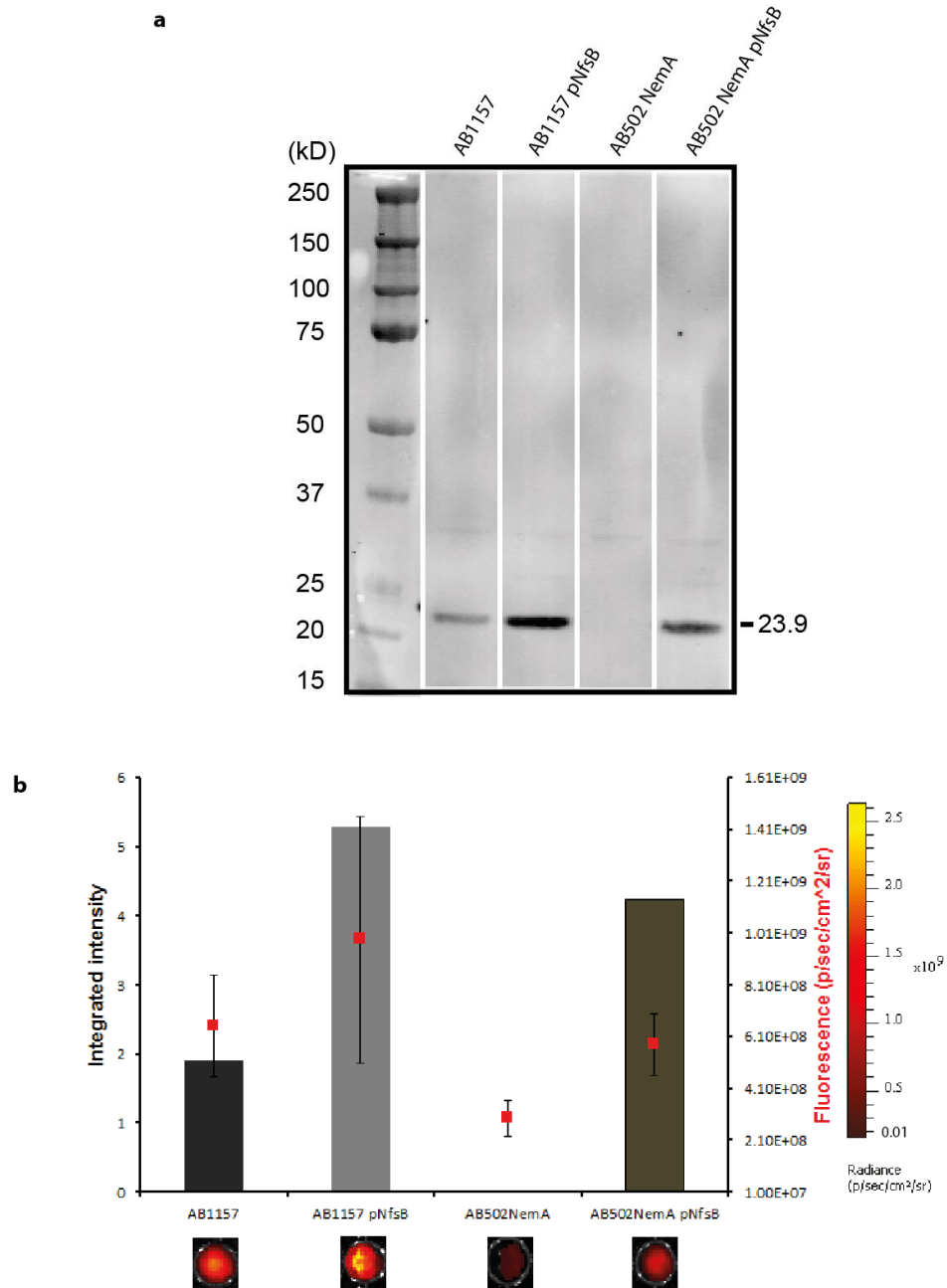


**Figure 5. Analysis of NfsB expression levels in *E. coli* and the effect of nitroreductase gene knockout on CytoCy5S activation.** a) Western blot of protein extracts from *E. coli* AB1157 and AB502NemA +/- pTrc NfsB probed with an anti-NfsB antibody. The band representing the NfsB protein is seen at 23.9 kDa. b) Graph showing the integrated intensities of bands from a western blot of protein extracts from *E. coli* AB1157 and AB502NemA +/- pTrc NfsB, probed with an anti-NfsB antibody (primary Y axis/bars). Fluorescence from live bacteria 1 h post incubation with CytoCy5S is represented on the secondary Y axis (red dots). Although the fluorescent signal from AB502NemA is significantly ( $P < 0.0001$ , Student's t-test) less than AB1157 expressing the full NTR complement, a signal is still evident, indicating that multiple NTRs (other than NfsA, NfsB and Nema) are capable of CytoCy5S activation. Error bars represent SEM.

### **The effect of CytoCy5S on bacterial cell viability *in vitro* and *in vivo*.**

As can be seen in Figure 6, coincubation of the probe with bacteria *in vitro* for a period of 7.5 h did not significantly affect the viability of bacterial cells. Similarly, no significant toxicity to bacteria was observed *in vivo* (Figure 6b) where bioluminescence from muscle localised *lux* tagged bacteria was used as a readout for bacterial cell viability. The decrease in luminescence that occurred over 72 hours in the untreated group was mirrored by the CytoCy5S treated group.

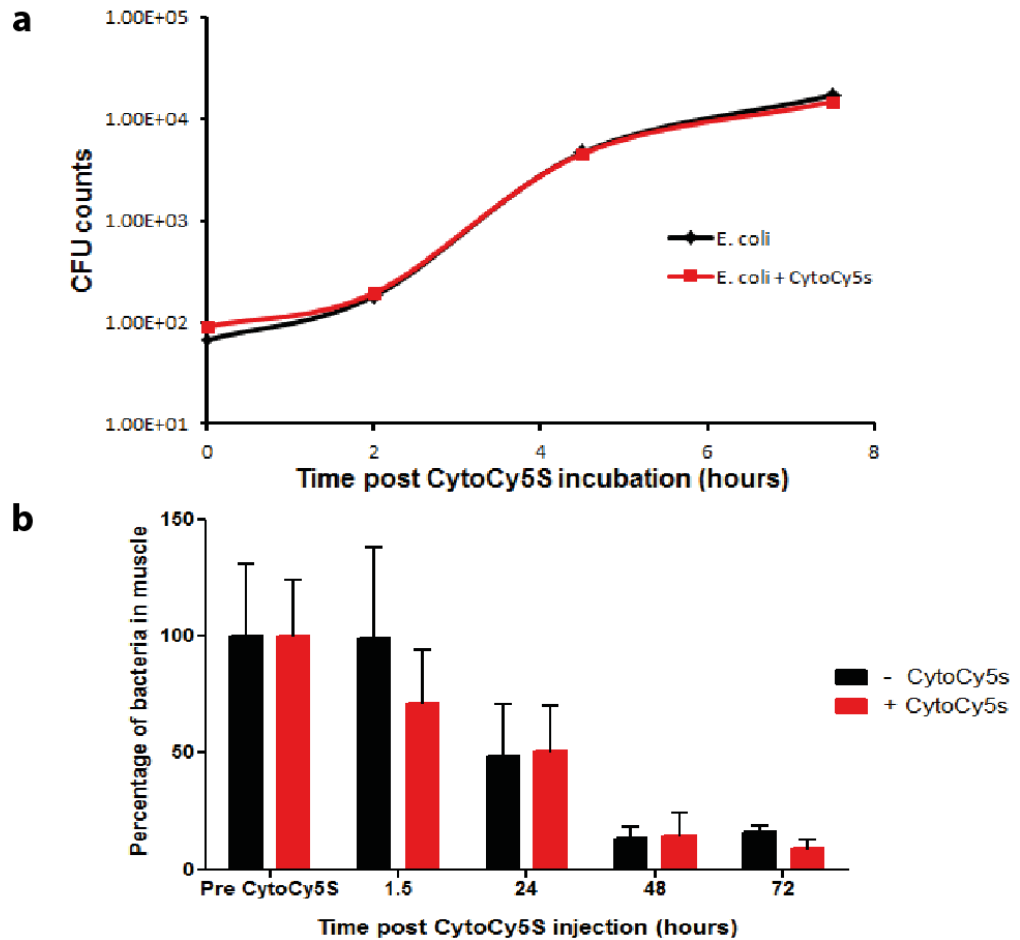


**Figure 6. Analysis of the effect of CytoCy5S on bacterial viability *in vitro* and *in vivo*.** a) *E. coli* MG1655 bacterial cultures were coincubated with 500 ng ml<sup>-1</sup> CytoCy5S at 37°C. At hourly timepoints aliquots from cultures (+/- CytoCy5S) were plated on selective agar and the resultant colony forming unit (cfu) counts were compared with untreated bacterial cultures. b) The effect of CytoCy5S on bacteria *in vivo* was assessed via correlation with luminescence from muscle bearing luminescent *E. coli* MG1655. Luminescence from infected muscle before injection of the fluorescent probe is represented as 100% (of bacteria in muscle) and changes in luminescence following probe injection are represented as a change in percentage. No significant difference (Student's t-test) in luminescence between mice that received CytoCy5S and mice that received PBS was observed at any timepoint tested. n=3 mice per group. Error bars represent SD for panel a and SEM for panel b.

### **Route of CytoCy5S administration for *in vivo* experiments.**

In order to determine the optimal route of probe administration, fluorescence from *E. coli* colonised 4T1 flank tumours was quantified following either intravenous (IV) or intraperitoneal (IP) injection of 100 ng CytoCy5S (Figure 7). Regions of interest (ROI) drawn around the tumours were used to determine the level of fluorescence from the tumour at various timepoints following CytoCy5S administration. Over the duration of the experiment there was no significant difference ( $p>0.05$ ) between the IV and IP groups. With this in mind it was determined that IP probe administration, which resulted in the highest level of fluorescence at each timepoint tested, is the optimal route of administration. IP injection is not only technically much easier than IV but also allows for repeated injections on a single day as opposed to IV where repeated injection in the tail vein would prove extremely difficult.

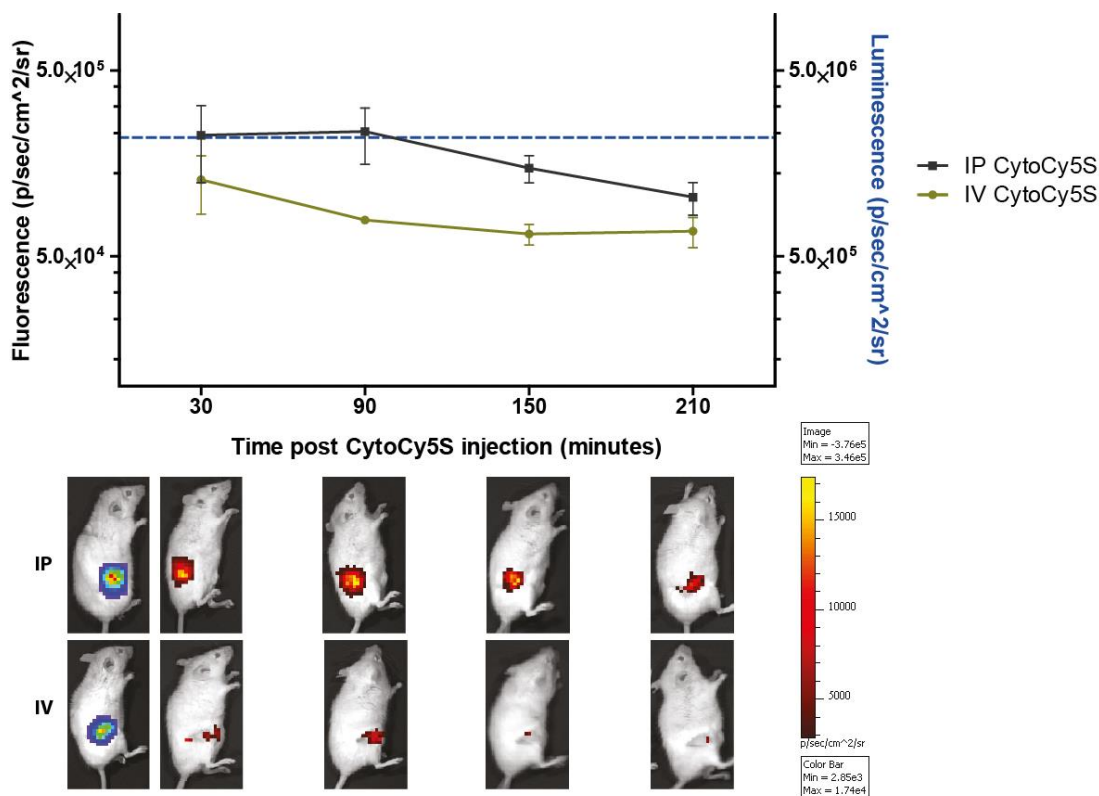


**Figure 7. Evaluation of intravenous versus intraperitoneal routes of administration of CytoCy5S for fluorescent imaging of tumour localised *E. coli*.** BALB/c mice bearing subcutaneous 4T1 flank tumours were colonised by luminescent *E. coli* MG1655. Following tumour colonisation mice received a 100 ng injection of CytoCy5S either via IP or IV administration. Mice were imaged for fluorescence at regular intervals post probe administration. No significant difference in fluorescence was observed between IV and IP groups ( $p>0.05$ ).  $n=3$  for both groups. Pictures of mice shown below the graphs are randomly selected representative images for each group. Error bars represent SEM. The dotted blue line represents the average luminescence value from mice across the course of the experiment.

### ***In vivo* fluorescence from bacterial activated CytoCy5S reflects bacterial numbers**

The utility of CytoCy5S for *in vivo* bacterial imaging was examined in various mouse models. BALB/c mice were directly injected in the quadriceps with escalating numbers of *E. coli* MG1655 or PBS. Mice received  $5 \times 10^2$ ,  $5 \times 10^4$ ,  $5 \times 10^6$  or  $5 \times 10^7$  bacteria before IP injection of 100 ng CytoCy5S. Use of *lux*-tagged bacterial cells permitted correlation with bacterial location, quantity and viability [29]. Luminescence imaging of mice showed that viable bacteria remained within the muscle tissue over time. The location of the fluorescent signal (corresponding to CytoCy5S) overlapped with the location of bacteria within the tissue as determined by luminescence (corresponding to *lux* luminescence from the same bacteria) (Figure 8a). A bacterial dose response was evident, and while the level of fluorescence from muscle bearing  $5 \times 10^2$  and  $5 \times 10^4$  bacteria was below the detection limit, strong and sustained fluorescence was observed from muscle bearing  $5 \times 10^6$  and  $5 \times 10^7$  bacteria (Figure 8a). IP injection of CytoCy5S showed no significant improvement on bacteria mediated fluorescence over IV (Figure 7), and hence IP administration was utilised in subsequent experiments for logistical reasons.

A probe dose response was also observed (Figure 8b). Fluorescence saturation *in vivo* was achieved at a probe dose of 100 ng and was maintained at equal levels to that measured from mice that received 150 ng of the probe at 24 h post probe injection. The fluorescent signal was maintained for over 72 h in mice that received  $5 \times 10^7$  bacteria plus CytoCy5S, with a peak fluorescent signal at 1 h post probe injection (Figure 8c). Mice that received an intramuscular injection of PBS instead of bacteria showed no fluorescence or bioluminescence from the hind limbs.

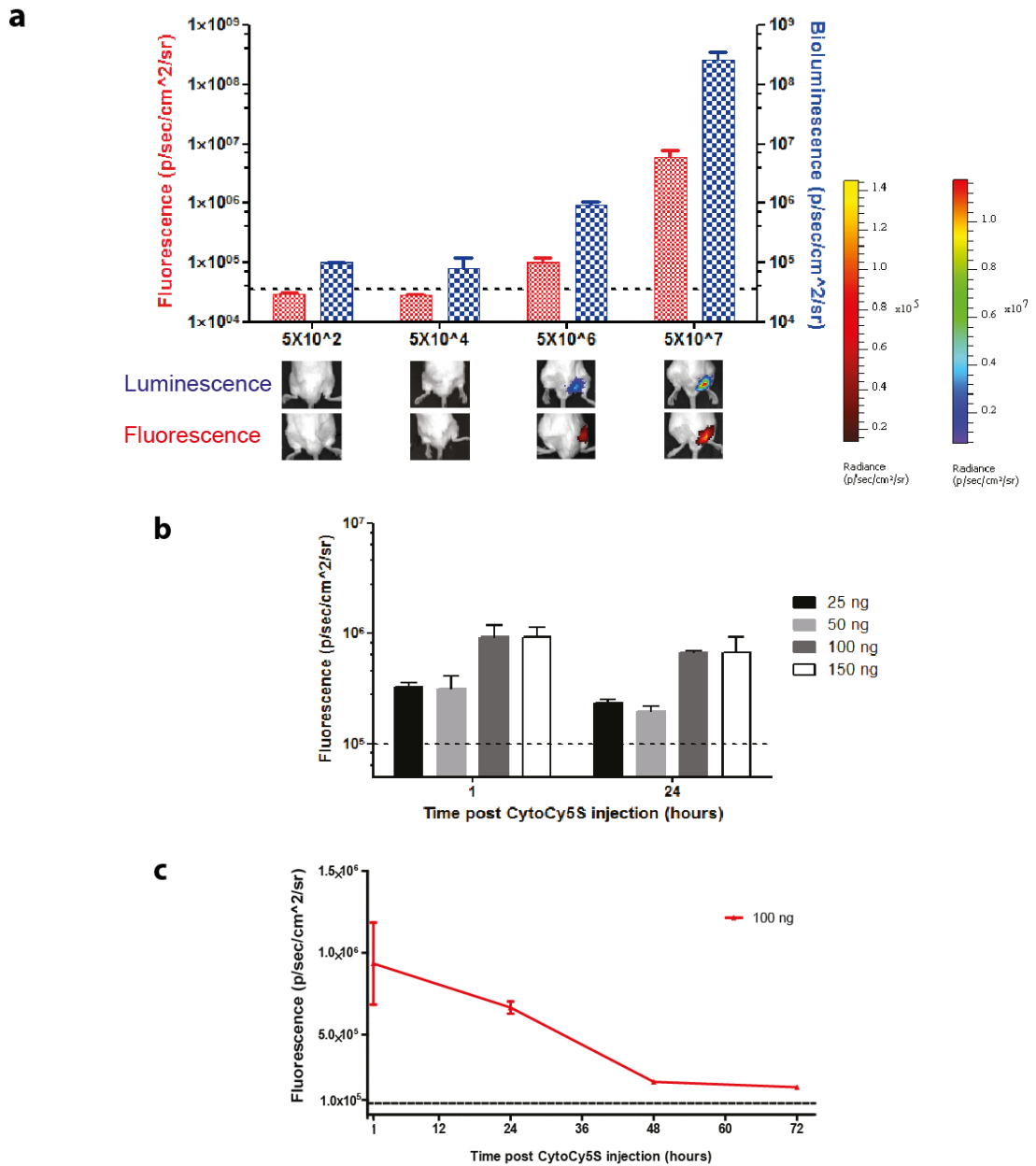


**Figure 8. *E. coli*-related CytoCy5S fluorescence *in vivo*.** a) An increase in fluorescence from quadriceps muscle injected with *E. coli* MG1655 was seen to correlate with increasing numbers of luminescent bacteria injected into the muscle. BALB/c mice were injected with  $5 \times 10^2$ ,  $5 \times 10^4$ ,  $5 \times 10^6$  or  $5 \times 10^7$  *E. coli* MG1655 in the right quadriceps and PBS in the left. 1 h post bacterial injection, mice received 100 ng CytoCy5S IP and were imaged for bioluminescence and for fluorescence. The dotted line represents autofluorescence from PBS injected limbs. Pictures of mice shown below the graphs are randomly selected representative images for each group. b) *In vivo* CytoCy5S dose escalation study showing the effect of CytoCy5S concentration on fluorescence from intramuscular bacteria. Mice received IP injections of 25 ng, 50 ng, 100 ng or 150 ng CytoCy5S. Fluorescence saturation from BALB/c mice bearing  $5 \times 10^6$  bacteria in the quadriceps was achieved at 100 ng CytoCy5S. The dotted line represents autofluorescence. c) Change in fluorescence from activated CytoCy5S within muscle localised *E. coli* MG1655 over time. A robust fluorescent signal exceeding autofluorescence was still evident at 72 h post probe injection.  $n=3$  in all cases. Error bars represent SEM.

### ***In vivo* imaging of *S. Typhimurium* infection in mice**

BALB/c mice were infected with  $1 \times 10^4$  bioluminescent *S. Typhimurium* UK-1 by tail vein injection and progression of infection to a chronic stage was monitored using BLI. Mice were deemed to have established infection once BLI showed bacterial luminescence concentrated to the liver and spleen (approximately four days post IV bacterial administration). When mice reached this peak state of infection CytoCy5S was administered. Fluorescence imaging 90 min post probe injection showed a strong signal from livers ( $2.38 \times 10^5$  p/sec/cm<sup>2</sup>/sr  $\pm$   $1.34 \times 10^4$ ) and spleens ( $3.08 \times 10^5$  p/sec/cm<sup>2</sup>/sr  $\pm$   $3.7 \times 10^4$ ) which correlated with the location of bacteria within the mice as determined by BLI (Figure 9b). Following imaging, mice were culled and the livers, spleens and kidneys were removed (Figure 9c). *Ex vivo* luminescence and fluorescence imaging of the organs confirmed that infection was confined to the liver and spleen with no luminescence or fluorescence apparent from other organs.

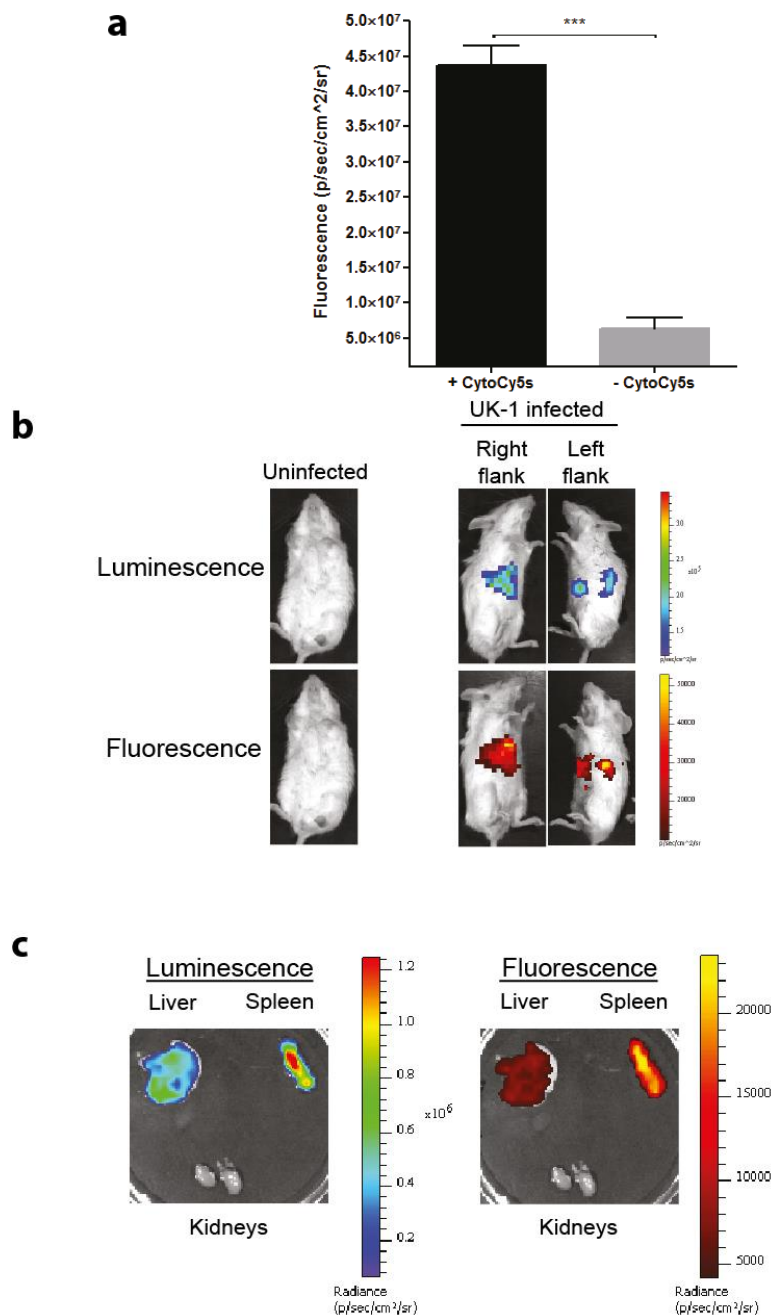


**Figure 9. *In vivo* imaging of *Salmonella* Typhimurium UK-1 infection.** a) Metabolically active *S. Typhimurium* UK-1 cells are capable of reducing CytoCy5S to its fluorescent form *in vitro*. A significant ( $P < 0.0001$ ) increase in fluorescence signal from *S. Typhimurium* UK-1 incubated *in vitro* with 50 ng CytoCy5S over autofluorescence from *S. Typhimurium* UK-1 alone was observed. b) BALB/c mice were infected with  $10^4$  *S. Typhimurium* UK-1 by tail vein injection. Use of *lux*-tagged bacteria permitted determination of the specific location of these bacteria within the host using BLI. Once established infection with *S. Typhimurium* UK-1 was confirmed by BLI, bacteria were tracked by fluorescence imaging of activated CytoCy5S 120 min post probe injection. The fluorescent signal produced following administration of 100 ng CytoCy5S colocalised with the luminescent signal from the bacteria. The pictures of mice in this panel are randomly selected representative images of infected mice.  $n = 3$  mice per group. c) *Ex vivo* BLI and FLI of the liver, spleen and kidneys (uninfected) of UK-1 infected mice shows that luminescence and fluorescence were localised to bacteria infected organs.

### ***In vivo* imaging of tumour targeting *E. coli***

We have previously demonstrated high-level, specific bacterial growth within mouse tumour xenografts [29]. BALB/c mice bearing subcutaneous 4T1 xenograft tumours were IV administered  $1 \times 10^5$  *E. coli* MG1655 and allowed one week to permit colonisation of the tumours and clearing of bacteria from the rest of the body. Following tumour colonisation as evidenced by BLI, CytoCy5S was IP administered and mice imaged for fluorescence at a range of time-points. A strong tumour-specific fluorescent signal was maintained in probe-administered mice for up to 4 h (Figure 10). Upon excision and dissection of tumours 8 h post probe injection, robust fluorescence from the tumour was still evident. Colocalisation of luminescence and fluorescence from the tumour confirmed that CytoCy5S activation was occurring specifically in the presence of bacteria. MG1655 colonisation of the tumour was further confirmed and quantified by plating of single cell suspensions from tumours on selective agar (data not shown). Mice bearing subcutaneous tumours that did not receive bacteria showed no fluorescence following IP injection of CytoCy5S. Similarly, mice that bore bacteria colonised tumours and did not receive any CytoCy5S showed no fluorescence. CytoCy5S can also be used to detect Gram-positive bacteria *in vivo*. BALB/c mice bearing subcutaneous CT26 flank tumours received an intratumoural injection of *B. breve*. Three days post injection of bacteria, mice received an IP injection of CytoCy5S and were imaged for fluorescence 1.5 h later. As was seen with *E. coli* colonised tumours, probe activation was confined to the tumour site and no off target activation of the probe was observed. The fluorescent signal from the tumour following bacteria mediated probe activation was

significantly ( $p < 0.01$ ) greater than that seen in mice that did not have bacteria colonised tumours.

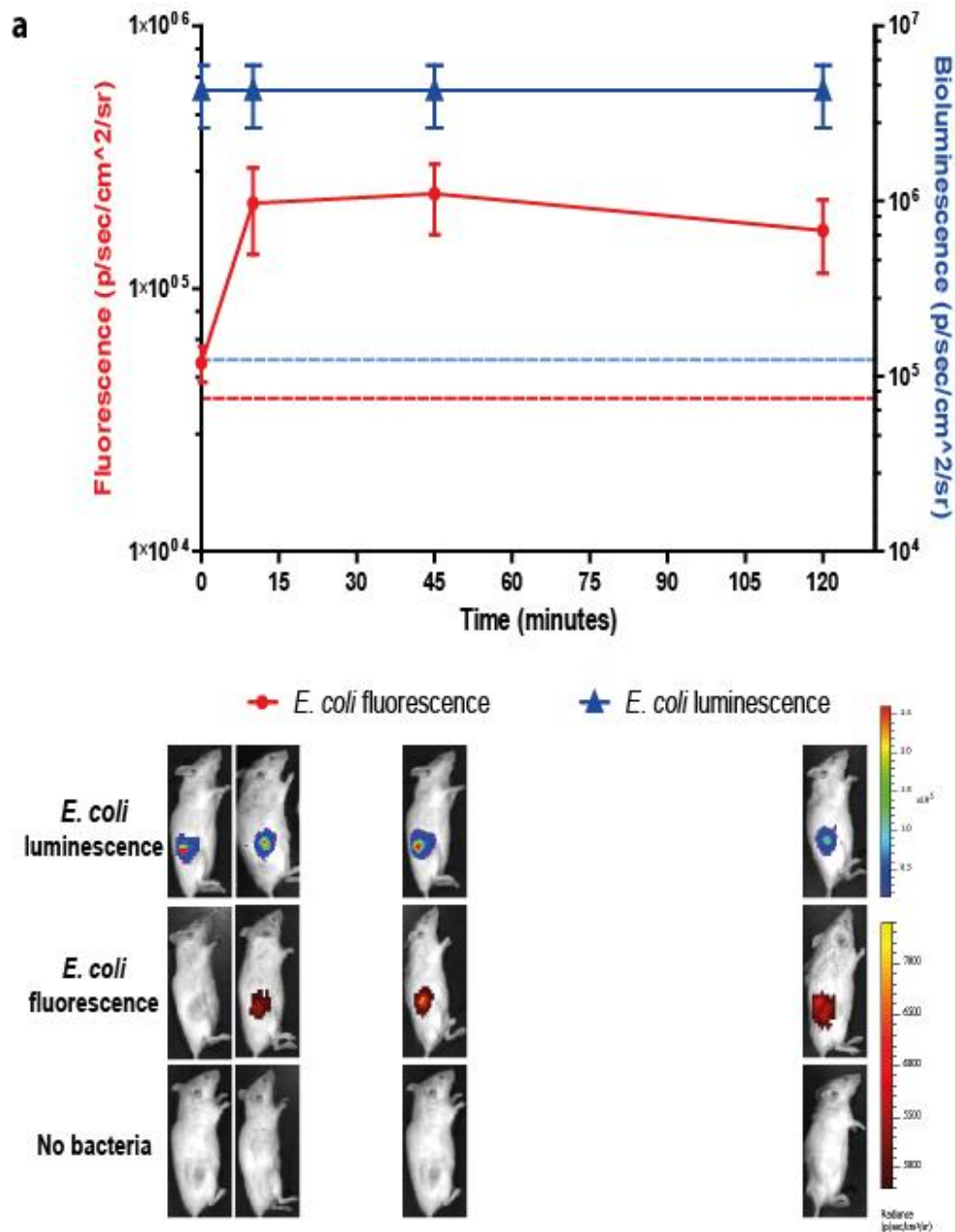


**Figure 10 (part 1). *In vivo* imaging of *E. coli* colonised tumours.** a) BALB/c mice bearing subcutaneous 4T1 flank tumours colonised with *E. coli* MG1655 or PBS show a tumour localised bioluminescent signal. Following IP injection of CytoCy5S, mice were imaged at various timepoints for fluorescence. A peak fluorescent signal was reached 45 min post CytoCy5S injection. Fluorescence from *E. coli* bearing mice that received CytoCy5S was maintained for over 120 min while no signal exceeding autofluorescence was evident in the PBS group. n=3 mice per group. Autoluminescence is represented as a dotted blue line on the graph and autofluorescence is shown as a dotted red line.

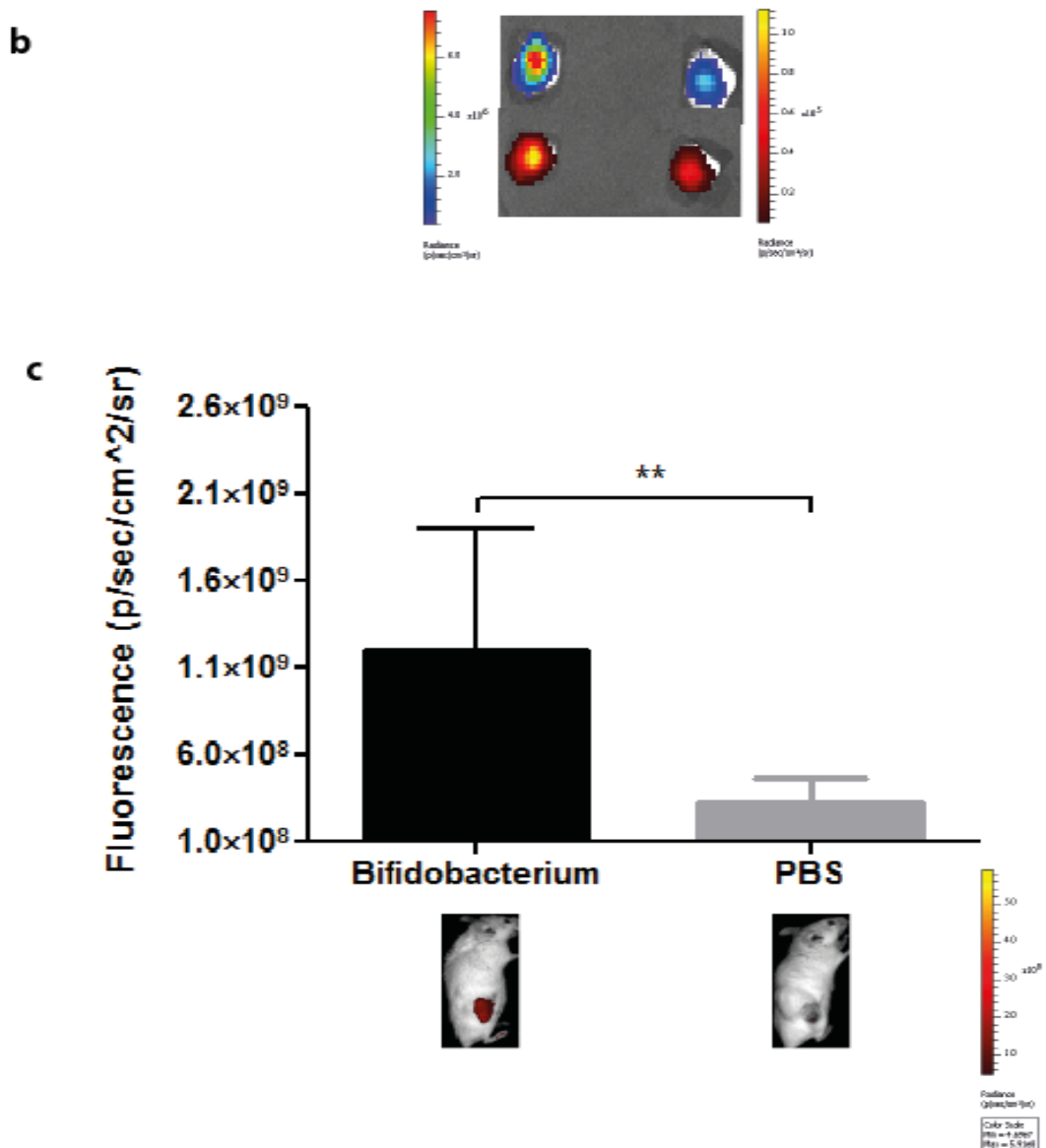


**Figure 10 (part 2). *In vivo* imaging of *E. coli* colonised tumours.** b) *Ex vivo* imaging of an *E. coli* colonised tumour from a mouse that received CytoCy5S. The dissected tumour maintained a strong fluorescent signal at 8 h post CytoCy5S injection c) BALB/c mice bearing subcutaneous CT26 flank tumours colonised with IT administered *B. breve* show a tumour localised fluorescent signal 1.5 h following IP administration of CytoCy5S. The level of fluorescence is significantly higher ( $p < 0.01$ ) than in mice that did not have bacteria colonised tumours (PBS group).  $n = 3$  mice per group. Pictures of mice shown below the graphs are randomly selected representative images for each group. Error bars represent SEM in (a) and (c).

## Discussion.

In this chapter, we describe a novel *in vivo* optical imaging system based on the exclusive activation of a fluorophore specific for bacterial nitroreductase enzymatic activity, to provide a highly targeted strategy for preclinical imaging of *in vivo* bacterial localisation is described. Natural levels of bacterial nitroreductases were shown to be capable of reducing the quenched fluorophore CytoCy5S to its fluorescent form *in vitro* in a range of bacteria, thereby demonstrating the versatility of the system for the non-invasive detection of metabolically active bacteria.

Beyond the strategies necessitating genetic engineering of bacteria, only a small number of other strategies have been reported. In addition to studies by Kong *et. al.* and Leevy *et. al.*, the maltodextrin-based system mentioned earlier and an *ex vivo*-labelling approach involving quantum dots (QD) have been described [33]. However, transiently labelled bacteria do not offer much by way of longitudinal monitoring due to dilution of the reporter. Furthermore, the QD system was restricted to certain Gram-negative species as a result of probe uptake issues. The probe-enzyme strategy outlined here is applicable to a broad range of Gram-negative and Gram-positive species, even traditionally poorly genetically tractable genera such as *Clostridium* and *Bifidobacterium*, while repeat *in situ* probe administration overcomes probe dilution, providing real-time read-out with a degree of quantitation. Fluorescence from activated CytoCy5S strongly correlated with the number of bacteria within the muscle and was seen to reduce over time in line with the reduction in luminescence observed from infected quadriceps. The considerable longevity of the fluorescent signal (72 h following IP injection of the probe) is most likely due to saturation of cells with CytoCy5S leading to steady and continual probe

activation as NTRs perpetually reduce single CytoCy5S molecules before becoming available for the activation of subsequent probe molecules.

Two studies involving CytoCy5S have been published by other groups. The first report of this probe, by Bhaumik and colleagues [25], exploited CytoCy5S as a reporting system for cancer gene therapy based on NTR activation of a prodrug (GDEPT), with CytoCy5S facilitating imaging of the NTR-engineered viral vector in mouse xenograft experiments. A subsequent publication described the utility of CytoCy5S for imaging of mouse xenograft growth using cancer cells engineered to stably express NTR [26]. Both papers demonstrated the utility of this probe in mice in terms of high sensitivity, low background and lack of toxicity to mammalian cells, and were entirely focused on reporting transfected cancer cells. Of interest, Bhaumik *et al.* observed that when a 10 x dose of probe was administered, fluorescence was evident from the abdominal region after 48 h. The authors proposed that this may be due to non-specific background signal due to NTR activity from *E. coli* and some other gut species, which might interfere with their desired imaging of transduced tumour cells, but that could be reduced by antibiotic administration.

The work described in this chapter is the first to demonstrate the potential for this probe as a specific bacterial imaging agent. This strategy proved to be exquisitely specific to bacterial cells, with no increase in organ fluorescence upon administration of probe to untreated mice. For example, in tumour experiments, tumours that did not harbour bacteria did not show a fluorescent signal, while activated CytoCy5S within infected mouse liver and spleen was readily observed with no off-site probe activation in uninfected organs. The reduction in fluorescence that resulted from the co-incubation of the NTR KO strain with CytoCy5S validates the specificity of this probe to nitroreductase activity, while demonstrating that a

broad range of relevant enzymes capable of its activation are present within a single strain. In the presence of the full complement of bacterial nitroreductases a robust and sustained fluorescent signal can be obtained and longitudinal fluorescence imaging can be carried out for up to 7.5 h post single administration.

The pursuit of highly targeted *in vivo* imaging strategies is an aim that unites a number of research fields. The application of this imaging strategy to the non-invasive detection of *Salmonella* infection *in vivo* represents an important addition to the current state of the art imaging systems. *In vitro* validation of functionality with other infectious disease-related agents such as *L. monocytogenes*, *E. coli* and *C. difficile* indicates applicability to *in vivo* monitoring of a wide range of infectious diseases in internal organs. Since common GIT commensal genera such as *Bifidobacterium* and *E. coli* also proved to activate the probe, this strategy can add value to other research fields involving microbiome research, probiotics etc. The ability of systemically circulating bacteria to specifically home to and grow within solid tumours to high numbers provided for the tumour localised production of NTR. Through the utilisation of this tumour-targeting phenomenon, it was possible to achieve highly targeted CytoCy5S activation specifically within the tumour site. Activation of CytoCy5S within the tumours also permitted non-invasive visualisation of the tumour. All current tumour imaging and therapy strategies strive to achieve high levels of specificity for tumours while avoiding healthy tissue. The tumour specific replication of systemically administered bacteria is a phenomenon common to all bacteria tested to date [34-40]. This capacity for tumour targeting makes bacteria ideal vectors for the delivery of genes, proteins or therapeutic payloads to the tumour microenvironment and the ability to image ‘bacterial therapeutics’ is of high value. Furthermore, this system could also be used as a

reporter for tracking conversion of NTR activated prodrugs such as CB1954 to analyse the therapeutic efficacy of treatment with these prodrugs [41].

## References

1. Cronin, M., et al., *Bacterial vectors for imaging and cancer gene therapy: a review*. Cancer Gene Therapy, 2012. **19**(11): p. 731-740.
2. Matthews, P.M., et al., *Technologies: preclinical imaging for drug development*. Drug Discovery Today: Technologies, 2013. **10**(3): p. e343-e350.
3. ECDC/EMA, *ECDC/EMA Joint Technical Report: The bacterial challenge: time to react*, 2009.
4. Rice, B.W., M.D. Cable, and M.B. Nelson, *In vivo imaging of light-emitting probes*. Journal of Biomedical Optics, 2001. **6**(4): p. 432-440.
5. Byrne, W.L., et al., *Use of optical imaging to progress novel therapeutics to the clinic*. J Control Release, 2013.
6. Tangney, M. and K.P. Francis, *In vivo optical imaging in gene & cell therapy*. Curr Gene Ther, 2012. **12**(1): p. 2-11.
7. Niska, J.A., et al., *Monitoring Bacterial Burden, Inflammation and Bone Damage Longitudinally Using Optical and  $\mu$ CT Imaging in an Orthopaedic Implant Infection in Mice*. PLoS ONE, 2012. **7**(10): p. e47397.
8. Riedel, C.U., et al., *Improved luciferase tagging system for *Listeria monocytogenes* allows real-time monitoring in vivo and in vitro*. Appl Environ Microbiol, 2007. **73**(9): p. 3091-4.
9. Nunes-Halldorson, V.d.S. and N.L. Duran, *Bioluminescent bacteria: lux genes as environmental biosensors*. Brazilian journal of Microbiology, 2003. **34**(2): p. 91-96.
10. Guglielmetti, S., et al., *Construction, characterization and exemplificative application of bioluminescent *Bifidobacterium longum* biovar longum*. Int J Food Microbiol, 2008. **124**(3): p. 285-90.
11. Foucault, M.L., et al., *In vivo bioluminescence imaging for the study of intestinal colonization by *Escherichia coli* in mice*. Appl Environ Microbiol, 2010. **76**(1): p. 264-74.
12. Hoffman, R.M. and M. Zhao, *Whole-body imaging of bacterial infection and antibiotic response*. Nature Protocols, 2006. **1**(6): p. 2988-2994.

13. *Clinicopathological statistics on registered prostate cancer patients in Japan: 2000 report from the Japanese Urological Association*. Int J Urol, 2005. **12**(1): p. 46-61.
14. White, A.G., et al., *Deep-red fluorescent imaging probe for bacteria*. Bioorganic & Medicinal Chemistry Letters, 2012. **22**(8): p. 2833-2836.
15. Leevy, W.M., et al., *Optical Imaging of Bacterial Infection in Living Mice Using a Fluorescent Near-Infrared Molecular Probe*. Journal of the American Chemical Society, 2006. **128**(51): p. 16476-16477.
16. Leevy, W.M., et al., *Noninvasive Optical Imaging of Staphylococcus aureus Bacterial Infection in Living Mice Using a Bis-Dipicolylamine-Zinc(II) Affinity Group Conjugated to a Near-Infrared Fluorophore*. Bioconjugate Chemistry, 2008. **19**(3): p. 686-692.
17. Ning, X., et al., *Maltodextrin-based imaging probes detect bacteria in vivo with high sensitivity and specificity*. Nat Mater, 2011. **10**(8): p. 602-7.
18. Orenga, S., et al., *Enzymatic substrates in microbiology*. J Microbiol Methods, 2009. **79**(2): p. 139-55.
19. Kong, Y., et al., *Imaging tuberculosis with endogenous  $\beta$ -lactamase reporter enzyme fluorescence in live mice*. Proceedings of the National Academy of Sciences, 2010. **107**(27): p. 12239-12244.
20. Rice, L.B. *Mechanisms of resistance and clinical relevance of resistance to  $\beta$ -lactams, glycopeptides, and fluoroquinolones*. in Mayo Clinic Proceedings. 2012. Elsevier.
21. Roldan, M.D., et al., *Reduction of polynitroaromatic compounds: the bacterial nitroreductases*. FEMS Microbiol Rev, 2008. **32**(3): p. 474-500.
22. Patel, P., et al., *A phase I/II clinical trial in localized prostate cancer of an adenovirus expressing nitroreductase with CB1954 [correction of CB1984]*. Mol Ther, 2009. **17**(7): p. 1292-9.
23. James, A.L., et al., *Fluorogenic substrates for the detection of microbial nitroreductases*. Lett Appl Microbiol, 2001. **33**(6): p. 403-8.
24. Cellier, M., et al., *2-Arylbenzothiazole, benzoxazole and benzimidazole derivatives as fluorogenic substrates for the detection of nitroreductase and aminopeptidase activity in clinically important bacteria*. Bioorg Med Chem, 2011. **19**(9): p. 2903-10.

25. Bhaumik, S., et al., *Noninvasive optical imaging of nitroreductase gene-directed enzyme prodrug therapy system in living animals*. Gene therapy, 2011. **19**(3): p. 295-302.
26. McCormack, E., et al., *Nitroreductase, a near-infrared reporter platform for in vivo time-domain optical imaging of metastatic cancer*. Cancer Res, 2013. **73**(4): p. 1276-86.
27. González-Pérez, M.M., et al., *Escherichia coli has multiple enzymes that attack TNT and release nitrogen for growth*. Environmental Microbiology, 2007. **9**(6): p. 1535-1540.
28. Mathur, H., et al., *Analysis of Anti-Clostridium difficile Activity of Thuricin CD, Vancomycin, Metronidazole, Ramoplanin, and Actagardine, both Singly and in Paired Combinations*. Antimicrobial Agents and Chemotherapy, 2013. **57**(6): p. 2882-2886.
29. Cronin, M., et al., *High resolution in vivo bioluminescent imaging for the study of bacterial tumour targeting*. PLoS One, 2012. **7**(1): p. e30940.
30. Baban, C.K., et al., *Bioluminescent bacterial imaging in vivo*. J Vis Exp, 2012(69).
31. Prosser, G., et al., *Discovery and evaluation of *Escherichia coli* nitroreductases that activate the anti-cancer prodrug CB1954*. Biochemical pharmacology, 2010. **79**(5): p. 678-687.
32. Valle, A., et al., *Study of the role played by NfsA, NfsB nitroreductase and NemA flavin reductase from Escherichia coli in the conversion of ethyl 2-(2'-nitrophenoxy) acetate to 4-hydroxy-(2H)-1, 4-benzoxazin-3 (4H)-one (D-DIBOA), a benzohydroxamic acid with interesting biological properties*. Applied microbiology and biotechnology, 2012. **94**(1): p. 163-171.
33. Leevy, W.M., et al., *Quantum dot probes for bacteria distinguish Escherichia coli mutants and permit in vivo imaging*. Chemical Communications, 2008(20): p. 2331-2333.
34. Yu, Y.A., Q. Zhang, and A.A. Szalay, *Establishment and characterization of conditions required for tumor colonization by intravenously delivered bacteria*. Biotechnol Bioeng, 2008. **100**(3): p. 567-78.
35. Cummins, J. and M. Tangney, *Bacteria and tumours: causative agents or opportunistic inhabitants?* Infectious agents and cancer, 2013. **8**(1): p. 1-8.

36. Tangney, M., *Gene therapy for cancer: dairy bacteria as delivery vectors*. Discovery medicine, 2010. **10**(52): p. 195.
37. Hoffman, R.M., *Tumor-seeking *Salmonella* amino acid auxotrophs*. Current opinion in biotechnology, 2011. **22**(6): p. 917-923.
38. Morrissey, D., G.C. O'Sullivan, and M. Tangney, *Tumour targeting with systemically administered bacteria*. Curr Gene Ther, 2010. **10**(1): p. 3-14.
39. Cronin, M., et al., *Orally administered bifidobacteria as vehicles for delivery of agents to systemic tumors*. Mol Ther, 2010. **18**(7): p. 1397-407.
40. Baban, C.K., et al., *Bacteria as vectors for gene therapy of cancer*. Bioeng Bugs, 2010. **1**(6): p. 385-94.
41. Lehouritis, P., C. Springer, and M. Tangney, *Bacterial-directed enzyme prodrug therapy*. J Control Release, 2013.

## Chapter 3: Development of a novel, nitroreductase activated, luminescent probe

Sections from this chapter have been published as

Vorobyeva, A. G., Stanton, M., Godinat, A., Lund, K. B., Karateev, G. G., Francis, K. P., ... & Dubikovskaya, E. A. (2015). **Development of a bioluminescent nitroreductase probe for preclinical imaging.** *PloS one*, 10(6).

## Abstract

Bacterial nitroreductases (NTRs) have been widely utilised in the development of novel antibiotics, degradation of pollutants, and gene-directed enzyme prodrug therapy (GDEPT) of cancer that reached clinical trials. In the case of GDEPT, since NTR is not naturally present in mammalian cells, the prodrug is activated selectively in NTR-transformed cancer cells, allowing high efficiency treatment of tumours. Currently, no bioluminescent probes exist for sensitive, non-invasive imaging of NTR expression. We therefore developed a "NTR caged luciferin" (NCL) probe that is selectively reduced by NTR, producing light proportional to the NTR activity. Here we report successful application of this probe for imaging of NTR *in vitro*, in bacteria and cancer cells, as well as *in vivo* in mouse models of bacterial infection and cancer. This novel tool should significantly accelerate the development of cancer therapy approaches based on GDEPT and other fields where NTR expression is important.

## Study Aim

The aim of this chapter was to characterise and develop a novel caged luciferin probe (NCL) for use in the *in vivo* detection of nitroreductase expressing bacteria. The probe was synthesised and designed by a collaborating lab in the EPFL at our request. This probe differs from CytoCy5S (Chapter 2) in that it is a luminescent probe, and while requiring genetic modification of the bacterium, bioluminescence typically offers increased sensitivity over fluorescence. This work aimed to determine the suitability of the probe for application to detection of bacterial infection and the localisation of bacteria in a live host.

## Introduction.

The nitroreductase (NTR) family of enzymes are widespread amongst bacteria and are known to metabolize nitrosubstituted compounds and quinones using NADH or NADPH as reducing agents [1-4]. They are important for the development of novel antibiotics being the main target for the treatment of infections caused by bacteria, e.g. *Mycobacterium tuberculosis* [5], *Helicobacter pylori* [6] and by parasites, e.g. *Trypanosoma* [7], *Giardia* and *Entamoeba* [8]. Their enzymatic activity in gut microbiota is linked to carcinogen production and etiology of colorectal cancer [9, 10]. In addition, they are used in biotechnology for degradation of environmental contaminants [1]. Due to their absence in mammalian cells they are also utilized as activating enzymes in gene-directed enzyme prodrug therapy (GDEPT) approaches for cancer chemotherapy [11] where the NTR gene is used to selectively transform cancer cells, providing unique targeted therapy of tumours over normal tissues [12]. The nitroaromatic prodrug CB1954, in conjunction with bacterial NTR, is promising for GDEPT and has reached clinical trials for prostate cancer [13]. Following the recent first approval in Europe of a gene therapy medicine, the potential for clinical application of GDEPT is increasing [14]. However, both preclinical and clinical development of NTR-based GDEPT systems has been severely hampered by the lack of imaging tools that allow sensitive *in vivo* evaluation of transgene expression in living subjects. Quantification of the level of transgene expression is extremely important because it is directly linked to the effectiveness of the therapy. Bioluminescence (BL) is currently the most sensitive optical *in vivo* imaging modality available, and has been applied to visualize multiple biological processes in small animals [15, 16]. It obviates most of the limitations of *in vivo* fluorescent

imaging [17], such as high tissue-derived autofluorescence, photobleaching, limited tissue penetration and lack of quantification. Several activatable fluorescent probes for NTR imaging *in vitro* have been previously described [18-22]. However, the only reported probe (CytoCy5S) for imaging of NTR *in vivo* relies on fluorescence (CytoCy5S) [23-25] and therefore possesses the limitations mentioned above. Similar to bioluminescent imaging, *in vivo* chemiluminescent imaging offers the advantages of high sensitivity due to low background and high signal-to-noise ratios. Prior studies have elegantly demonstrated the application of chemiluminescence for imaging of myeloperoxidase activity [26] and beta-galactosidase activity [27] *in vivo*. However, although chemiluminescence has the additional advantage of not requiring luciferase transfected cells for the generation of light, expression of this enzyme allows more elaborate disease models to be developed due to the researcher's ability to define its spatial localization and regulation. Moreover, most chemiluminescent agents suffer from low quantum yield, short maximal photon wavelength emission and high instability. For example, the quantum yield of aqueous luminol chemiluminescence is  $1.23 \pm 0.20\%$  [28] with a maximal emission of 424 nm [29], while the reported quantum yield of firefly BL is  $41.0 \pm 7.4\%$  [30], that is about 40 times higher, with D-hydroxyluciferin and D-aminoluciferin having wavelength at 560 nm and 603 nm respectively [31]. Recently, Zhang et al. [32] showed the advantage of using both near-infrared fluorescent and chemiluminescent imaging in combination, while addressing the wavelength issue associated with luminol chemiluminescence *in vivo* by shifting it into the near-infrared region utilising quantum dots. BL is based on the interaction of a small molecule D-luciferin with firefly luciferase that results in the generation of photons of light. The system can be "tuned" through "caging" of the luciferin scaffold to image and

quantify activities of biological molecules. Target-mediated selective removal of the caging moiety leads to production of free D-luciferin and subsequent generation of photons by luciferase, that can be quantified [33]. While this strategy was previously used by us and others to study biological processes (delivery and biodistribution of cell penetrating peptide conjugates [34], cell surface glycosylation [35], hydrogen peroxide fluxes [36], fatty acids uptake [37]) and image enzyme activity (beta-galactosidase [38], caspases [39-41], furin [42] and beta-lactamase [43], no bioluminescent probes have been previously reported for imaging of NTR. Here, we describe the development of novel NTR-specific bioluminescent probe, termed Nitroreductase Caged Luciferin (NCL). Our results demonstrate that this probe can be used for non-invasive real-time imaging of NTR activity *in vitro*, in live bacteria and mammalian cells, as well as in preclinical models of cancer and bacterial infection.

## Materials and Methods

***Chemical materials and synthesis.*** The synthetic procedures and characterisation are detailed in [44]

***Kinetics of NCL reaction with NTR by fluorescence.*** Fluorescence was measured using a Tecan Infinite M1000 (Tecan Austria GmbH) plate reader. Kinetic measurements of NCL (5–50  $\mu\text{M}$ ) uncaging by NTR (0.25  $\mu\text{g ml}^{-1}$ ) were performed in the presence of NADH (500  $\mu\text{M}$ ) at 37°C in PBS buffer (pH 7.4). The kinetics rate of luciferin release from NCL was measured by fluorescence at 330 nm excitation and 530 nm emission wavelengths. The fluorescence calibration curve for luciferin was used to calculate the rate. Kinetic parameters  $K_m$  and  $V_{\text{max}}$  were determined from Michaelis-Menten model and Lineweaver-Burk plot was used to display the data. The  $k_{\text{cat}}$  value was calculated by dividing the  $V_{\text{max}}$  value, obtained from the data acquired for the determination of the corresponding  $K_m$  values for the probe, by the concentration of the nitroreductase in the assay.

***Bioluminescent imaging of NTR with NCL in enzyme assay.*** *In vitro* imaging studies were performed in clear bottom black 96 well plates from Becton Dickinson and Company. An IVIS Spectrum (PerkinElmer) was used to measure the amount of bioluminescent imaging (BLI) signal production. The data are presented as pseudocolour images indicating light intensity (red being the most intense and blue the least intense), which are superimposed over the grayscale reference photographs. Bioluminescence was quantified using region of interest (ROI) analysis of individual wells and the average signal expressed as the total number of photons emitted per second per  $\text{cm}^2$  per steradian ( $\text{p/sec/cm}^2/\text{sr}$ ) from each of the three wells was calculated by using the Living Image software. Total luminescence was calculated

by integrating the area under corresponding kinetic curves. Luciferase buffer was prepared as following: 2 mM ATP, 5 mM MgSO<sub>4</sub> in PBS (pH 7.4). Stock solutions of luciferase in luciferase buffer, NADH, NCL, luciferin and NTR in PBS (pH 7.4), were freshly prepared and aliquoted in a 96-well plate to give the following final concentrations in the total volume of 100  $\mu$ l/well: luciferase (60  $\mu$ g ml<sup>-1</sup>), NADH (100  $\mu$ M), NTR (10  $\mu$ g ml<sup>-1</sup>), luciferin or NCL (0.25–5  $\mu$ M); luciferin and NCL were added at the last step with a multichannel pipette from the additional 96-well plate. Bioluminescence signal from the plate was acquired immediately every 1 min with 0.5 s integration time for 30 min.

***Bacterial strains, plasmids and culture conditions.*** *E. coli* K-12 MG1655 (- luc gene) and *E. coli* K-12 AB1157, containing the luciferase expressing pUC57 Click beetle red (CBR) plasmid (+ luc gene) was a kind gift from Daniel Ansaldi (Perkin Elmer). The NTR triple mutant, *E. coli* K-12 AB502NemA, was a kind gift from Dr Antonio Valle (University of Cádiz, Cádiz, Spain) and was transformed with the pUC57 CBR plasmid for production of luciferase. *E. coli* MG1655 lux, expressing lux luciferase, was generated as previously described [45]. All strains were grown aerobically at 37°C in Luria Bertani (LB) medium supplemented with 100  $\mu$ g ml<sup>-1</sup> ampicillin (Amp).

***Bioluminescent imaging of NTR activity by NCL in E. coli.*** An IVIS-100 (PerkinElmer) was used to measure the amount of BLI signal production. Stock solutions of luciferin and NCL in PBS (pH 7.4) were freshly prepared and aliquoted in a 96-well plate to give the final concentrations (1–250  $\mu$ M) in the total volume of 200  $\mu$ l/well. The volume of bacterial suspension was 150  $\mu$ l/well. Bioluminescence signal from the plate was acquired immediately every 2 min with 10 s integration time for 1 h.

***Bioluminescent imaging of bacteria reduced NCL in a luciferase producing cancer cell line.*** 4T1 or 4T1 rluc cells were plated at a density  $5 \times 10^4$  cells/well in two 6-well plates for 24 h. A culture of *E. coli* AB1157 that contained 100  $\mu$ M NCL was incubated at 37°C for 1 h to allow sufficient time for reduction of the probe to occur before centrifugation and removal of the supernatant. The bacterial supernatant was then filter sterilised before addition of 500  $\mu$ l to appropriate wells containing either 4T1 or 4T1 rluc cells. Control wells were treated with supernatant from an *E. coli* culture that did not contain NCL. Plates were imaged using the IVIS Lumina at regular timepoints for a total of 2 h. The observed BLI signal was quantified using ROI analysis with Living Image software.

***Ethics statement.*** All animal procedures were performed in accordance with the national ethical guidelines prescribed by the Health Products Regulatory Authority (HPRA). Protocols were approved by the animal ethics committee of University College Cork (AERR #2010/003 and #2012/015). All efforts were made to minimise suffering.

***Bacterial administration and imaging of bacterial nitroreductase in mice.*** Bacteria were grown at 37°C in a shaking incubator until reaching OD<sub>600</sub> of 0.6 in LB medium, containing 100  $\mu$ g/ml Amp. Cultures were harvested by centrifugation (4000  $\times$  g for 10 min) and washed three times in PBS. After washing, bacteria were resuspended in one tenth volume of PBS. Mice were kept at a constant room temperature (22°C) in a conventional animal colony. Standard laboratory food and water were provided ad libitum. Mice were afforded an adaptation period of at least 4 days before the beginning of experiments. Female BALB/c mice (Harlan, Oxfordshire, UK) in good condition, without infections, weighing 18–22 g and 6–8 weeks old, were kept as previously described [46] and were included in experiments.

BALB/c mice were anaesthetized and the fur on the rear legs was removed. Mice were injected directly into the right quadriceps muscle at a depth of approximately 5 mm with 50  $\mu$ l of bacteria suspended in PBS. The concentration of bacterial suspensions used for injection ranged from  $10^6$  to  $10^9$  bacteria/ml. Mice also received an intramuscular injection of 50  $\mu$ l sterile PBS in the left rear quadriceps (control) and *E. coli* lux MG1655 (positive control). 1 h post bacterial injection, mice received an IP injection of 200  $\mu$ l of 10 mM NCL probe (0.8 mg) or 200  $\mu$ l of 10 mM D-luciferin potassium salt (0.63 mg) in PBS. For *in vivo* experiments involving varying concentrations of the probe, the concentration of NCL probe injected was 200  $\mu$ l of 1, 10 or 20 mM solutions in PBS (0.08, 0.8 or 1.6 mg of NCL probe). Mice were imaged for bioluminescence at regular intervals beginning immediately after probe injection using IVIS 100. Mice that were infected with bacteria for experimental purposes were monitored for signs of illness for the duration of the experiment. No adverse symptoms were reported. Following bioluminescence imaging, or at experiment end, animals were euthanized by cervical dislocation.

***Mice and tumour induction.*** As described in Chapter 2.

***Imaging of nitroreductase in a mouse model of subcutaneous cancer.*** 6-8 week old BALB/c mice bearing subcutaneous 4T1luc+/- flank tumours were IV injected with *E. coli* MG1655 (lux +/-). Once tumour colonisation had occurred (approx. 1 week post bacterial injection) as determined by luminescence imaging of mice that received luminescent *E. coli*, mice were injected IP with NCL or D-luciferin. Mice were imaged for luminescence 4 h post probe administration and the level of luminescence was quantified using ROI drawn around the tumour site.

***Statistical analysis.*** As detailed in Chapter 2.

## Results

### Probe design

The reduction of nitroaromatic compounds can occur through one- or two-electron mechanism [1]. Two types of bacterial NTRs have been described and they are classified according to the oxygen dependence. The NTRs used in our study (NfsA, NfsB) are type I oxygen-insensitive NTRs, they catalyse the reduction of the nitro group by addition of a pair of electrons, and their activity does not depend on the level of oxygen. However, the oxygen-sensitive NTRs (type II) catalyse the reduction of the nitro group by the addition of one electron, forming the nitro anion radical, which is oxidized back to the nitro group by oxygen. Bacteria contain both types of nitroreductases with type I being the most characterized among other NTRs. The independence of reduction from the level of oxygen in *E. coli* had been previously demonstrated for an NTR-sensitive coumarin probe (7-nitrocoumarin-3-carboxylic acid) suggesting the prevalent involvement of type I NfsA and NfsB possibly along with other uncharacterized NTRs [47]. The design and synthesis of the NCL probe was carried out by Anzhelika Vorobyeva at the Ecole Polytechnique Federale de Lausanne.

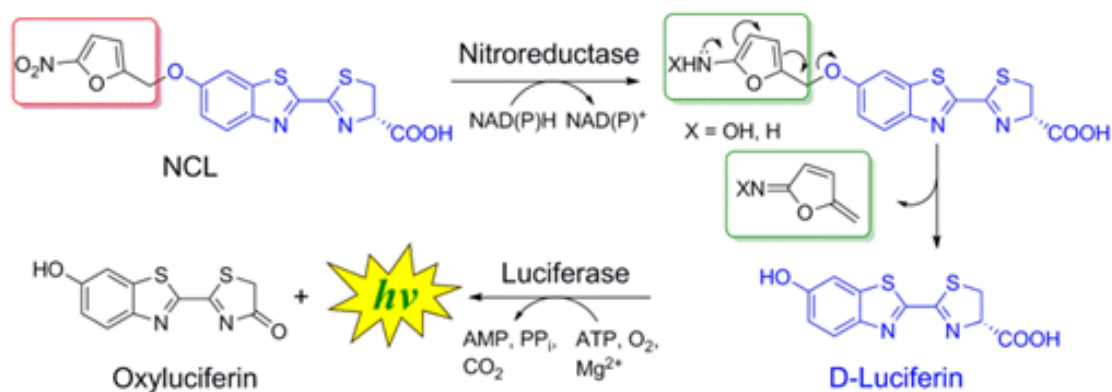


**Figure 1. General strategy for imaging of NTR activity with Nitroreductase Caged Luciferin (NCL) probe.** NCL is a luminescent probe composed of D-luciferin attached to a nitrofuryl moiety that acts as a chemical “cage”. Reduction of the nitrofuryl nitro group by NTR promotes the cleavage of the C-O bond (uncaging) leading to the subsequent release of luciferin. This free luciferin is oxidised by luciferase to emit a photon of light.

The suitability of exploiting NTR activity as a means to selectively distinguish bacterial cells from host background has previously been demonstrated [48]. Several NTR-related enzymes have been identified in mammalian cells and they functionally relate to type I NTRs (NAD(P)H-quinone oxidoreductase (DT-diaphorase EC 1.6.99.2) and xanthine dehydrogenase EC 1.17.1.4). They can potentially contribute to reduction of nitroaromatics, although they are not phylogenetically related and do not exhibit the typical domain characteristic of NTR family. These properties were investigated in the study on FMISO imaging reagent, a derivative of nitroimidazole used as a hypoxia PET tracer [49]. It was reported that under hypoxic conditions xanthine dehydrogenase is converted to xanthine oxidase that reduces FMISO and other nitroimidazole-containing compounds. Similarly, eukaryotic NTRs that are functionally related to type II (aldehyde oxidase EC 1.2.3.1, cytochrome c oxidase EC 1.9.3.1, and NADPH cytochrome P450 reductase EC 1.6.2.4) can potentially reduce nitroaromatics anaerobically and are generally used as targets for hypoxia-activated prodrugs and imaging agents [50]. Therefore, several important factors need to be taken into account when designing the compounds activated selectively by bacterial or mammalian enzymes. For bacterial NTRs the activation is largely dependent on the redox potential of the nitroaromatics. For example, nitrofurans display relatively high redox potentials (reported from -250 to -270 mV) and are reductively activated by NAD(P)H nitroreductases of enteric bacteria. At the same time metronidazole (nitroimidazole) is only activated by anaerobic enzymes showing low redox potentials (-480 mV) in some bacteria and protozoa, making it well tolerated in humans when used as an antibiotic [51]. Substrate specificity of the designed compounds is also important, for example CB1954 prodrug is efficiently reduced by bacterial NTRs and a human DT-diaphorase (NQO2) while being a poor

substrate for a human paralogue NQO1 enzyme [52]. These and other important aspects of selectivity of bioreductive prodrugs are discussed in more details in a recent review by Wilson and Hay [53]. The overall probe design is based on caging of D-luciferin with nitrofuryl moiety resulting in "Nitroreductase Caged Luciferin" (NCL) probe (Figure 1). 5-Nitrofuryl was selected as a cage as its derivatives (nitrofurazone, nitrofurantoin) were shown to be efficiently activated by NTR in bacteria [51]. Upon the reduction of the nitro group by NTR the resulting electron-donating amino group promotes the cleavage of the C-O bond (uncaging), leading to the subsequent release of luciferin which is oxidized by luciferase and a photon of light is emitted. Therefore, release of free luciferin followed by light production is only possible in the presence of NTR.

### **Bioreductive activation of NCL in cell-free assays**

The specificity of probe uncaging by incubating NCL with a recombinant NTR enzyme from *E. coli* (NfsA) in the presence of NADH as a cofactor was investigated. The resulting data demonstrate rapid conversion of NCL into free luciferin under these conditions, the calculated values of rate constant and NCL half-life, were  $5.8 \times 10^{-3}$  s and 119.5 s respectively (data not shown). Next, the Michaelis-Menten kinetic parameters for the NTR-specific cleavage of NCL probe was determined using fluorescence to monitor release of luciferin ( $\lambda_{\text{ex/em}} = 330/530$  nm) as the caged probe is not fluorescent. Both  $V_{\text{max}}$  and  $K_{\text{m}}$  values were found to be comparable to those previously reported for a NTR fluorescent substrate [20] and were determined to be  $0.057 \mu\text{M s}^{-1}$  and  $24.7 \mu\text{M}$  respectively. Catalytic efficiency of probe reduction by NTR ( $k_{\text{cat}}/K_{\text{m}}$ ) was determined to be  $2.25 \times 10^7 \text{ M}^{-1} \text{ s}$ , which is two orders higher than that of luciferin-luciferase reaction ( $1.07 \times 10^5 \text{ M}^{-1} \text{ s}$ ) [54]. To evaluate if the probe can be used as a reporter of NTR activity, the effect of the NTR inhibitor dicoumarol (competitive with NADH) on the efficiency of NCL uncaging was investigated. A gradual concentration-dependent decrease in signal was observed (Figure 2a) indicating that the uncaging of NCL depends on the activity of NTR. The quantitative capability of the probe against the amount of NTR was assayed by fluorescence ( $\lambda_{330/530}$ ) and it was found that the detection limit was  $0.15 \mu\text{g/ml}$ . To determine the utility of NCL as a bioluminescent reporter, the light emission from increasing concentrations of NCL ( $0.25\text{--}5 \mu\text{M}$ ) in the presence or absence of NTR and firefly luciferase was measured (Figure 2b). The resulting signal was concentration-dependent and no significant light was produced in the absence of NTR, resulting in high signal to background noise ratios even at relatively low

concentrations of the probe in comparison to that previously reported [36,42]. In addition, NCL demonstrated an average 70% conversion into luciferin, the highest uncaging efficiency among existing caged luciferin substrates reported to date [36,42].

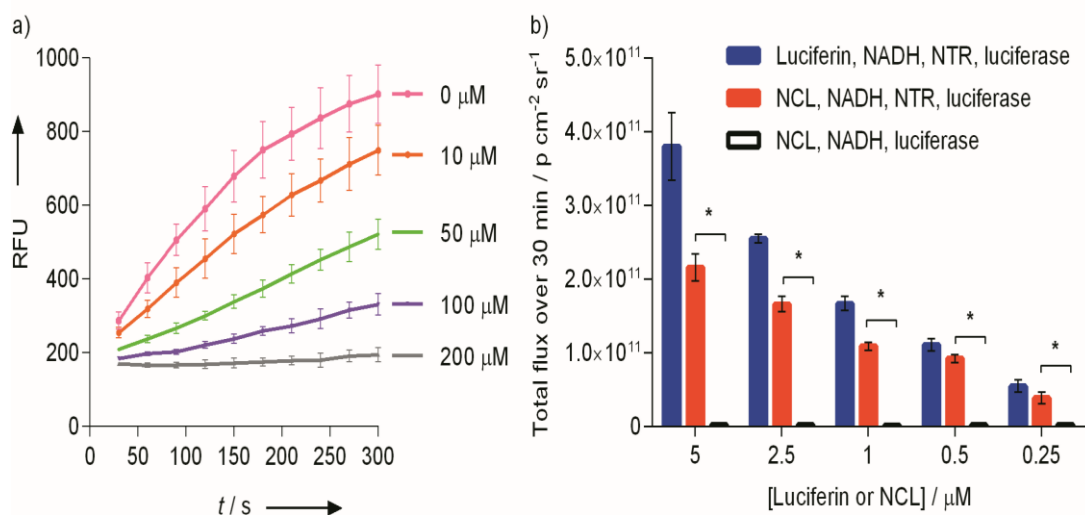


**Figure 2. Evaluation of NTR-specific uncaging of NCL probe.** a) NCL (20  $\mu\text{M}$ ) uncaging by NTR (0.5  $\mu\text{g/ml}$ ) in the presence of NADH (100  $\mu\text{M}$ ) was inhibited by dicoumarol (0 to 200  $\mu\text{M}$ ). b) Total luminescence over 30 min from luciferin or NCL (0.25-5  $\mu\text{M}$ ) with NADH, luciferase, and NTR, compared with the control (no NTR), \* $p < 0.001$ .

## Imaging of NTR activity in *E. coli*

The validation of NCL in a live biological system was initially approached by utilising bacteria as a source of both NTR and luciferase and comparing the level of luminescence obtained using this novel system with the luminescent signal acquired when the established D-luciferin system was used as a positive control (Figure 3). The potential of NCL probe for imaging NTR in *E. coli* naturally expressing NTR [2–4] and engineered to express luciferase was also investigated. The resulting signal from NCL or luciferin control was compared between several *E. coli* strains: *E. coli* engineered to stably express luciferase (*E. coli* CBR) and a strain of *E. coli* (NTR KO luc+) with three well-described NTR genes knocked out (NfsA, NfsB and NemA). Addition of NCL to *E. coli* CBR (*E. coli* luc+) resulted in probe reduction and the subsequent production of an imageable luminescent signal that exceeded background luminescence from *E. coli* CBR in the absence of NCL. When compared with luminescence from NCL treated, NTR KO *E. coli* a significant ( $p < 0.05$ ) decrease in luminescence was observed. This demonstrates that *E. coli* NTRs are responsible for probe uncaging as the reduced NTR activity of the NTR triple KO strain was less capable of probe reduction to liberate free luciferin. As was expected based on the *in vitro* data shown in Figure 3, probe uncaging by *E. coli* did not result in the production of a signal commensurate with that seen with *E. coli* CBR + D-luciferin.

The data presented in Figure 4a show a significant signal above background was detected from *E. coli* luc+ in comparison with *E. coli* wt, indicating the need for luciferase presence for light production. Both wt and NTR KO luc+ strains showed similar levels of luciferase expression when treated with luciferin. However, with

NCL the signal from the parent strain was significantly higher than from the NTR mutant strain (NTR KO luc+), demonstrating probe selectivity for detection of NTR activity in bacteria. The presence of a signal in wells with NTR KO luc+ strain indicates that reduction of the nitrofuryl cage is not exclusive or specific to any of the three major *E. coli* NTRs (NfsA, NfsB and NemaA) and that cage reduction can be achieved at detectable levels in the presence of the remaining NTRs in *E. coli*. In *E. coli*, several nitroreductases (NfsA [2], NfsB [3], YdjA [4]) and reductases (NemaA [55]) are characterized, while the exact functions of other reductase proteins remain unclear. Recent studies [4] indicate that *E. coli* reductases could also have additional nitroreductase activity. The signal dependence on different numbers of bacteria was also investigated and significant signals were evident at concentrations of bacteria as low as  $10^4$  cells/ml ( $1.5 \times 10^3$  cells/well) (Figure 4c). The average efficiency of probe uncaging in bacteria was calculated to be 35% (Figure 4d).

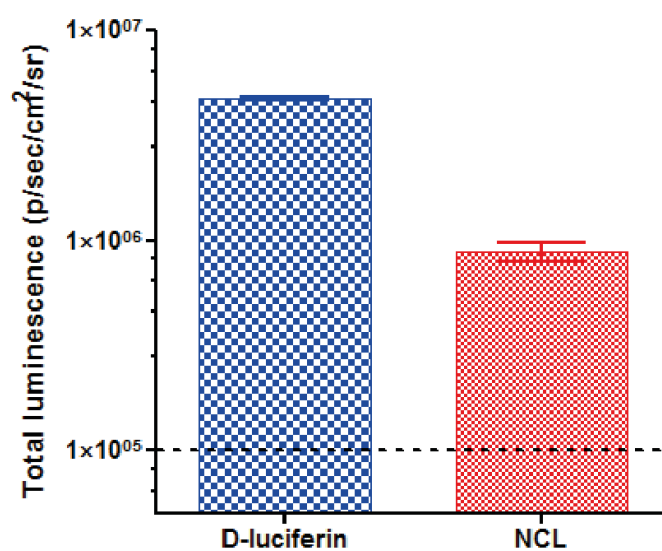


**Figure 3. Comparison of total luminescence from *E. coli* CBR incubated with D-luciferin or NCL.** Total luminescence acquired over 4 h was compared between *E. coli* incubated with either D-luciferin or NCL. A high level of luminescence was recorded from wells containing *E. coli* + NCL ( $8.8 \times 10^5$  (p/sec/cm<sup>2</sup>/sr)) which is comparable with that recorded from wells containing *E. coli* + D-luciferin ( $4.7 \times 10^6$  (p/sec/cm<sup>2</sup>/sr)).

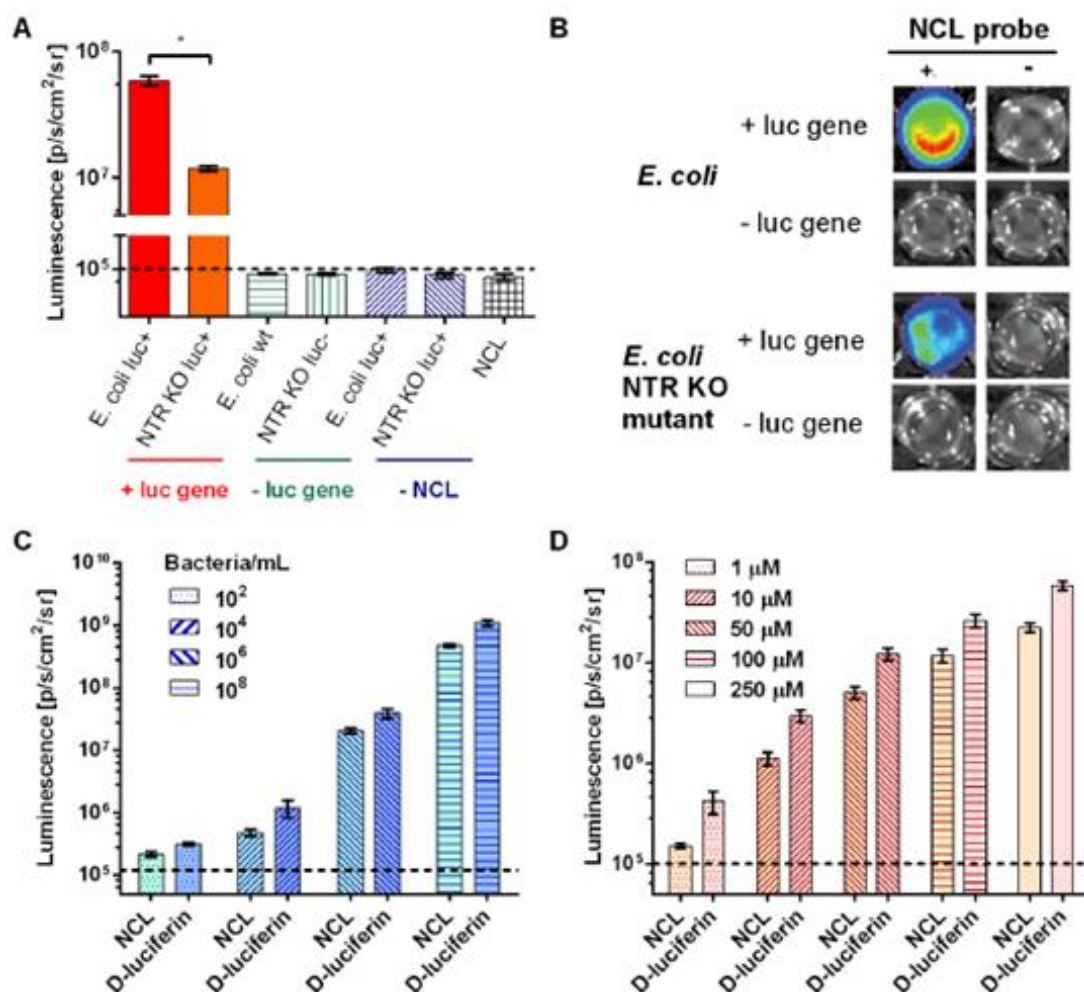


**Figure 4. Light production in *E. coli* by NTR-mediated uncaging of NCL.** a) Light output from NCL (300 μM) after 2 h incubation in luciferase-expressing *E. coli* (+ luc gene) is significantly higher than in NTR mutant (NTR KO luc+) (\*p < 0.001) and in wild type (- luc gene). The dashed line indicates the background. b) Overlay of a photographic image and bioluminescence from the assay described. c) Bioluminescence from 100 μM NCL probe and luciferin incubated with various concentrations of luciferase expressing *E. coli* AB1157 (10<sup>2</sup>–10<sup>8</sup> bacteria/ml) for 10 min before imaging. d) Bioluminescence from luciferase expressing *E. coli* luc+ (10<sup>8</sup> bacteria/ml) incubated with various concentrations of NCL or luciferin (1–250 μM) for 10 min before imaging. Error bars represent SD in all cases.

### **Effect of NCL on bacteria cell viability**

The effect of the NCL probe on the growth and the viability of bacteria *in vitro* was tested by comparing CFU from cultures that were grown in the presence of NCL with cultures grown in the absence of the probe. A fresh *E. coli* culture grown with 100  $\mu$ M NCL did not show any significant difference in the number of CFU over a 4 h time-course when compared with bacteria grown in the absence of the probe (Figure 5). This result demonstrates that NCL does not affect the growth or viability of *E. coli in vitro* at the concentration tested.

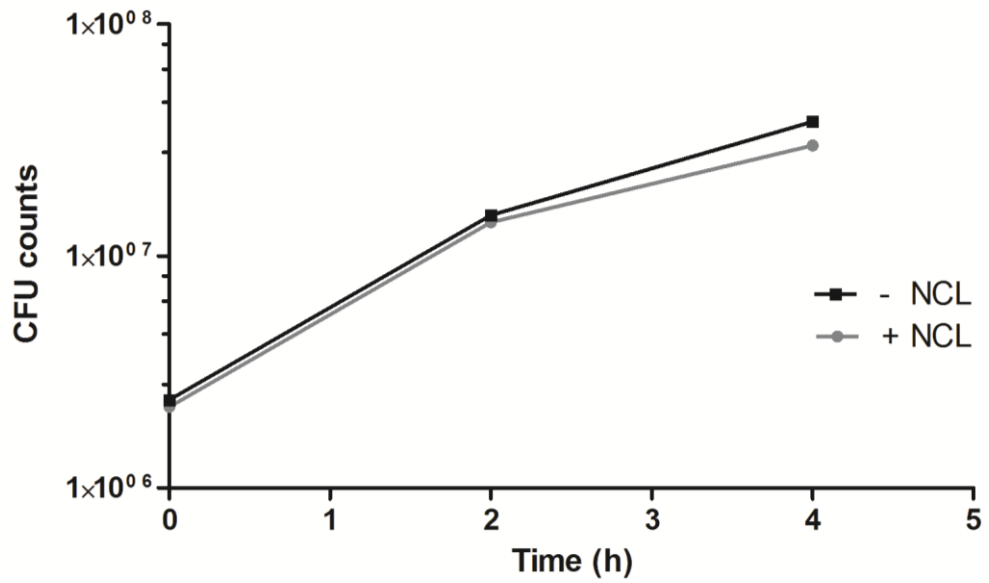


**Figure 5. NCL does not affect the viability of *E. coli in vitro*.** *E. coli* AB1157 CBR were incubated with 100  $\mu$ M NCL and cultured at 37°C for 4 h. Aliquots of the bacterial culture were taken every hour and plated on selective agar overnight. No significant difference ( $p > 0.05$ ) in CFU counts between NCL treated and untreated bacteria was observed. Error bars represent SD.  $n=3$ .

***In vitro* light production from bacteria activated NCL with 4T1 cells as the source of luciferase**

*In vitro* incubation of NCL in the presence of wt *E. coli* AB1157 and luciferase producing 4T1 murine breast cancer cells (4T1 luc) resulted in the production of light. Following NCL reduction by bacterial nitroreductases, free luciferin entered 4T1 cells where cell produced luciferase was available for completion of the luciferase-luciferin reaction and production of light. Luminescence from wells containing NCL, bacteria and 4T1 luc cells was detected using the IVIS Lumina and the intensity of light produced was quantified. Luminescence was measured 2 h post incubation with NCL (or PBS) and was determined to be significantly greater ( $p=0.048$ ) than luminescence from wells that contained wild type 4T1 cells and luciferase producing (CBR+) *E. coli* in the presence of NCL. The luminescence signal from samples that contained the luc+ cancer cells, bacteria and NCL was determined to be 220% greater than wild type 4T1 cancer cells plus CBR+ bacteria and NCL 2 h post probe incubation ( $3.06 \times 10^6$  vs  $1.39 \times 10^6$  p/sec/cm<sup>2</sup>/sr) (Figure 6).

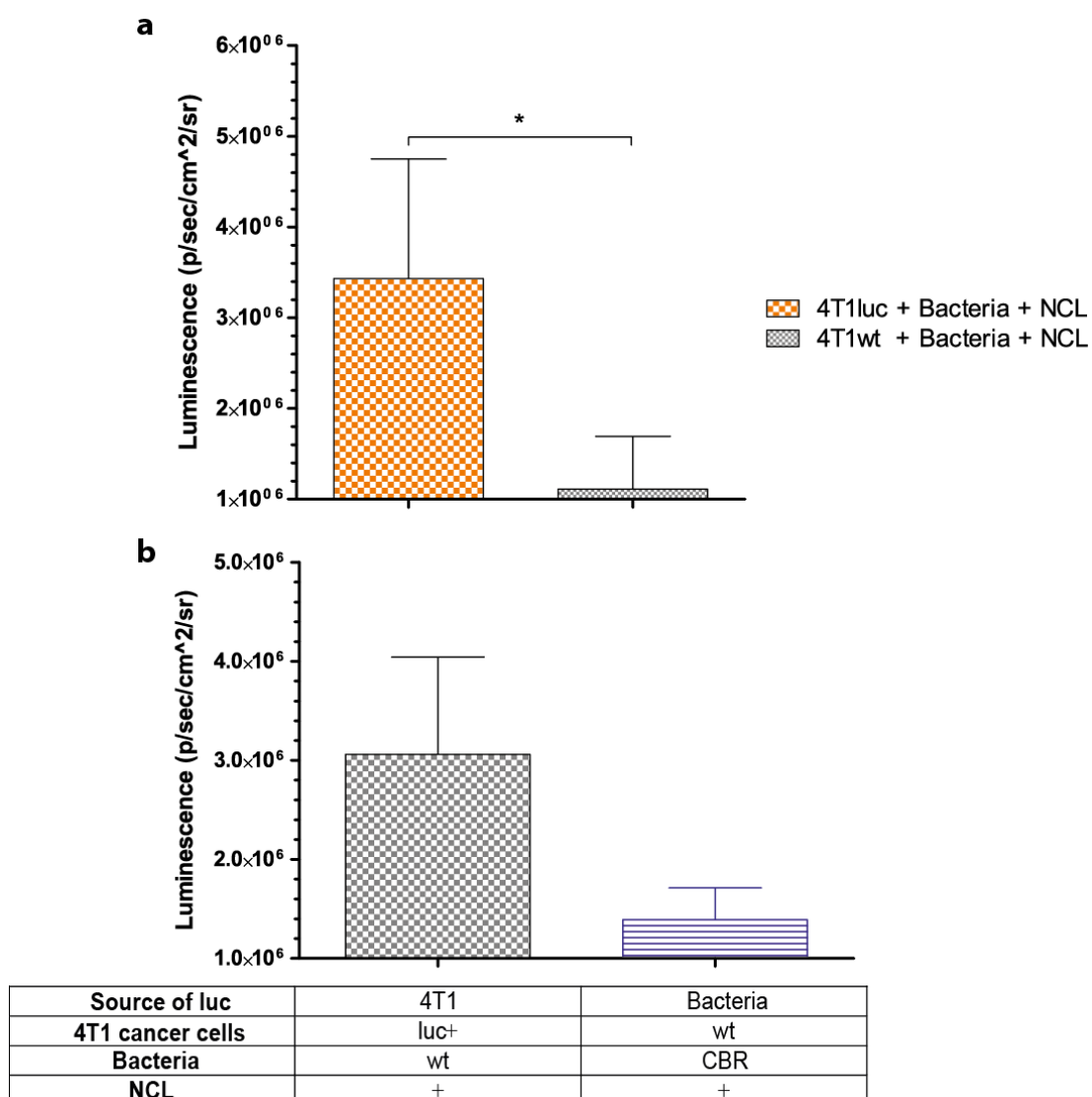


**Figure 6. *In vitro* light production from bacteria activated NCL with cancer cells as the source of luciferase.** a) An increase in luminescence was observed *in vitro* when luc+ cancer cells were incubated with bacteria activated NCL. 10 min post NCL incubation, luminescence from these wells was observed to be significantly greater ( $p < 0.05$ ) than from wells containing wild type 4T1 cells. b) Light production from uncaged NCL with either cancer cells or bacterial cells as the source of luciferase. Luminescence readings taken from wells containing NCL and 4T1 cells +/- luc and E coli +/- CBR 2 h post incubation with NCL.

### **Route of NCL administration for *in vivo* experiments**

In order to determine the optimal route of NCL administration to BALB/c mice, luminescence from *E. coli* infected quadriceps muscles was quantified following either intravenous (IV) or intraperitoneal (IP) injection of 20 mM NCL (Figure 7). Regions of interest drawn around the mouse hind legs were used to determine the level of luminescence from the infected muscle at various timepoints following NCL administration. Over the duration of the experiment there was no significant difference ( $p>0.05$ ) between the IV and IP groups. With consideration to this result it was decided to proceed with IP probe administration. IP injection presents a technically more simple method of probe injection than IV and also facilitates repeated probe injection in a single day, if necessary, which is in contrast to IV injection where repeated injection into the lateral tail vein is unfeasible.

### **Luminescence from NCL outlasts D-luciferin *in vivo*.**

BALB/c were injected with  $5 \times 10^7$  *E. coli* CBR and IP injected with either NCL or D-luciferin. Mice were imaged from luminescence from infected muscle for 48 h and the level of signal acquired was compared between the two groups. In keeping with the *in vitro* data, luminescence from D-luciferin injected mice exceeded NCL over the first 4 h. However, the difference in luminescence was not significant. When the luminescent signal was tracked over the course of 48 h, mice that received NCL were shown to maintain a luminescent signal that exceeded background (uninfected muscle) while luminescence from limbs containing bacteria and D-luciferin returned to background levels after less than 18 h (Figure 8).

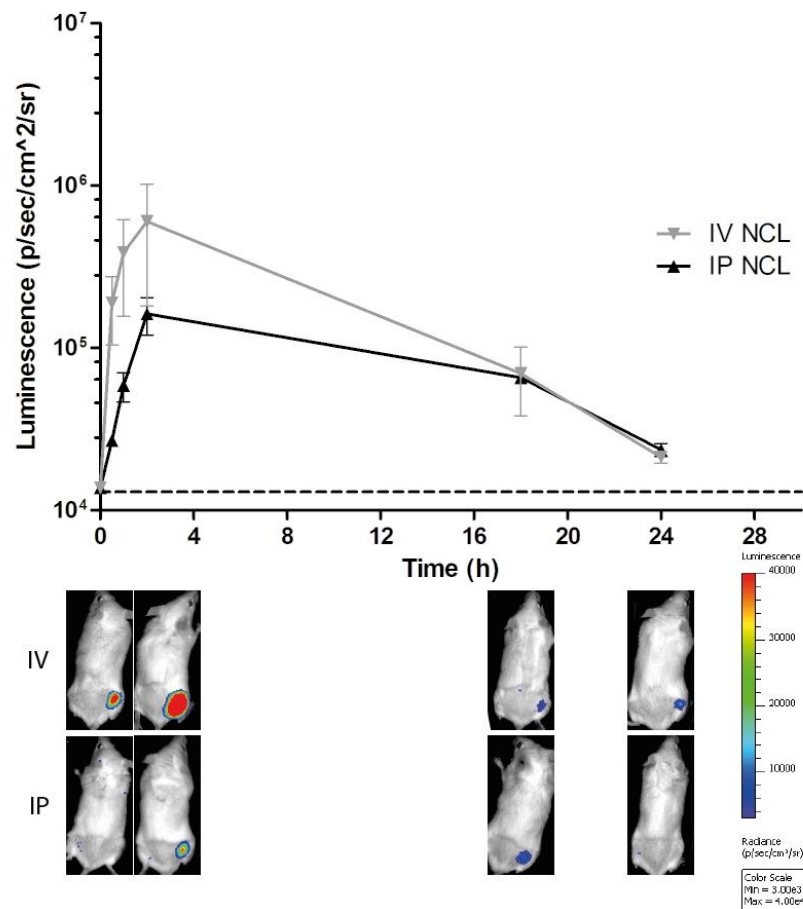


**Figure 7. Evaluation of intravenous versus intraperitoneal routes of administration of NCL for luminescent imaging of *E. coli* infected quadriceps.** BALB/c mice were injected with 10<sup>7</sup> *E. coli* in the quadriceps. Following muscle infection mice received a 20 mM injection of NCL either via IP or IV administration. Mice were imaged for luminescence at regular intervals post probe administration. No significant difference in fluorescence was observed between IV and IP groups ( $p > 0.05$ ).  $n = 4$  for both groups. Pictures of mice shown below the graphs are randomly selected representative images for each group. Error bars represent SEM. The dotted black line represents the average luminescence value from uninfected limbs.

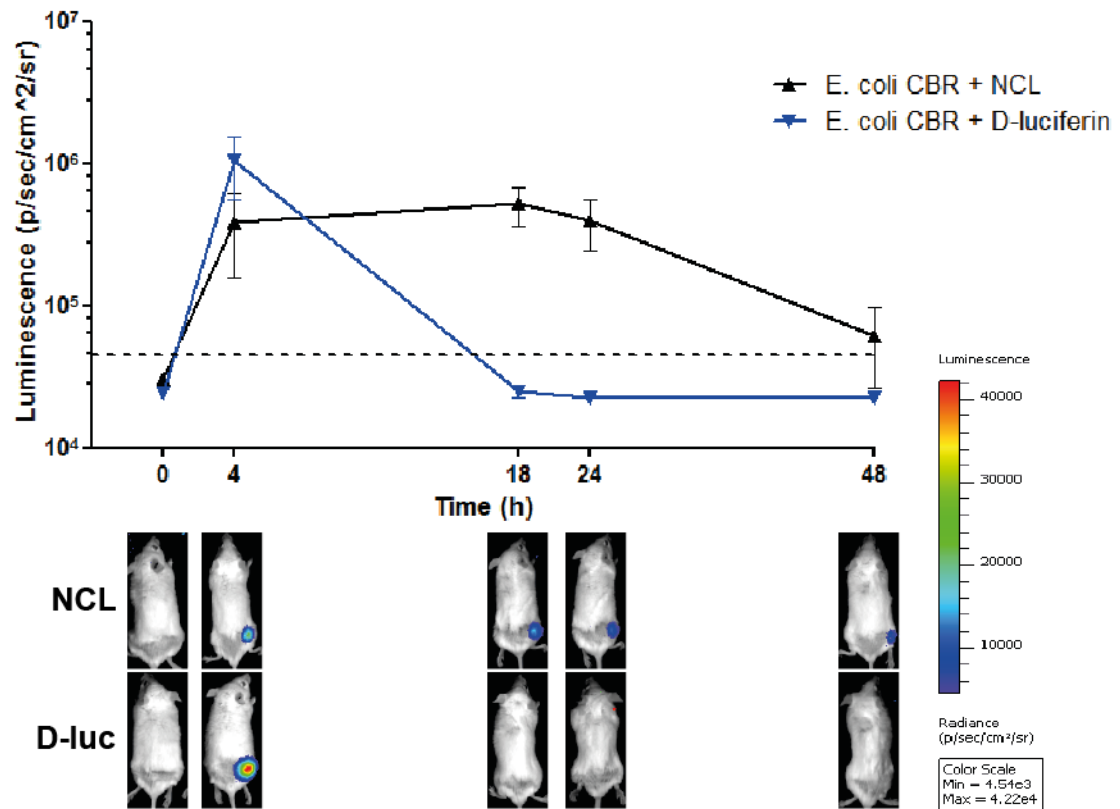


**Figure 8. Duration of luminescence from NCL and D-luciferin. Luminescence from infected muscle is maintained for longer following NCL injection than following D-luciferin.** BALB/c mice with *E. coli* infected quadriceps were injected with either NCL or D-luciferin and tracked for changes in luminescence over 48 h. Luminescence from mice that received D-luciferin was initially higher than NCL but had returned to background levels after approximately 18 h post probe injection. Luminescence from mice that received NCL was maintained for over 48 h. n=3. Error bars represent SEM. Images shown below the graph are representative of mice in that group.

### ***In vivo* comparison of NCL with CytoCy5S**

As a further characterisation of the NCL probe a direct comparison with CytoCy5S (Chapter 2) was made *in vivo* in an intramuscular infection model. BALB/c mice with *E. coli* infected ( $5 \times 10^6$ ) quadriceps were imaged for fluorescence or luminescence to establish the level of background signal. Mice were then injected with either CytoCy5S or NCL and imaged accordingly 1 h post probe administration. The relative increase in signal compared to the previously established background level was calculated by dividing the ROI reading at 1 h by the background reading. The fold increase in signal for both probes is shown in Figure 9. A 4.47 fold increase in fluorescence from infected muscle was observed in mice that received CytoCy5S while a slightly higher, and non-significant ( $p>0.05$ ), increase was observed in mice that received NCL (4.76 fold increase).

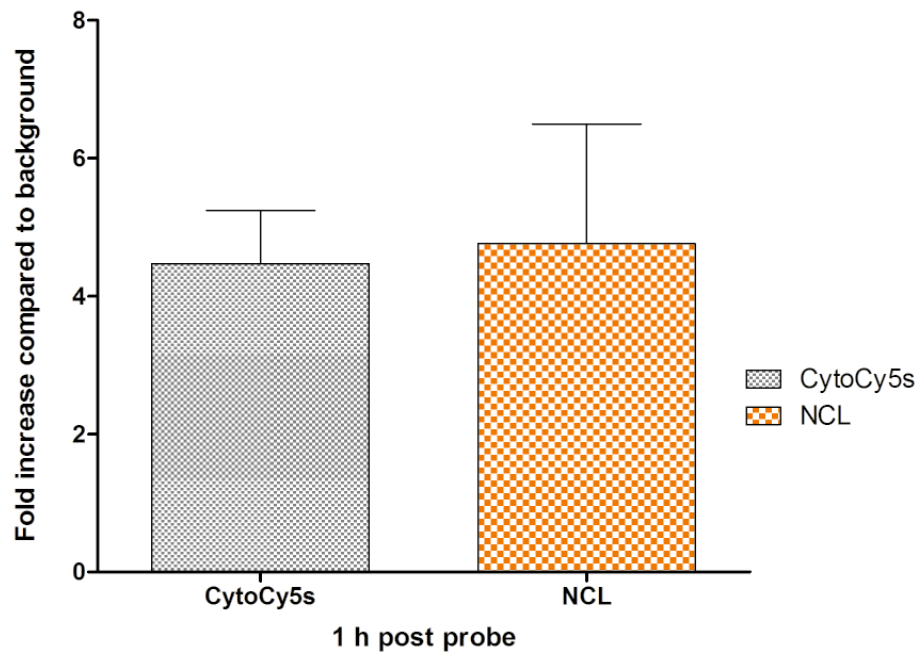


**Figure 9. Direct comparison of the increase in *in vivo* signal from *E. coli* between CytoCy5S and NCL treated mice.** BALB/c mice with *E. coli* infected quadriceps received an IP injection of either CytoCy5S or NCL. Mice were imaged for fluorescence (CytoCy5S) or luminescence (NCL) 1 h post probe administration and the relative increase in signal compared to pre-probe background signal was determined. Mice that received NCL showed a slightly higher increase in signal compared to mice that received CytoCy5S (4.76 fold vs 4.47 fold). Error bars represent SEM. n=3.

### **Imaging of bacterial NTR *in vivo* in a mouse model of intramuscular infection**

The utility, and importantly, the specificity, of the probe *in vivo* was examined in a mouse model of thigh muscle infection, again utilising bacteria as the source of both NTR and luciferase. BALB/c mice were injected in quadriceps with various numbers of *E. coli* luc+ ( $5 \times 10^4 - 5 \times 10^7$ ), followed by IP injection of NCL 30 min later (Figure 10a). Animals were imaged at various time points over 24 h (Figure 10c). Signal from the probe was detected 20 min post injection lasting for as long as 24 h and correlated with the amount of probe injected. The intensity increased over the first 4 h reaching plateau afterwards. The total photon flux produced during this time was approximately 1/3 of the total flux detected from the mice injected with luciferin, demonstrating high efficiency of uncaging by bacterial NTR *in vivo* (Figure 10b).

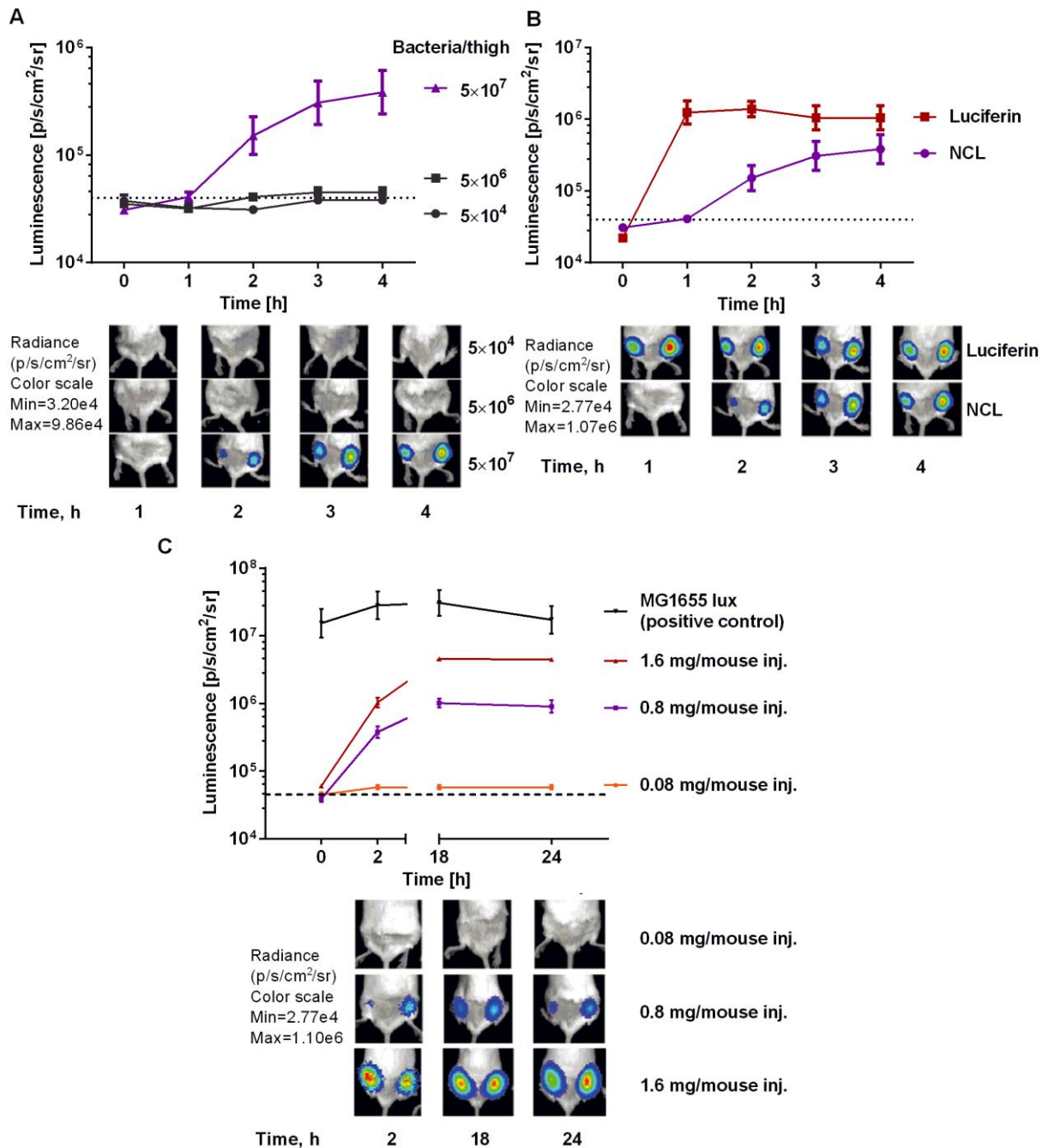


**Figure 10.** *In vivo* activation of NCL probe by luciferase and nitroreductase expressing *E. coli* in a mouse model of thigh infection. a). Luminescence over 4 h from *E. coli luc+* infected quadriceps ( $5 \times 10^4$ – $5 \times 10^7$  bacteria) after IP injection of 0.8 mg NCL probe (200  $\mu$ l of 10 mM solution in PBS). b). Luminescence over 4 h from *E. coli luc+* infected quadriceps ( $5 \times 10^7$  bacteria) following IP injection of 0.8 mg of probe or 0.63 mg of luciferin (200  $\mu$ l of 10 mM solution in PBS). c). Luminescence imaging of mice over 24 h bearing  $5 \times 10^7$  bacteria treated with various (0.08, 0.8 and 1.6 mg) NCL probe concentrations (200  $\mu$ l of 1, 10 and 20 mM solutions of NCL in PBS). As a positive control, mice were injected with equal amounts of *E. coli* MG1655 expressing lux luciferase that doesn't require exogenous substrate for light production [45]. The signal was collected over 24 h, n = 3. Images of mice shown below the graph are randomly selected representative images of mice in the group.

### **Imaging of bacterial NTR activity in a mouse model of *Salmonella* infection**

As a means for testing the ability of NCL to act as a probe for the non-invasive detection of infectious bacteria, BALB/c mice were intravenously injected with luc+ *Salmonella enterica* Typhimurium UK-1 (*Salmonella* CBR). A subset of mice received lux tagged *Salmonella* to facilitate luminescence imaging of bacterial localisation *in vivo* and thereby allow for the determination of when a chronic infection had been established in the liver and spleen of the mice. Once this group of mice showed signs of chronic infection by BL imaging (4 days post bacteria injection), the remaining mice received an IP injection of 10 mM NCL. Mice were then imaged for the presence of a luminescent emanating from within infected organs where NCL had been reduced by NTR expressing *Salmonella* CBR. However, the low level of BL detected in mice that received lux tagged *Salmonella* strongly indicates that the level of infection of the liver or spleen was low. As a result of this, the NCL was most likely not reduced in adequate amounts to produce sufficient light for *in vivo* detection using the IVIS. No luminescent signal above background (obtained from uninfected mice) was detected in mice that received *Salmonella* CBR + NCL (Figure 11).

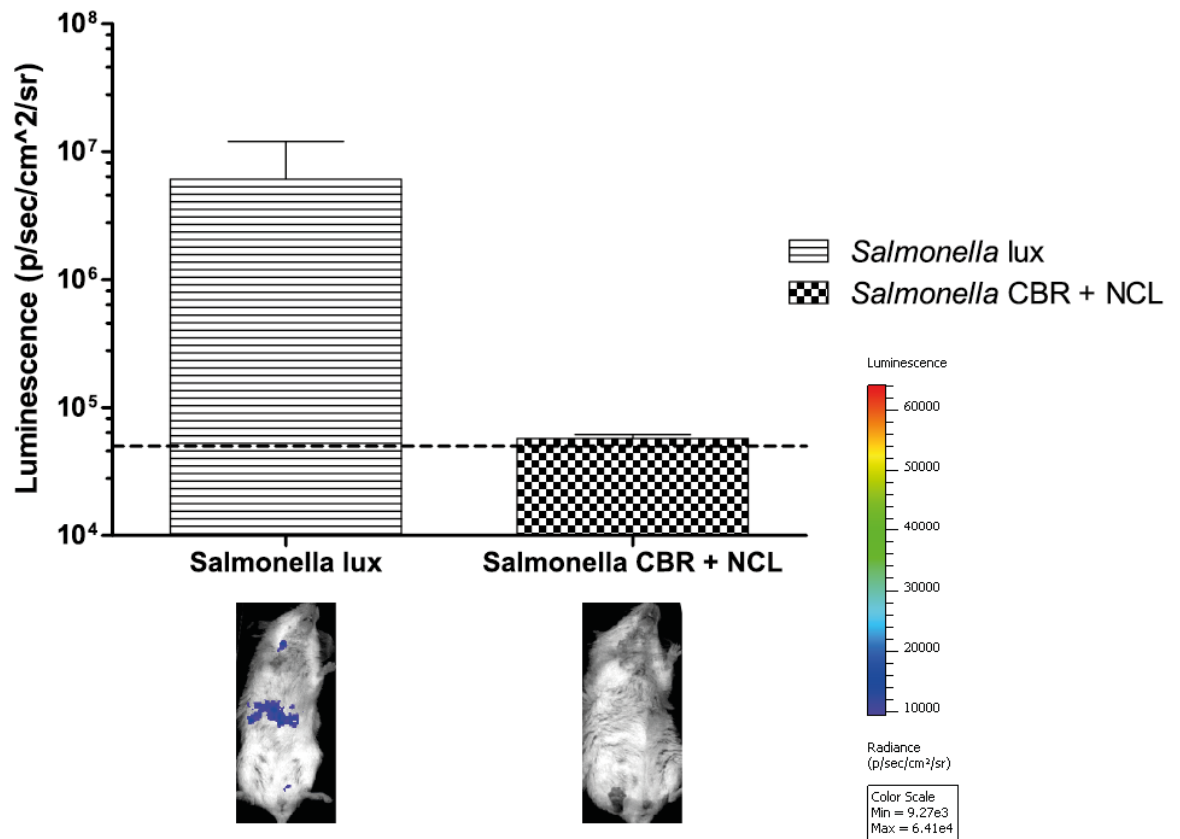


**Figure 11. *In vivo* detection of infection from NTR expressing *Salmonella* CBR using NCL.** BALB/c mice received an IV injection of *Salmonella enterica* Typhimurium UK1 wt, CBR or lux. Mice that received lux tagged *Salmonella* were then tracked by BLI for the onset of chronic infection in the liver and spleen. Once infection was determined to have occurred four days post bacteria injection, mice that had been infected with *Salmonella* CBR received an IP injection of 10 mM NCL and were imaged for luminescence from *Salmonella* colonised organs. No luminescent signal that exceeded control luminescence from wt *Salmonella* infected mice (dotted black line) was observed. Images were collected 45 min post probe injection. n=3. Pictures are of representative mice from each group.

### **Imaging of NTR activity in subcutaneous xenograft model of cancer**

In order to further determine the utility of NCL the probe was investigated as a tool for imaging tumours in a cancer xenograft model in mice (Figure 12). BALB/c mice bearing subcutaneous 4T1luc tumours were injected via the lateral tail vein with  $5 \times 10^5$  *E. coli* MG1655. One week post bacterial injection, mice that received lux tagged bacteria were imaged for luminescence to confirm that tumour colonisation had occurred. Following this, the remainder of mice (that had received wild type *E. coli* or PBS) were IP injected with NCL. Mice were imaged for luminescence 4 h post probe injection, and bacteria-containing 4T1luc tumour bearing mice showed a strong, tumour localised luminescent signal ( $1.69 \times 10^8$ ) and no luminescence from any organs of the body indicating that probe activation had been confined to the bacteria colonised tumour site. Luminescence from these tumours was significantly greater ( $p < 0.05$ ) than luminescence from mice bearing bacteria colonised tumours that did not receive NCL, mice bearing tumours + bacteria and mice with 4T1 wt (luc-) tumours colonised with *E. coli* and injected with NCL. Low level luminescence was observed in tumours of mice bearing luc+ tumours that did not receive bacteria but were injected with NCL, ( $1.69 \times 10^7$ ) which was a log fold lower than the bacteria + NCL group, and not significantly greater than control groups.

This experiment demonstrated the utility of NCL for use in a murine model of cancer where the tumour is the source of luciferase and the tumour colonising bacteria were the source of NTR.

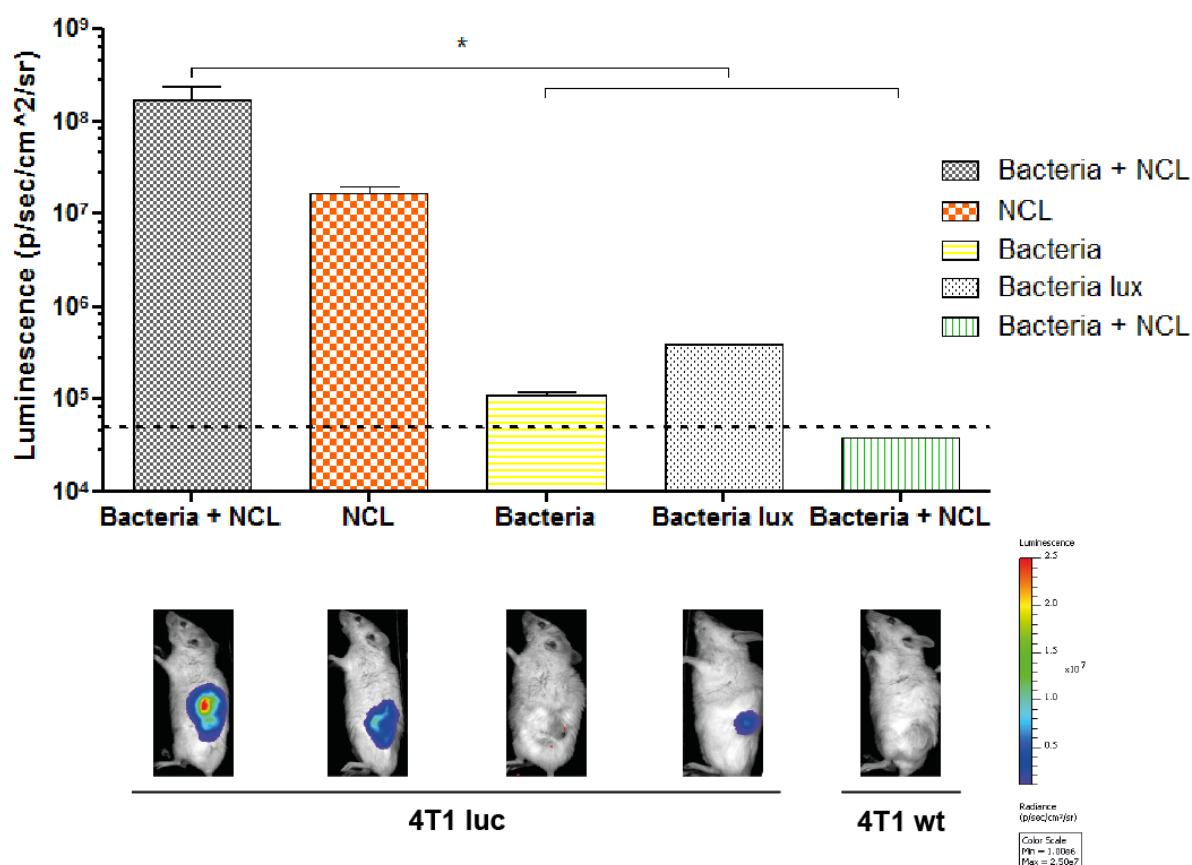


**Figure 12. Bacterial mediated *in vivo* imaging of NCL in a murine model of cancer.** BALB/c mice bearing subcutaneous 4T1luc tumours were colonised with *E. coli*. Following IP injection of NCL, mice were imaged for luminescence. Active NCL luminescence from bacteria colonised tumours was observed to be a log fold higher than from uncolonised tumours and significantly greater ( $p < 0.05$ ) than in mice that did not receive probe or bore luc- 4T1 tumours and received bacteria + NCL. Error bars represent SEM.  $n = 3-5$ . The dotted line represents autoluminescence and the images of mice below the graph are randomly chosen images representative of the group.

## Discussion

In this chapter, a novel caged luciferin probe was tested and evaluated in multiple *in vitro* and *in vivo* models. NCL was demonstrated to be effective for real-time imaging of NTR activity *in vitro* in live bacteria and mammalian cells, as well as *in vivo* where NCL was utilised for the non-invasive detection of bacteria in models of thigh infection and a preclinical model of cancer. This novel reagent has the potential to significantly simplify screening of prodrugs *in vivo* and accelerate the preclinical development of enzyme-activatable therapeutics for translation into the clinic.

Cell free assays demonstrated 70% conversion of caged NCL to free luciferin which is higher than all other caged luciferins currently available. In the presence of luc+ *E. coli*, NCL reduction was achieved and the role of the major *E. coli* NTRs was evaluated. Comparison of probe uncaging between NTR competent bacteria and NTR KO strains showed that while the three main *E. coli* NTRs play a major role in NCL uncaging, the remainder of the reductases are also capable of uncaging the probe at detectable levels. Bacterial cell viability assays were used to determine the effect of NCL on the viability of cells *in vitro* and the results demonstrated that the probe does not affect bacterial viability. When cancer cells were used as the source of luciferase and bacteria provided NTR, NCL activation was seen to be significantly greater ( $p < 0.05$ ) than probe free controls and also exceeded the luminescent signal from wells that contained cancer cells in co-culture with luc+ NTR producing bacteria at 2 h post NCL incubation.

*In vivo* testing of NCL revealed that  $10^7$  bacteria localised to the thigh muscle are required for the production of light on a level sufficient for detection using the IVIS Lumina. The level of luminescence observed was also shown to be dependent

on the concentration of probe administered to mice bearing muscle localised *E. coli*. Direct comparison of NCL with the fluorescent probe CytoCy5S (discussed in Chapter 2) showed that the observed increase in signal 1 h post probe incubation in a model of thigh infection was higher in mice that received NCL. This further highlights the utility of this luminescent probe. However, in a model of *Salmonella* infection, no luminescence was observed from the liver or spleen of infected mice. Analysis of images obtained from mice that were infected with luminescent *Salmonella* indicated that the degree of infection (as determined by the number of bacteria in the liver or spleen) may not have been sufficient to allow for NCL uncaging at an imageable level.

When NCL was applied to a murine cancer model for tumour imaging, it was shown that a strong, tumour localised luminescent signal can be acquired when the 4T1 tumour acts as the source of luc and tumour colonising *E. coli* express NTRs specifically within the tumour site following colonisation. In the absence of injected *E. coli*, a high level of probe uncaging was still observed. This may be due to the presence of other bacteria within the tumour following natural colonisation.

## References

1. Oliveira, I.M., Bonatto, D. , Henriques, J. A., *Nitroreductases: Enzymes with Environmental, Biotechnological and Clinical Importance*. Current Research, Technology and Education Topics in Applied Microbiology and Microbial Biotechnology, ed. A. Méndez-Vilas. Vol. 2. 2010, Spain: Formatex Badajoz.
2. Prosser, G.A., et al., *Discovery and evaluation of Escherichia coli nitroreductases that activate the anti-cancer prodrug CB1954*. Biochem Pharmacol, 2010. **79**(5): p. 678-87.
3. Zenno, S., et al., *Biochemical characterization of NfsA, the Escherichia coli major nitroreductase exhibiting a high amino acid sequence homology to Frp, a Vibrio harveyi flavin oxidoreductase*. J Bacteriol, 1996. **178**(15): p. 4508-14.
4. Zenno, S., et al., *Gene cloning, purification, and characterization of NfsB, a minor oxygen-insensitive nitroreductase from Escherichia coli, similar in biochemical properties to FRase I, the major flavin reductase in Vibrio fischeri*. J Biochem, 1996. **120**(4): p. 736-44.
5. Cellitti, S.E., et al., *Structure of Ddn, the deazaflavin-dependent nitroreductase from Mycobacterium tuberculosis involved in bio-reductive activation of PA-824*. Structure, 2012. **20**(1): p. 101-12.
6. Jenks, P.J. and D.I. Edwards, *Metronidazole resistance in Helicobacter pylori*. Int J Antimicrob Agents, 2002. **19**(1): p. 1-7.
7. Patterson, S. and S. Wyllie, *Nitro drugs for the treatment of trypanosomatid diseases: past, present, and future prospects*. Trends in Parasitology, 2014. **30**(6): p. 289-298.
8. Pal, D., et al., *Giardia, Entamoeba, and Trichomonas enzymes activate metronidazole (nitroreductases) and inactivate metronidazole (nitroimidazole reductases)*. Antimicrob Agents Chemother, 2009. **53**(2): p. 458-64.
9. Louis, P., G.L. Hold, and H.J. Flint, *The gut microbiota, bacterial metabolites and colorectal cancer*. Nat Rev Micro, 2014. **12**(10): p. 661-672.
10. McBain, A.J. and G.T. Macfarlane, *Ecological and physiological studies on large intestinal bacteria in relation to production of hydrolytic and reductive*

- enzymes involved in formation of genotoxic metabolites. J Med Microbiol*, 1998. **47**(5): p. 407-16.
11. Xu, G. and H.L. McLeod, *Strategies for enzyme/prodrug cancer therapy. Clin Cancer Res*, 2001. **7**(11): p. 3314-24.
  12. Cronin, M., et al., *Bacterial vectors for imaging and cancer gene therapy: a review. Cancer Gene Ther*, 2012. **19**(11): p. 731-40.
  13. Patel, P., et al., *A phase I/II clinical trial in localized prostate cancer of an adenovirus expressing nitroreductase with CB1954 [correction of CB1984]. Mol Ther*, 2009. **17**(7): p. 1292-9.
  14. Bryant, L.M., et al., *Lessons learned from the clinical development and market authorization of Glybera. Human gene therapy Clinical development*, 2013. **24**(2): p. 55-64.
  15. Massoud, T.F. and S.S. Gambhir, *Molecular imaging in living subjects: seeing fundamental biological processes in a new light. Genes & Development*, 2003. **17**(5): p. 545-580.
  16. Prescher, J.A. and C.H. Contag, *Guided by the light: visualizing biomolecular processes in living animals with bioluminescence. Curr Opin Chem Biol*, 2010. **14**(1): p. 80-9.
  17. Leblond, F., et al., *Pre-clinical whole-body fluorescence imaging: Review of instruments, methods and applications. J Photochem Photobiol B*, 2010. **98**(1): p. 77-94.
  18. Cui, L., et al., *A new prodrug-derived ratiometric fluorescent probe for hypoxia: high selectivity of nitroreductase and imaging in tumor cell. Org Lett*, 2011. **13**(5): p. 928-31.
  19. James, A.L., et al., *Fluorogenic substrates for the detection of microbial nitroreductases. Lett Appl Microbiol*, 2001. **33**(6): p. 403-8.
  20. Li, Z., et al., *7-((5-Nitrothiophen-2-yl)methoxy)-3H-phenoxazin-3-one as a spectroscopic off-on probe for highly sensitive and selective detection of nitroreductase. Chem Commun (Camb)*, 2013. **49**(52): p. 5859-61.
  21. Li, Z., et al., *Nitroreductase detection and hypoxic tumor cell imaging by a designed sensitive and selective fluorescent probe, 7-[(5-nitrofuran-2-yl)methoxy]-3H-phenoxazin-3-one. Anal Chem*, 2013. **85**(8): p. 3926-32.

22. Shi, Y., S. Zhang, and X. Zhang, *A novel near-infrared fluorescent probe for selectively sensing nitroreductase (NTR) in an aqueous medium*. Analyst, 2013. **138**(7): p. 1952-5.
23. Bhaumik, S., et al., *Noninvasive optical imaging of nitroreductase gene-directed enzyme prodrug therapy system in living animals*. Gene Ther, 2012. **19**(3): p. 295-302.
24. McCormack, E., et al., *Nitroreductase, a near-infrared reporter platform for in vivo time-domain optical imaging of metastatic cancer*. Cancer Res, 2013. **73**(4): p. 1276-86.
25. Sekar, T.V., et al., *Noninvasive theranostic imaging of HSV1-sr39TK-NTR/GCV-CB1954 dual-prodrug therapy in metastatic lung lesions of MDA-MB-231 triple negative breast cancer in mice*. Theranostics, 2014. **4**(5): p. 460-74.
26. Gross, S., et al., *Bioluminescence imaging of myeloperoxidase activity in vivo*. Nat Med, 2009. **15**(4): p. 455-61.
27. Liu, L. and R.P. Mason, *Imaging beta-galactosidase activity in human tumor xenografts and transgenic mice using a chemiluminescent substrate*. PLoS One, 2010. **5**(8): p. e12024.
28. Ando, Y., et al., *Development of a quantitative bio/chemiluminescence spectrometer determining quantum yields: re-examination of the aqueous luminol chemiluminescence standard*. Photochem Photobiol, 2007. **83**(5): p. 1205-10.
29. White, E.H. and D.F. Roswell, *Chemiluminescence of Organic Hydrazides*. Accounts of Chemical Research, 1970. **3**(2): p. 54-&.
30. Ando, Y., et al., *Firefly bioluminescence quantum yield and colour change by pH-sensitive green emission*. Nat Photon, 2008. **2**(1): p. 44-47.
31. Viviani, V.R., et al., *Bioluminescence of Beetle Luciferases with 6'-Amino-d-luciferin Analogues Reveals Excited Keto-oxyluciferin as the Emitter and Phenolate/Luciferin Binding Site Interactions Modulate Bioluminescence Colors*. Biochemistry, 2014. **53**(32): p. 5208-5220.
32. Zhang, N., et al., *Enhanced detection of myeloperoxidase activity in deep tissues through luminescent excitation of near-infrared nanoparticles*. Nat Med, 2013. **19**(4): p. 500-5.

33. Razgulin, A., N. Ma, and J. Rao, *Strategies for in vivo imaging of enzyme activity: an overview and recent advances*. Chem Soc Rev, 2011. **40**(7): p. 4186-216.
34. Goun, E.A., et al., *Molecular transporters: synthesis of oligoguanidinium transporters and their application to drug delivery and real-time imaging*. Chembiochem, 2006. **7**(10): p. 1497-515.
35. Cohen, A.S., et al., *Real-time bioluminescence imaging of glycans on live cells*. Journal of the American Chemical Society, 2010. **132**(25): p. 8563-8565.
36. Van de Bittner, G.C., et al., *In vivo imaging of hydrogen peroxide production in a murine tumor model with a chemoselective bioluminescent reporter*. Proc Natl Acad Sci U S A, 2010. **107**(50): p. 21316-21.
37. Henkin, A.H., Cohen, A. S., Dubikovskaya, E. A., Park, H. M., Nikitin, G. F., Auzias, M. G., Kazantzis, M., Bertozzi, C. R., Stahl, A. , *Real-time noninvasive imaging of fatty acid uptake in vivo*. ACS Chem Biol, 2012. **7**: p. 1884–1891.
38. Wehrman, T.S., et al., *Luminescent imaging of beta-galactosidase activity in living subjects using sequential reporter-enzyme luminescence*. Nat Methods, 2006. **3**(4): p. 295-301.
39. Hickson, J., et al., *Noninvasive molecular imaging of apoptosis in vivo using a modified firefly luciferase substrate, Z-DEVD-aminoluciferin*. Cell Death Differ, 2010. **17**(6): p. 1003-10.
40. Scabini, M., et al., *In vivo imaging of early stage apoptosis by measuring real-time caspase-3/7 activation*. Apoptosis, 2011. **16**(2): p. 198-207.
41. Shah, K., et al., *In vivo imaging of S-TRAIL-mediated tumor regression and apoptosis*. Mol Ther, 2005. **11**(6): p. 926-31.
42. Dragulescu-Andrasi, A., G. Liang, and J. Rao, *In vivo bioluminescence imaging of furin activity in breast cancer cells using bioluminogenic substrates*. Bioconjug Chem, 2009. **20**(8): p. 1660-6.
43. Yao, H., M.K. So, and J. Rao, *A bioluminogenic substrate for in vivo imaging of beta-lactamase activity*. Angew Chem Int Ed Engl, 2007. **46**(37): p. 7031-4.
44. Vorobyeva, A.G., et al., *Development of a Bioluminescent Nitroreductase Probe for Preclinical Imaging*. PloS one, 2015. **10**(6).

45. Cronin, M., et al., *High resolution in vivo bioluminescent imaging for the study of bacterial tumour targeting*. PloS one, 2012. **7**(1): p. e30940.
46. Cronin, M., et al., *Bacterial-mediated knockdown of tumor resistance to an oncolytic virus enhances therapy*. Molecular Therapy, 2014. **22**(6): p. 1188-1197.
47. Mercier, C., et al., *Characteristics of major Escherichia coli reductases involved in aerobic nitro and azo reduction*. Journal of applied microbiology, 2013. **115**(4): p. 1012-1022.
48. Stanton, M., et al., *In Vivo Bacterial Imaging without Engineering; A Novel Probe-Based Strategy Facilitated by Endogenous Nitroreductase Enzymes*. Current gene therapy, 2015. **15**(3): p. 277-288.
49. Prekeges, J.L., et al., *Reduction of fluoromisonidazole, a new imaging agent for hypoxia*. Biochemical pharmacology, 1991. **42**(12): p. 2387-2395.
50. Krohn, K.A., J.M. Link, and R.P. Mason, *Molecular imaging of hypoxia*. Journal of Nuclear Medicine, 2008. **49**(Suppl 2): p. 129S-148S.
51. Sisson, G., et al., *Enzymes associated with reductive activation and action of nitazoxanide, nitrofurans, and metronidazole in Helicobacter pylori*. Antimicrob Agents Chemother, 2002. **46**(7): p. 2116-23.
52. Celli, C.M., et al., *NRH: quinone oxidoreductase 2 (NQO2) catalyzes metabolic activation of quinones and anti-tumor drugs*. Biochemical pharmacology, 2006. **72**(3): p. 366-376.
53. Wilson, W.R. and M.P. Hay, *Targeting hypoxia in cancer therapy*. Nature Reviews Cancer, 2011. **11**(6): p. 393-410.
54. Branchini, B.R., et al., *Site-directed mutagenesis of firefly luciferase active site amino acids: a proposed model for bioluminescence color*. Biochemistry, 1999. **38**(40): p. 13223-30.
55. Miura, K., et al., *Molecular cloning of the nemA gene encoding N-ethylmaleimide reductase from Escherichia coli*. Biol Pharm Bull, 1997. **20**(1): p. 110-2.

## Chapter 4: Exploitation of endogenous bacterial enzymes for cancer therapy.

Sections from this chapter have been published as

Stanton M., Lehouritis P., McCarthy F.O., Jeavons M. and Tangney M. **Activation of multiple chemotherapeutic prodrugs by the natural enzymolome of tumour-localised probiotic bacteria.** *Journal of Controlled Release*. Under review

&

Lehouritis, P., Cummins, J., Stanton, M., Murphy, C. T., McCarthy, F. O., Reid, G., ... & Tangney, M. (2015). **Local bacteria affect the efficacy of chemotherapeutic drugs.** *Scientific reports*, 5.

## Abstract

Some chemotherapeutic drugs (prodrugs) require activation by an enzyme for efficacy. We and others have demonstrated the ability of probiotic bacteria to grow specifically within solid tumours following systemic administration, and we hypothesised that the natural enzymatic activity of these tumour-localised bacteria may be suitable for activation of certain such chemotherapeutic drugs.

Wild type probiotic bacteria such as *E. coli* Nissle and *Bifidobacterium breve* were screened against a panel of popular prodrugs. All strains were capable of activating at least one prodrug. *E. coli* Nissle 1917 was selected for further studies because of its ability to activate numerous prodrugs and its robust nature. HPLC data confirmed biochemical transformation of prodrugs to their toxic counterparts. Further analysis demonstrated that multiple enzymes can complement prodrug activation, while simultaneous activation of multiple prodrugs (CB1954, 5-FC and Fludarabine Phosphate) by *E. coli* was confirmed, resulting in significant efficacy improvement over single drugs. Experiments in mice harbouring murine tumours validated *in vitro* findings, with significant reduction in tumour growth and increase in survival of mice treated with probiotic bacteria and a combination of prodrugs.

These findings demonstrate the ability of probiotic bacteria, without the requirement for genetic modification, to enable high-level activation of multiple prodrugs specifically at the site of action.

## **Study Aim**

The aim of the work presented in this chapter was to develop a Bacterial Directed Enzyme Prodrug Therapy (BDEPT) based on the activation of multiple prodrugs by endogenously produced bacterial enzymes. It was hypothesised that native bacterial enzymes could be used to specifically activate prodrugs within a tumour site to elicit a therapeutic response while minimising off-target effects.

## Introduction

One of the primary limitations of classical chemotherapy is insufficient tumour selectivity because the therapeutic drug concentration required at the tumour is not achievable without inducing systemic toxicity. Emerging technologies have thus focused on increasing the specificity of the therapeutic agent to the tumour site. Bacteria have the capacity to preferentially proliferate within tumours [1]. The mechanism for this phenomenon is believed to be a function of the nature of the tumour and involves a number of physical characteristics, including leaky tumour vasculature; the tumour microenvironment offering protection from the immune system; as well as a low oxygen and rich nutrient environment derived from dying tumour cells on which bacteria thrive [2]. Tumour targeting by bacteria has been repeatedly demonstrated by several groups over the years with a broad range of genera (e.g. bifidobacteria, salmonellae, clostridia) [3-9]. The use of non-pathogenic strains is preferable for safety reasons, which traditionally necessitates genetic modification in order to provide expression of heterologous therapeutic agents, either by the bacterium itself, or via plasmid transfer to host cells (bactofection) [3].

Enzyme-directed prodrug therapy is a broad term used to describe two-step strategies which aim to localise chemotherapeutic activity to the site of the tumour, thereby limiting adverse side effects and permitting administration of higher drug doses. Traditionally, a gene coding for an enzyme that has the ability to convert a non-toxic prodrug to a toxic drug is used to arm a cancer gene therapy vector (e.g. virus [10] ligand [11], antibody [12], bacterium [13]). Firstly, the vector is administered to the patient in order to deliver the gene to the tumour cells. There, the gene becomes expressed and sensitises the cells to a specific prodrug. In the second step, the relevant prodrug is administered to the patient and is converted to a toxic

drug specifically by enzyme-expressing tumour cells resulting in localized toxicity while sparing distant healthy tissue. Various species of bacteria have been examined as tumour-specific gene delivery vehicles in this context at clinical and pre-clinical levels [14, 15] and to date, bacteria have been genetically engineered to over-express genes coding for therapeutic enzymes [14, 16] (Figure 1).

It was hypothesised that; i) since bacteria grow specifically within solid tumours following systemic administration, tumour-localised bacteria may be conceived as a tumour-specific enzymatic reservoir capable of local activation of prodrugs; ii) since bacterial genes are employed in gene therapy strategies to activate prodrugs, native expression of such therapeutic genes by a bacterium may be sufficient to mediate prodrug activation; iii) a given bacterium contains multiple enzymes capable of activation of various prodrugs, so it may be possible to use multiple prodrugs in conjunction with bacteria to treat cancer.

Previously, the Tangney lab has shown that various probiotic bacteria can specifically colonise tumours in murine models [3, 17-19]. In this chapter it is reported that probiotic bacterial species can activate multiple prodrugs, without the need for genetic modification.

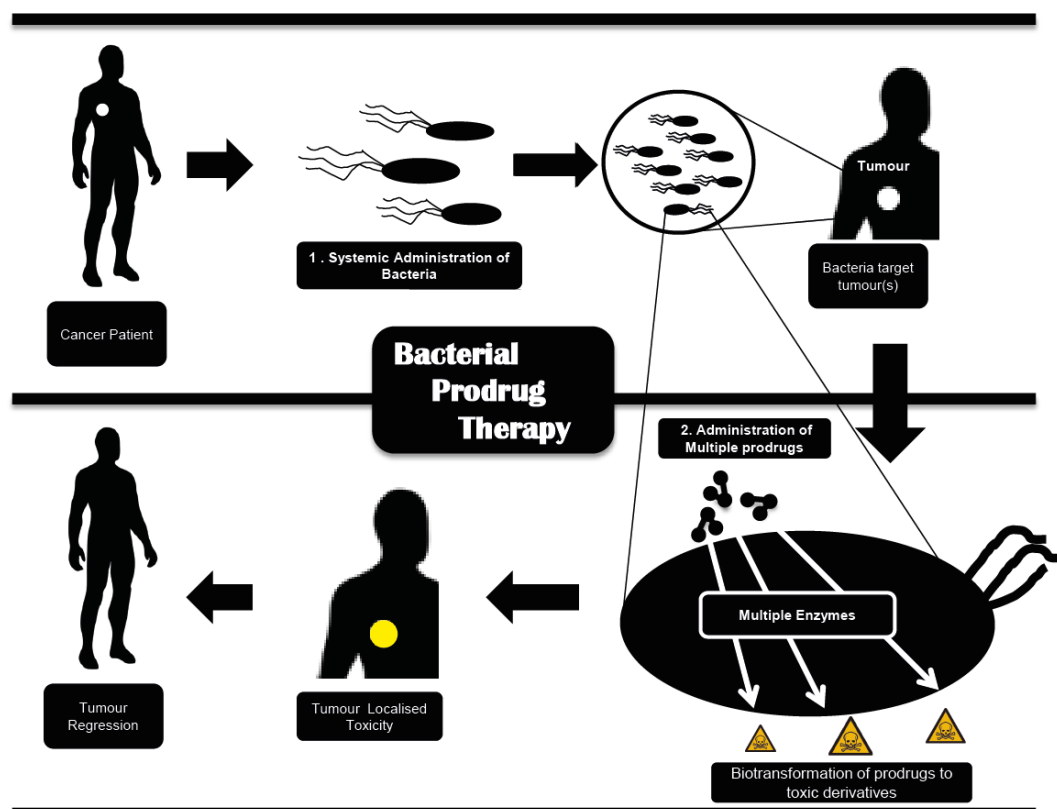


**Figure 1. Schematic representation of bacterial directed enzyme prodrug therapy (BDEPT).** Systemically administered bacteria are capable of selectively colonising solid tumours *in vivo*. These tumour localised bacteria produce a range of unique bacterial enzymes within the tumour site, some of which may be exploited for the tumour targeted activation of administered prodrugs resulting in highly localised toxicity and tumour regression.

## Materials and methods

**Bacteria and cell lines.** Bacteria were cultured as described in Chapter 2. Lewis Lung Carcinoma (LLC), 4T1 (mouse mammary carcinoma) and CT26 (mouse colorectal carcinoma) cells were purchased from ATCC and were propagated according to the supplier's instructions. The murine recycled prostate cancer cell line TRAMPC1 was kindly provided by Ciavarra RP [20] of Eastern Virginia Medical School, Norfolk USA, and propagated as described in [21].

**Drugs.** All drugs and enzymes were purchased from Sigma except: Etoposide Phosphate (Santa Cruz), Capecitabine (Santa Cruz), AQ4N (R&D), Nelarabine (A&B), and Vidarabine (Santa Cruz). Drugs were resuspended in H<sub>2</sub>O or DMSO, with appropriate control vehicle utilised accordingly in all experiments.

**Cell cytotoxicity assay.** Microtitre plates (96-well) were pre-seeded with 4000 cells/well in appropriate medium for each cell line and allowed to attach overnight. On the day of the assay, bacteria were cultured to log-phase and a subculture ratio, corresponding to an OD<sub>600nm</sub> of 0.2 determined for each strain, was exposed for 2 h (4 h in the case of IC<sub>50</sub>s) to drug in falcon tubes containing DMEM in a tissue culture incubator. Falcon content was filter-sterilized to remove presence of bacteria (using 0.2 µm pore filters (Sarstedt) before adding 200 µl per well. Plates were incubated until cells in control (untreated) had achieved confluent growth. Cytotoxicity was quantified using an MTS staining with the Cell Titre 96 AQueous One solution Cell Proliferation Assay (Promega). The plates were incubated with normal media (80 µl) and MTS solution (20 µl) in a 37°C incubator for approximately 2 h (until distinct change of colour occurred).

**Bacterial plating assay.** Bacteria were grown to log phase and plated directly on to agar plates containing the appropriate growth medium with 200  $\mu$ M CB1954 or without. Colonies were counted and scored after an overnight incubation at 37°C. Survival of bacteria in the presence of CB1954 was expressed in relation to untreated controls.

**Bacterial lysis and heat inactivation.** Bacteria were heat inactivated at 95 °C for 40 min. Lysis was facilitated by sonication using three 10 sec pulses (at 20 Kz, 50 W). Between each pulse, samples were incubated on ice for 30 sec. A 20-fold drop in optical density was considered sufficient lysis.

**Bacterial prodrug susceptibility assay.** Overnight bacterial cultures were used to inoculate fresh LB medium +/- prodrugs and transferred into 96 well format (300 $\mu$ l/well) for automated tracking in a plate reader. The change in optical density at 600 nm (37°C) of each individual well was monitored over several hours (in a Spectra max M2 device) in the presence of drugs.

**HPLC and Mass spectrometry analysis:** The results described were obtained using a Waters Micromass LCT Premier mass spectrometer (Instrument number KD160). Analysis was performed in ESI + mode using a gradient elution method to identify unknowns in the sample. An external reference standard of Leucine enkephalin was infused in order to confirm mass accuracy of the Mass Spectrometer (MS) data acquired. The samples were run in triplicate to ensure consistency and data were analysed by Masslynx 4.1 software. HPLC conditions: A waters Alliance 2695 with a 2996 Photodiode Array detector and Waters Xbridge C18 5  $\mu$ m 150 x 4.6 mm was used for the chromatographic separation with mobile phase: Acetonitrile (containing

0.1 % formic acid) and Water (containing 0.1 % formic acid) using the following gradient: 0 min (10:90); 0.5 min (10:90); 5 min (90:10); 10 min (100:0); 11 min (100:0); 11.1 min (10:90); 14 min (10:90). A flow rate of 0.5 ml/min, sample run time of 14 min and injection volume of 1 – 30 µl was used. For CB1954 the following gradient was used: 0 min (10:90); 0.5 min (10:90); 26 min (30:70); 27 min (10:90); 30 min (10:90). A flow rate of 1 ml/min, sample run time of 30 min and injection volume of 10 µl was used. The MS conditions were as follows: the samples were subjected to ESI + ionisation and acquired from 90 to 1250 m/z at a capillary voltage of 3.00 kV, sample cone of 30V and a source temperature of 140°C. An external Enkephalin in Water/Acetonitrile (ESI + m/z= 556.2771) for exact mass correction using Lockspray was used. The UV conditions were set at a sampling rate of 1 spectrum/second, scanning wavelengths from 195-400 nm at a resolution of 1.2 nm.

***Murine experiments.*** As described in Chapter 2

***Animals and Tumour Induction:*** All murine experiments were carried out according to the methods described in Chapter 2.

***Bacterial and drug administration:*** Overnight cultures of *E. coli* were re-inoculated into fresh LB (1/50 dilution) and incubated shaking at 37 °C until they reached an OD<sub>600</sub> of 0.7. Cells were then washed twice in PBS. Tumours were administered 10<sup>6</sup> *E. coli* in an injection volume of 50 µl by intratumoral (IT) injection. The viable count of each inoculum was determined by retrospective plating onto LB agar. Two h post bacterial administration, drug (CB1954 20 mg/kg) was administered by intraperitoneal (IP) injection in an injection volume of 50 µl. The drug was subsequently

administered on days 3, 6, 9, and 11 and animals not receiving drug were administered an equal volume of PBS vehicle.

***Image acquisition and formation.*** As described in Chapter 2 and 3.

***Cytospins.*** Exudate from drug treated tumours was collected post culling in a 1.5 ml tube and centrifuged at 1000 rpm for 5 minutes to pellet any tissue or debris in the sample. The supernatant was removed and was cytospun and stained using pro-diff I and II (Braidwood Laboratories BAPROD1). Cytospin images are representative of at least two independent samples. Images were captured using a DP70 digital microscope camera and Olympus DP-Soft823 version 3.2 software (Mason Technologies Dublin, Ireland).

***Statistical analysis.*** All statistical analysis was carried out in accordance with the methods outlined in Chapter 2.

## Results

### Effect of prodrugs on bacterial cell survival *in vitro*

While activated prodrugs have been shown to be highly effective at killing mammalian cells, we determined to investigate the effect these drugs would have on bacterial cell viability following drug activation by endogenous bacterial enzymes. A panel of bacteria were analysed for changes in viability in the presence or absence of the prodrug CB1954 (200  $\mu$ M) by growing bacterial cultures on LB agar +/- CB1954. While the plating efficiency of the *E. coli* Nissle strain did not change between CB1954 treated and untreated cultures, *E. coli* MG1655 was seen to be almost entirely ablated in the presence of CB1954 (Figure 2). A similar result was seen when *B. breve* was grown with 200  $\mu$ M CB1954 while *L. lactis* showed no change in plating efficiency between treated and untreated cultures. These data indicate that prodrug activation by bacteria can have serious effects on the viability of a bacteria population following drug activation (Figure 2a). With this in mind, *E. coli* Nissle was chosen as the ideal candidate for further studies as it exhibits a high level of prodrug activation and, importantly, is itself not killed by the activated prodrug. In order to demonstrate this, the effect of a range of prodrugs on *E. coli* Nissle growth over time in liquid culture was also analysed (Figure 2b). No significant effect ( $p>0.05$ ) on bacterial cell growth was observed with any prodrug tested, even when prodrug concentrations exceeded those that are effective at cancer cell killing (Figure 2b).

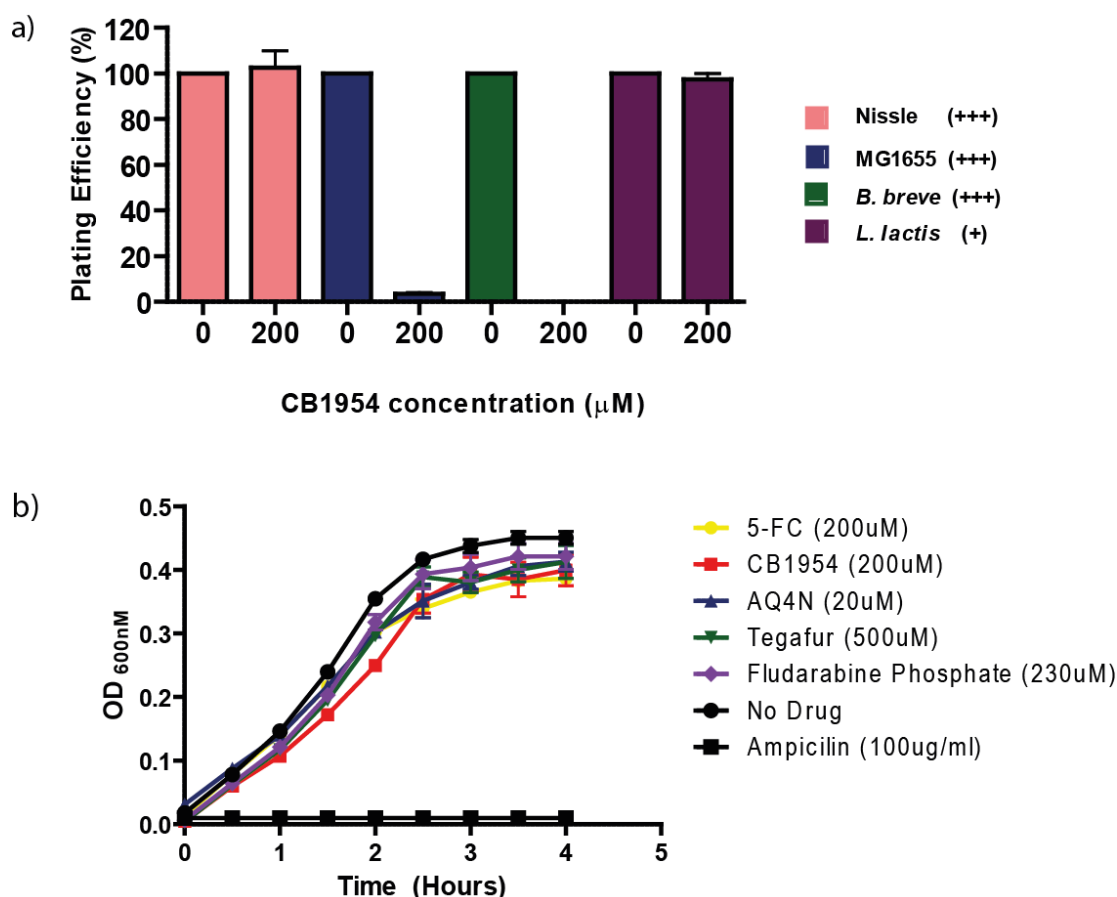


**Figure 2: *In vitro* evaluation of effects of CB1954 on probiotic bacterial survival.** a) Bacterial survival in the presence of CB1954. *E. coli* Nissle cells in logarithmic phase were plated directly on to LB plates containing CB1954 (200μM) and grown overnight. The plating efficiency shown is normalised to cfu counts from plain LB plates (+: prodrug efficacy on cancer cells). b) Prodrug influence on bacterial growth. Prodrugs were incubated with bacteria in LB medium and the change in optical density at 600 nm was monitored over time at 37°C. Data represent the average and standard error of four technical replicates. These data are representative of 2 independent experiments.

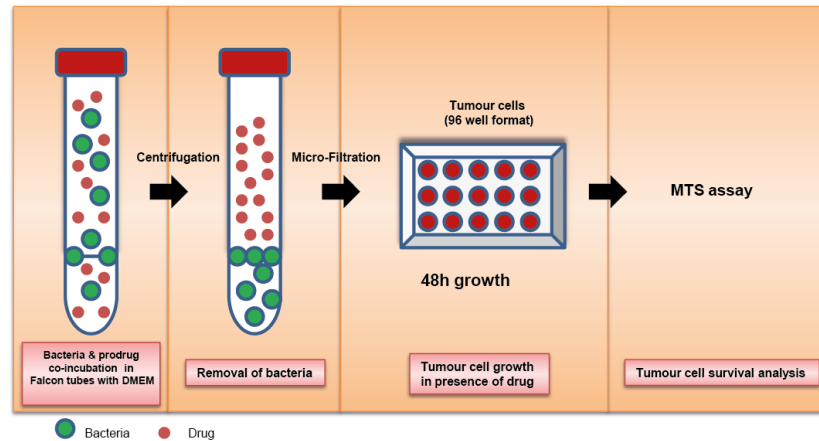


**Figure 3. Schematic of *in vitro* cell kill assay.** Bacteria and Drug are mixed in DMEM medium, and co-incubated for 3h at 37°C. The drug is separated from bacteria using centrifugation and microfiltration. The filter sterilised DMEM containing the transformed drug is applied to tumour cells in a 96 well plate. Tumour cell viability is evaluated via MTS assay for end-point measurements.

## **Validation of prodrug co-activation by High Performance Liquid Chromatography (HPLC)**

In order to validate prodrug activation at the molecular level, a sample of two prodrugs (CB1954 and 5-FC) was examined by HPLC. The chromatogram shown in Figure 4 displays the analysis of drugs pre- and post-incubation with *E. coli* Nissle. The data confirmed prodrug activation and metabolites related to CB1954 and 5-FC activation by *E. coli* Nissle were identified by peaks at 10.08 (CB1954) and 3.88 (5-FC). As a positive control and a reference, purified nitroreductase B enzyme + CB1954 was used and the HPLC chromatogram of each strain alone was used as a negative control (not shown). By comparison, when CB1954 was co-incubated with bacteria, similar retention time peaks are formed to the reference, confirming that a biochemical transformation has taken place.

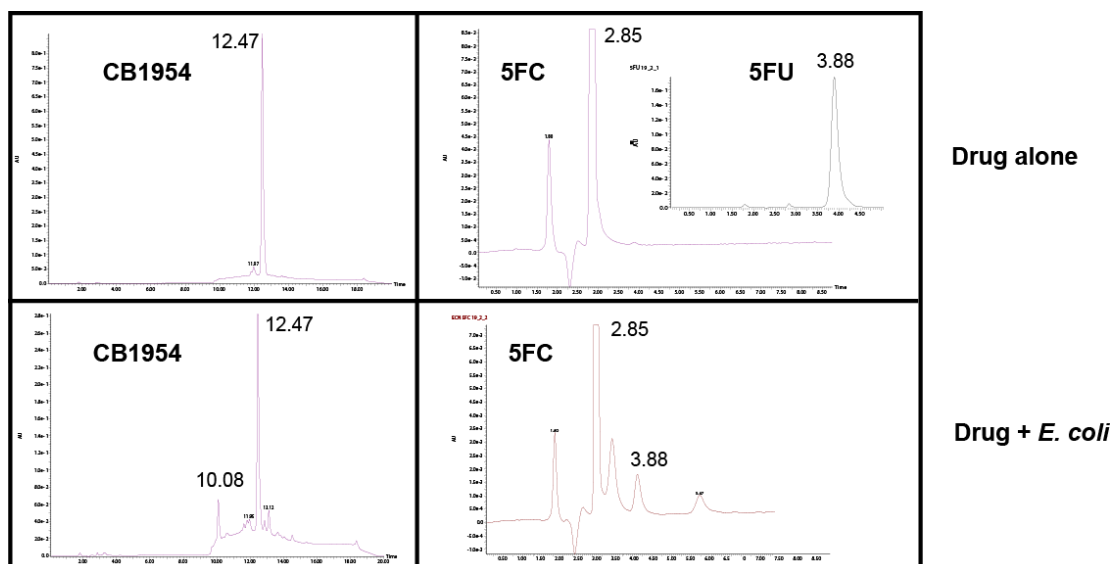


**Figure 4. Validation of prodrug co-activation by (HPLC).** HPLC chromatogram of supernatants of *E. coli* previously co-incubated with prodrugs in PBS at 37°C. Top; drugs alone (purified 5-FU is run as a control), bottom: Single drug-bacterial incubations.

***E. coli* is capable of activating a range of prodrugs and inducing cancer cell killing.**

Various cell lines were cultured and incubated with supernatant from *E. coli* Nissle +/- a range of prodrugs. The percentage of cells that survived in the presence of *E. coli* Nissle activated prodrug was determined by comparison with cell numbers from wells that were not treated with prodrug. A high level of cell killing (ranging from 80 to 98%) was observed across all cell lines tested and in the presence of all prodrugs tested (Figure 5).

Given the focus of this study on exploiting the natural enzymolome of bacteria, the ability of multiple endogenous enzymes from *E. coli* to contribute to the activation of a range of prodrugs was examined (Figure 5). Five prodrugs (Tegafur, Fludarabine, AQ4N, CB1954 and 5-FC) were co-incubated with *E. coli* Nissle and the cytotoxic effects on cancer cells examined. A very high level of cell killing was observed across the full range of prodrugs tested following activation by bacteria.

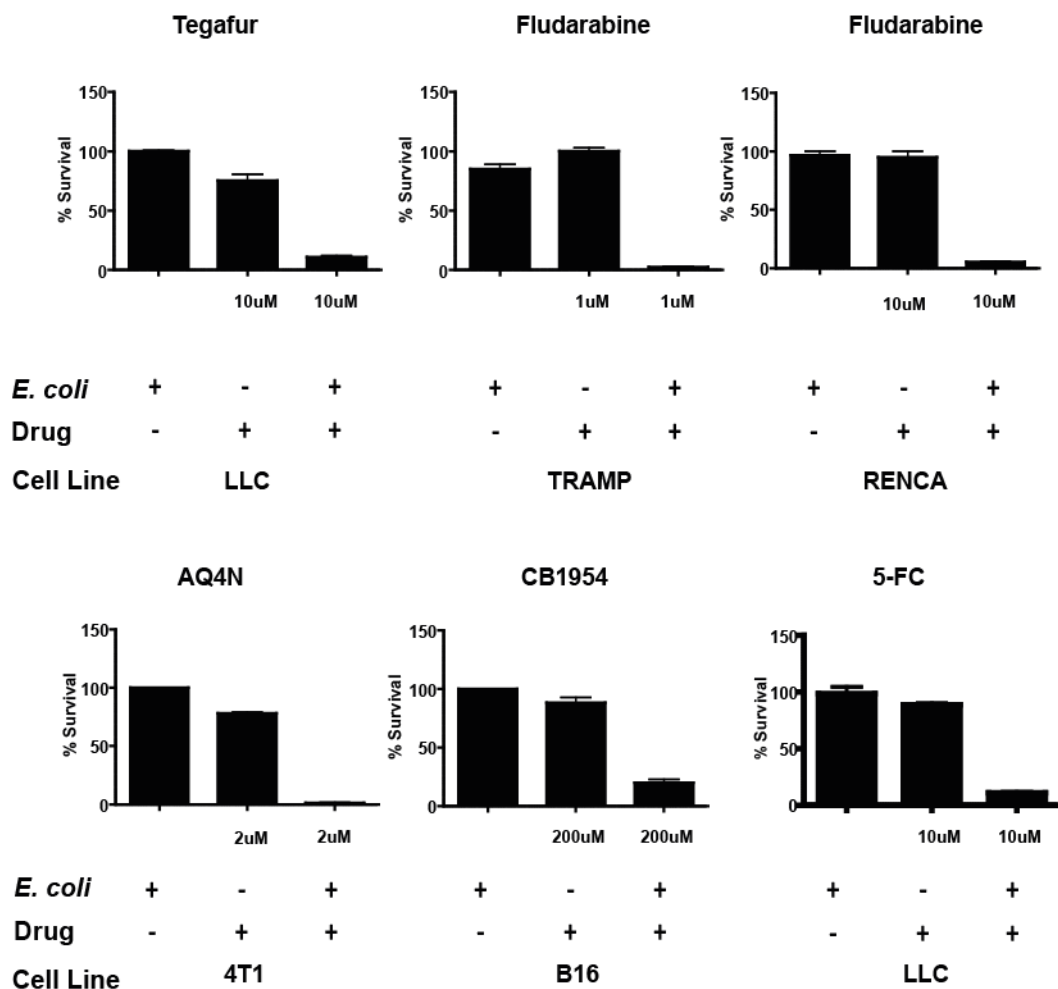


**Figure 5. Various prodrugs can be activated by *E. coli* and elicit cancer cell killing *in vitro*.** Therapeutic efficacy of *E. coli* in conjunction with prodrugs on multiple cell lines. Survival was measured by the MTS assay and is expressed relative to untreated cells. Data represent the average and standard error of four technical replicates. These data are representative of 2 independent experiments.

**Tumour colonising *E. coli* Nissle activates CB1954 and elicits a therapeutic effect *in vivo*.**

BALB/c mice bearing subcutaneous CT26 flank tumours were IT injected with *E. coli* Nissle or PBS, and IP injected with CB1954 (20 mg/kg) or PBS every 3 days and monitored over time (Figure 6). As expected, the PBS:PBS and PBS:CB1954 groups showed the greatest increases in tumour volumes over time. Considerably decreased tumour volume was observed in the Bacteria:CB1954 group compared with the drug alone group at all time-points analysed. A significant increase in median survival (26 days vs. 8 days,  $p=0.028$ ) was observed in the Bacteria:CB1954 group compared with the CB1954 alone group (Figure 6b), indicating drug activation by the intratumoural bacteria. These data indicate increased anti-tumour activity in tumours containing bacteria and CB1954. Bacteria alone did not significantly affect tumour volume relative to PBS administration although some reduction is evident in bacteria administered tumours, suggesting that bacteria alone may have a mild anti-tumour effect.

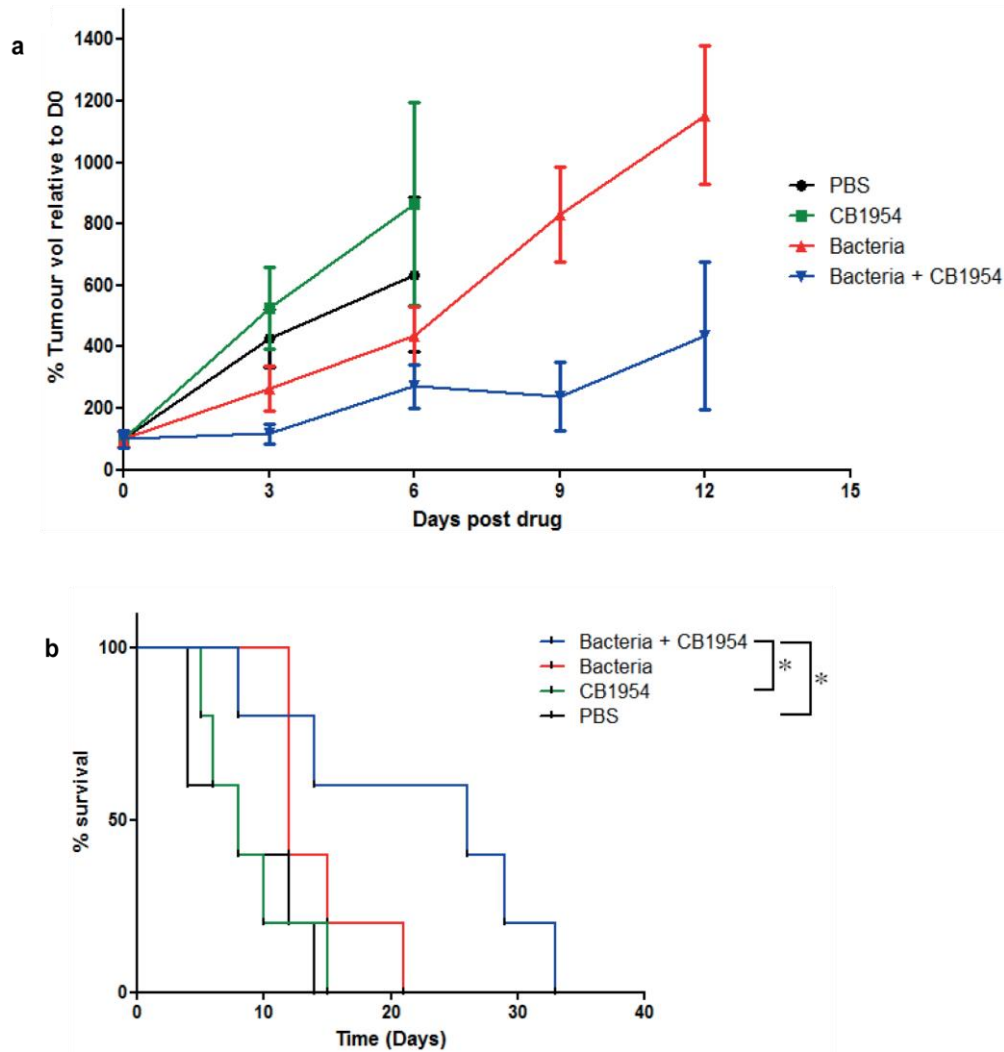


**Figure 6. Tumour colonising *E. coli* Nissle activates CB1954 to elicit a therapeutic response.** a) Subcutaneous flank CT26 tumours growing in BALB/c mice were injected IT with *E. coli* Nissle or PBS vehicle alone. CB1954 (20 mg/kg) was injected IP for the duration of the experiment at 3 day intervals. a) Tumour volume (%) relative to the first day of CB1954 injection (day 0) is shown. b) The median survival post Day 0 of the CB1954 + bacteria group was significantly greater than that of the CB1954 alone group (26 days vs. 8 days,  $P = 0.0374$ ). Data are expressed as mean  $\pm$  SEM of 3-5 individual mice per group.

### ***In vivo* optical imaging of NTR activity during CB1954 tumour therapy using CytoCy5S.**

The ability to monitor therapeutic effect using optical imaging provides researchers with a valuable tool for pre-clinical research. Having demonstrated the utility of CytoCy5S as a bacterial activated fluorescent reporter system in Chapter 2 [22], we aimed to develop a system whereby native bacterial NTRs could be used for both therapy and imaging in the same experiment. Since CB1954 is an NTR activated prodrug, it stood to reason to use CytoCy5S in conjunction with CB1954 to longitudinally monitor the response of BALB/c mice to CB1954 therapy. Mice bearing subcutaneous CT26 flank tumours were IT injected with *E. coli* Nissle or PBS and then received an IP injection of CB1954 or vehicle control. Mice were treated and imaged 3 times per week and changes in tumour volume were recorded following caliper measurement. No noticeable correlation between tumour localised fluorescence and tumour volume was detected. However, the strong fluorescent signal ( $> 10^9$  p/sec/cm<sup>2</sup>/sr) evident at day 17 (post first drug/probe injection) and the steady increase in fluorescence over time shows that bacterial numbers within the tumour increased over the course of the experiment.

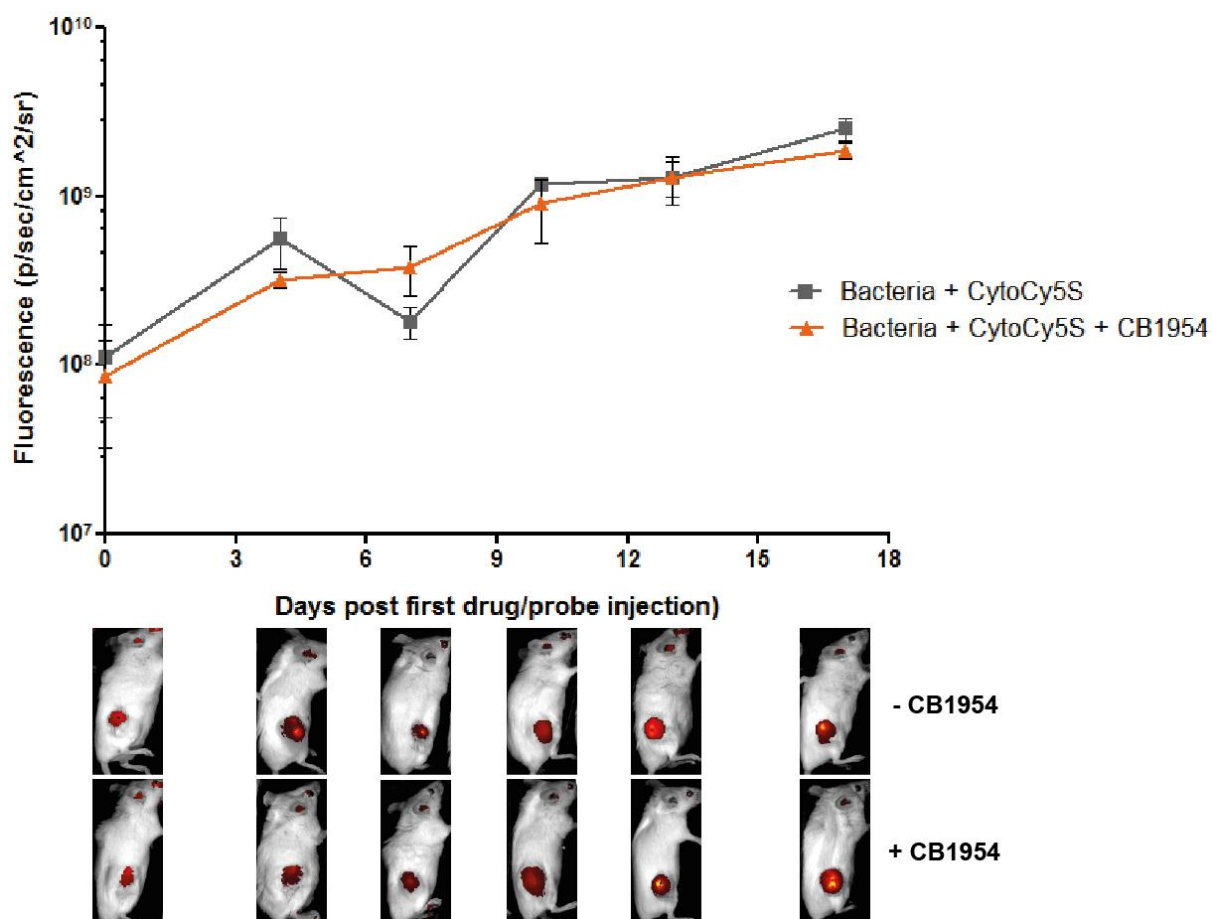


**Figure 7. *In vivo* optical imaging of nitroreductase activity during CB1954 tumour therapy using CytoCy5S.** BALB/c mice bearing subcutaneous CT26 flank tumours colonised with *E. coli* Nissle (via IT injection) were injected with CytoCy5S and CB1954 every 3 days. Mice were imaged for fluorescence on each treatment day. Fluorescence from tumours increased over time but no significant difference ( $p > 0.05$ ) was observed between mice that received CB1954 and mice that just received bacteria and CytoCy5S.

### **A cocktail of prodrugs can be activated by bacteria *in vitro*.**

Although the activation of individual prodrugs in the presence of bacteria was demonstrated by HPLC in Figure 4, it was important to determine whether or not a cocktail of prodrugs could be activated by a single bacterium. The effect of a cocktail of 3 prodrugs, Fludarabine phosphate, 5-FC and CB1954, on cancer cell survival was evaluated and it was shown that the combination of all 3 prodrugs, in the presence of *E. coli*, elicited the most effective level of cancer cell killing (Figure 8). Having established that *E. coli* are capable of activating multiple prodrugs in combination to achieve cancer cell killing, the cocktail of CB1954 and 5-FC was chosen for future cocktail experiments as they proved to be the most cytotoxic prodrugs in *in vitro* screens. The cocktail (CB1954 and 5-FC) did not have any effect on bacterial viability (Figure 8b). The supernatant from CB1954 and 5-FC in combination with *E. coli* was subjected to HPLC analysis and the chromatogram peaks formed by the cocktail of drugs when the prodrugs were pre-incubated with bacteria showed that metabolites were formed, as evidenced by peaks at 10.08 (CB1954) and 3.88 (5-FC) showing that both prodrugs were metabolised.

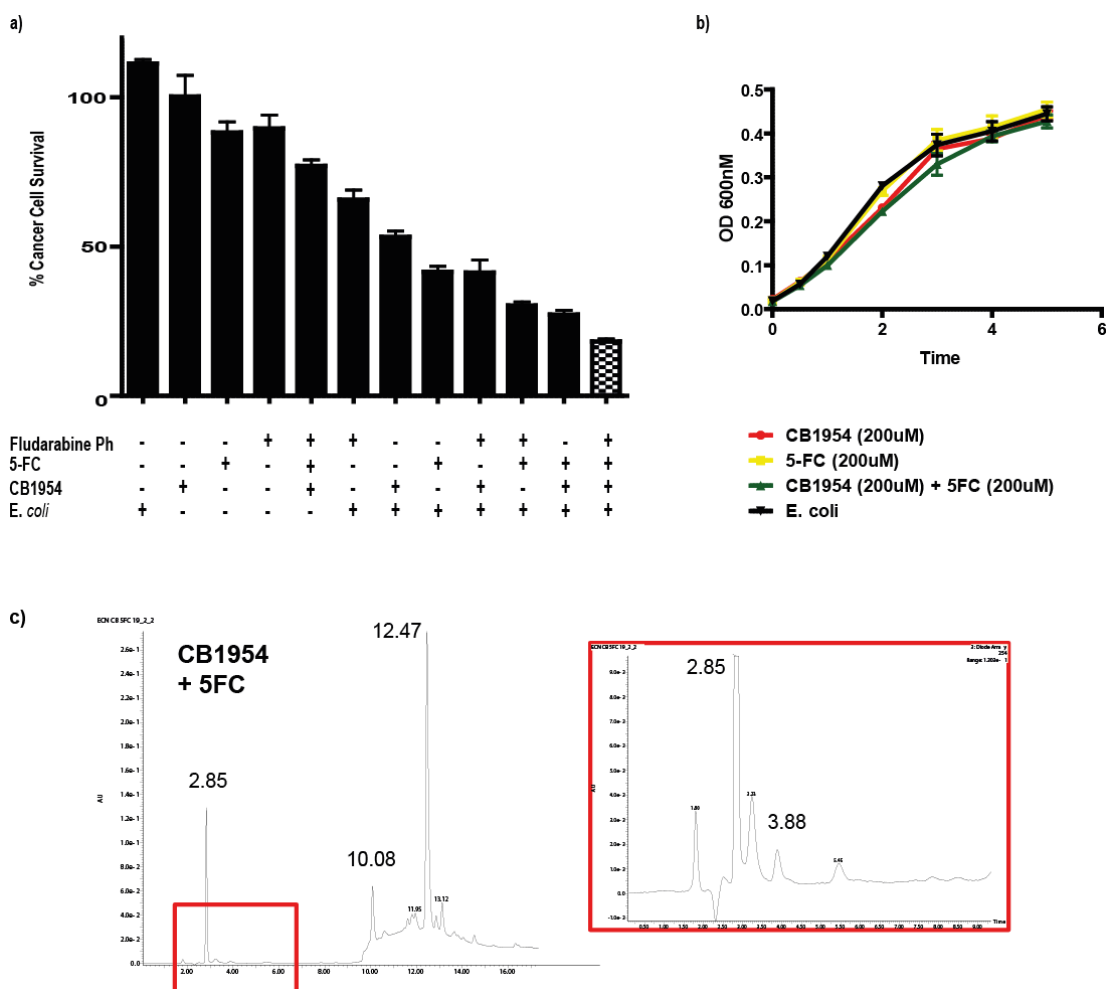


**Figure 8. *E. coli* Nissle can activate a prodrug cocktail consisting of CB1954 and 5-FC *in vitro*.** a) Cancer cell survival in the presence of multiple prodrugs. Bacteria were incubated with prodrugs for 1h. Fludarabine phosphate (5 $\mu$ M), 5-FC (2 $\mu$ M), CB1954 (25 $\mu$ M). b) Prodrug influence on bacterial growth. Prodrugs were incubated with bacteria in LB medium and the change in optical density at 600 nm was monitored over time at 37°C. (CB1954: 200 $\mu$ M, 5-FC: 500 $\mu$ M, FP (Fludarabine phosphate): 20 $\mu$ M). c) HPLC chromatogram of supernatants of *E. coli* previously co-incubated with a cocktail of CB1954 and 5-FC at 37°C. Red rectangle: Magnification of 5-FC profile in this reaction.

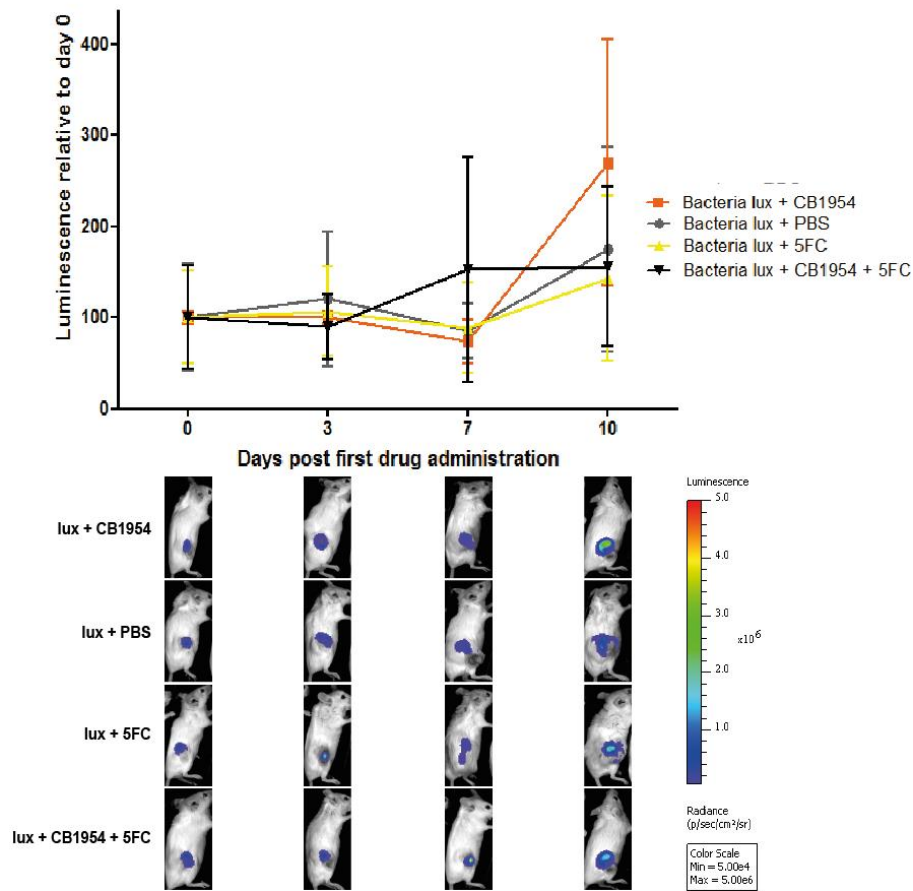
### ***In vivo* tumour therapy utilising a cocktail of CB1954 and 5-FC prodrugs**

In order to replicate *in vitro* observations, the efficacy of *E. coli* as a tumour-specific drug-activating agent was examined in tumour bearing mice in conjunction with CB1954 and 5-FC (Figure 9). BALB/c mice bearing subcutaneous CT26 flank tumours were colonised with *E. coli* Nissle via IT injection of bacteria. On the same day as bacterial injection, mice received an intraperitoneal (IP) injection of CB1954 or 5-FC or both drugs. Drug injections were repeated 3 times per week for the duration of the experiment. Therapeutic efficacy was determined by tracking changes in tumour volume (caliper measurement) and by calculating the median survival of mice (Figure 9c). Mice that received bacteria and either CB1954 or 5-FC alone showed increased median survival compared with control groups (PBS, 5-FC, CB1954, 5-FC/CB1954) ( $p < 0.05$ ) while the combination of both drugs in the presence of tumour localised bacteria was shown to increase median survival more than bacteria with either drug alone. Mice that received bacteria and a cocktail of CB1954 and 5-FC showed significantly greater median survival ( $p < 0.01$ ) than mice that received PBS or drugs without bacteria. While the increase in median survival of the bacteria plus cocktail group was not statistically significantly greater than the bacteria + 5-FC or CB1954 groups ( $p > 0.16$ ), the increase in survival does indicate that the drugs had a complimentary effect and represent a viable treatment option.

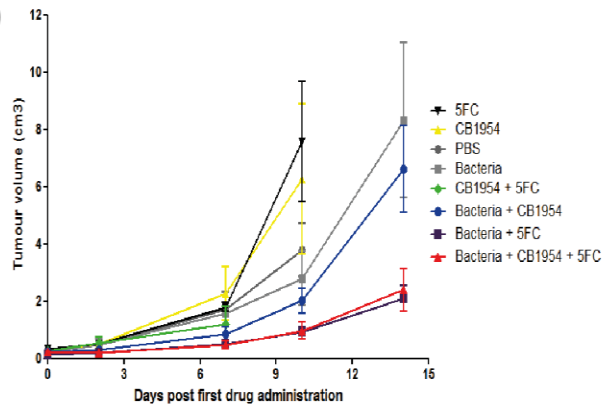
While CB1954 and 5-FC were not seen to be significantly toxic to bacteria *in vivo*, it was important to determine whether or not these drugs would have an effect on the viability of bacteria *in vivo* within the tumour site. Therefore, a subset of mice received an intratumoural injection of luminescent *E. coli* encoding the bacterial lux operon allowing for non-invasive *in vivo* imaging of viable tumour colonising bacteria throughout the experiment. The ability to track live bacteria using

luminescence imaging allowed for protensive monitoring of the effect drug treatment was having on bacterial cell numbers within the tumour when compared with mice that did not receive drug. Longitudinal luminescence readings demonstrated that the drug cocktail did not have a negative impact on bacterial numbers and in some cases the number of bacteria within the tumour increased over time. The persistence of bacteria within the tumour for prolonged periods of time allows for repetition of drug administrations as the levels of bacterial enzymes within the tumour are not diminished following drug treatment.

a)



b)



c)

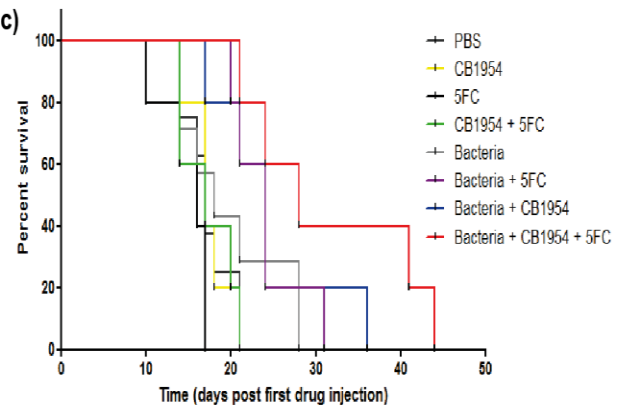


**Figure 9. Tumour therapy via *in vivo* activation of prodrugs.** BALB/c mice bearing subcutaneous CT26 flank tumours colonised by *E. coli* Nissle 1917 received IP injections of CB1954 + PBS, 5-FC + PBS, CB1954 + 5-FC or PBS three times per week. Tumours were monitored for changes in volume and luminescence (where applicable) from live bacteria on each treatment day. a) The change in bacterial luminescence (relative to day 0) from tumour colonising luminescent *E. coli* is shown. Luminescence remains stable across the range of time-points indicating that bacterial levels within the tumour remained constant throughout the experiment. b) Changes in CT26 tumour volume were monitored until the first death in the group determined by a predefined endpoint. c) Survival plot of each group starting from the first day of bacteria/drug administration. Mice that received bacteria and both drugs showed significantly increased median survival ( $p < 0.01$ ) compared with groups that did not receive bacteria.

### **Immune cell recruitment to the tumour following drug activation by tumour localised bacteria.**

Following the culling of mice that had received bacteria and 5-FC or CB1954, tumours were resected and dissected for analysis. Some drug treated mice harboured tumours containing a yellow exudate. This was not observed in mice that did not receive drug and was deemed to be indicative of recruitment of immune cells to the tumour site following drug activation by bacteria. This exudate was collected and subjected to cytopinning and staining to facilitate further analysis of the cells present in the infiltrate. Microscopic analysis of the cytopun samples revealed the presence of immune cells only, of multiple types. While the vast majority of the cells were dead by the time of analysis, it was possible to distinguish macrophages, eosinophils and lymphocytes in samples from mice that had received either CB1954 or 5-FC. However, as a result of the majority of cells in the samples being dead at the time of analysis, the clarity of cell morphology was compromised and some of the cell components appear diffuse while the cytoplasm and nuclei were not always intact as is common of apoptotic cells or cells. Lymphocytes were characterised by the appearance of large nuclei surrounded by a thin cytoplasm with a circular shape while macrophages were characterised by their large size and presence of a large, darkly stained nucleus surrounded by lightly stained cytoplasm and were more abundantly found in samples from mice that had received 5-FC prodrug. Eosinophils were identified by their large nuclei (appearing as a single nucleus in dead cells) and multiple granules present in the cytoplasm while neutrophils were characterised by the presence of a multi-lobed, crescent shaped nucleus that was darkly stained. Figure 10 shows representative images of each of these immune cell types as found

in the samples from drug treated mice. While no exudate sample was collected from mice that received the CB1954 and 5-FC cocktail treatment, it is thought that this was due to an absence of exudate in these tumours at the specific time of culling (= experiment end) and does not necessarily mean that these tumours never contained an exudate, but rather that it was absent due to increased life span of these treated mice. Exudate which may have been present in the tumours at earlier timepoints may have been cleared by the time of culling. Immune cells were clearly identifiable in all samples tested (from single drug groups) and interestingly, a distinct absence of non-immune or cancer cells was observed. No samples appeared to contain easily identifiable cancer cells.

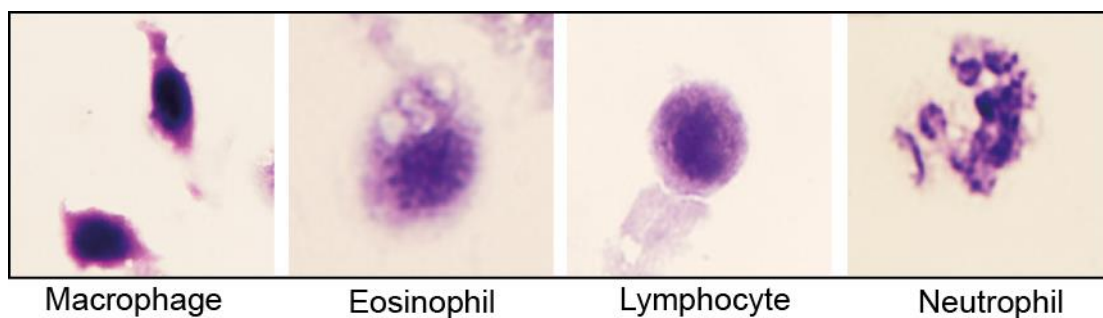


**Figure 10. Immune cell recruitment to the tumour following drug activation by tumour localised bacteria.** Exudate collected from the tumours of mice that had received CB1954 and/or 5-FC was cytopun and stained. The resultant samples were analysed by microscopy and multiple immune cells were detected in all samples analysed. Despite the fact that the cells were dead and displayed common signs of apoptosis such as fragmented nuclei, it is still possible to distinguish multiple forms of immune cell. The most abundant forms of immune cells found in samples were macrophages, lymphocytes and eosinophils. Images are representative of cells observed in each sample tested.

## Discussion

In this chapter, we investigated the use of wild type probiotic bacteria in conjunction with prodrugs for the treatment of solid tumours. Although traditionally prodrug research involves sophisticated drug design pegged to a specific gene followed by incorporation of that gene in a vector, our approach was in reverse. We decided to investigate the use of non-genetically engineered probiotic bacteria and exploit their natural enzymolome in order to activate multiple prodrugs even if their corresponding endogenous enzymes were unknown. Although most bacteria examined as anticancer agents are inherently toxic or attenuated, we have chosen to work with probiotic bacteria as they have a good safety profile.

Since many of the enzymes used in existing prodrug activating strategies have a bacterial origin, we reasoned that the natural enzymolome of wild type bacteria would be capable of activating a broad class of prodrugs either alone or as cocktails. An ideal therapeutic strain would be free from the burden of genetic modification but still be capable of activating multiple drugs. This would broaden the options for a clinician, giving them the freedom to choose from a panel of prodrugs in order to treat patients on a case by case. In addition, it would allow them to change the prodrug depending on therapeutic response, but also permit the usage of multiple prodrugs simultaneously or consecutively in order to maximise efficacy.

We began by screening several probiotic strains against popular prodrugs with different mechanisms of action of which some have unknown corresponding enzymes. Our aim was to find a strain that satisfies the criteria mentioned above. We discovered that the Gram-negative *E. coli* Nissle was able to increase the toxicity of all the examined prodrugs, while the Gram-positive bacteria could only influence a fraction of those. Currently, the molecular basis for this is unknown; however, this

observation prompted us to advance this study with *E. coli*. While CB1954 was activated by most strains, *E. coli* strains and *B. breve* could activate it to high levels and such an activation was confirmed biochemically. However, we found that *B. breve* and *E. coli* MG1655 were sensitive to CB1954 while *E. coli* Nissle was not (Figure 2). The aetiology for this sensitivity differential is unclear; however, it formed the basis to eliminate *B. breve* and MG1655 from further studies and focus on *E. coli* Nissle. By exploiting its enzymatic reservoir, it was possible to find a prodrug to treat any cancer cell line (Figure 5). Only the genes required for activation of CB1954, Fludarabine phosphate and 5-FC are known [23] [24] [25]; the enzymes that activate AQ4N and Tegafur in bacteria are unknown. In order to gain further insight into prodrug activation by multiple genes, we chose to use the prodrug CB1954 which is activated by nitroreductases described in earlier chapters.

The concept of several enzymes acting in concert on a single drug is intriguing and suggests towards prodrug design around ubiquitous enzymes or enzyme families rather than relying on one gene. The ability to simultaneously activate prodrugs of different mechanistic classes is an important finding (which has never been described in this context, to our knowledge) that could potentially be used to treat resistant cancers. We show several different types of cocktails that can be activated, one of which was a combination of 3 prodrugs (Figure 8). To show proof of principle at the molecular level, we analysed one of the cocktail reactions (CB1954 and 5-FC) by HPLC (Figure 8).

Finally, we replicated our *in vitro* data *in vivo*, by showing that wild type *E. coli* could enhance the cytotoxicity of CB1954 and 5-FC. The possibility of using one single organism to activate multiple prodrugs is very attractive in this field of research. However, fine-tuning a therapy using a cocktail of multiple drugs poses

technical challenges beyond the scope of this study, and we acknowledge that this is an artificial system. *E. coli* Nissle is a promising agent and further exploration of its enzymatic repertoire may lead to the discovery of new enzyme/prodrug combinations, thus expanding the existing prodrug arsenal and giving rise to new therapeutic strategies. The ability to non-invasively track the therapeutic response to a therapy through the use of optical imaging of unmodified bacteria (Figure 7) represents a novel development in the field. Although the data presented in Figure 7 show little more than proof of concept, the potential applications of this system are clear to see. Combined imaging and therapy with CytoCy5S and a prodrug of choice could be used to detect the level of bacteria colonisation of the tumour to better inform the researcher with regard to optimal treatment timepoints. For example, had *E. coli* MG1655 been used as the tumour colonising strain in conjunction with CB1954 we would expect a proportion of the bacteria to be killed by CB1954 following each treatment (if *in vitro* results from Figure 2 were recapitulated). In this scenario, CytoCy5S imaging could be carried out on a daily basis and when fluorescence levels showed that tumour colonisation was at an optimal level the next round of CB1954 could be administered, potentially leading to increased efficacy.

Overall, these findings demonstrate the ability of probiotic bacteria, without the requirement for genetic modification, to enable high-level activation of multiple prodrugs specifically at the site of action, which may provide ‘old drugs’ with a new lease of life, and/or improve the therapeutic window of new or existing drug regimes.

## References

1. Cummins, J. and M. Tangney, *Bacteria and tumours: causative agents or opportunistic inhabitants?* Infect Agent Cancer, 2013. **8**(1): p. 11.
2. Morrissey, D., G.C. O'Sullivan, and M. Tangney, *Tumour targeting with systemically administered bacteria.* Curr Gene Ther, 2010. **10**(1): p. 3-14.
3. Baban, C.K., et al., *Bacteria as vectors for gene therapy of cancer.* Bioeng Bugs, 2010. **1**(6): p. 385-94.
4. Zhao, M., et al., *Tumor-targeting bacterial therapy with amino acid auxotrophs of GFP-expressing Salmonella typhimurium.* Proc Natl Acad Sci U S A, 2005. **102**(3): p. 755-60.
5. Stritzker, J., et al., *Myristoylation negative msbB-mutants of probiotic E. coli Nissle 1917 retain tumor specific colonization properties but show less side effects in immunocompetent mice.* Bioeng Bugs, 2010. **1**(2): p. 139-45.
6. Minton, N.P., *Clostridia in cancer therapy.* Nat Rev Microbiol, 2003. **1**(3): p. 237-42.
7. Nguyen, V.H., et al., *Genetically engineered Salmonella typhimurium as an imageable therapeutic probe for cancer.* Cancer Res, 2010. **70**(1): p. 18-23.
8. Nemunaitis, J., et al., *Pilot trial of genetically modified, attenuated Salmonella expressing the E. coli cytosine deaminase gene in refractory cancer patients.* Cancer Gene Ther, 2003. **10**(10): p. 737-44.
9. Roberts, N.J., et al., *Intratumoral injection of Clostridium novyi-NT spores induces antitumor responses.* Sci Transl Med, 2014. **6**(249): p. 249ra111.
10. Schepelmann, S., et al., *Suicide gene therapy of human colon carcinoma xenografts using an armed oncolytic adenovirus expressing carboxypeptidase G2.* Cancer Res, 2007. **67**(10): p. 4949-55.
11. Spooner, R.A., et al., *A novel vascular endothelial growth factor-directed therapy that selectively activates cytotoxic prodrugs.* Br J Cancer, 2003. **88**(10): p. 1622-30.
12. Springer, C.J. and I.I. Niculescu-Duvaz, *Antibody-directed enzyme prodrug therapy (ADEPT): a review.* Adv Drug Deliv Rev, 1997. **26**(2-3): p. 151-172.
13. Lehouritis, P., C. Springer, and M. Tangney, *Bacterial-directed enzyme prodrug therapy.* J Control Release. **170**(1): p. 120-31.

14. Lehouritis, P., C. Springer, and M. Tangney, *Bacterial-directed enzyme prodrug therapy*. J Control Release, 2013. **170**(1): p. 120-31.
15. Cunningham, C. and J. Nemunaitis, *A phase I trial of genetically modified Salmonella typhimurium expressing cytosine deaminase (TAPET-CD, VNP20029) administered by intratumoral injection in combination with 5-fluorocytosine for patients with advanced or metastatic cancer. Protocol no: CL-017. Version: April 9, 2001*. Hum Gene Ther, 2001. **12**(12): p. 1594-6.
16. Friedlos, F., et al., *Attenuated Salmonella targets prodrug activating enzyme carboxypeptidase G2 to mouse melanoma and human breast and colon carcinomas for effective suicide gene therapy*. Clin Cancer Res, 2008. **14**(13): p. 4259-66.
17. Cronin, M., et al., *High resolution in vivo bioluminescent imaging for the study of bacterial tumour targeting*. PLoS One, 2012. **7**(1): p. e30940.
18. Cronin, M., et al., *Bacterial-mediated knockdown of tumor resistance to an oncolytic virus enhances therapy*. Mol Ther, 2014. **22**(6): p. 1188-97.
19. Tangney, M., *Gene therapy for cancer: dairy bacteria as delivery vectors*. Discov Med, 2010. **10**(52): p. 195-200.
20. Somers, K.D., et al., *Orthotopic treatment model of prostate cancer and metastasis in the immunocompetent mouse: efficacy of flt3 ligand immunotherapy*. Int J Cancer, 2003. **107**(5): p. 773-80.
21. Ahmad, S., et al., *Prostate stem cell antigen DNA vaccination breaks tolerance to self-antigen and inhibits prostate cancer growth*. Mol Ther, 2009. **17**(6): p. 1101-8.
22. Stanton, M., et al., *In Vivo Bacterial Imaging without Engineering; A Novel Probe-Based Strategy Facilitated by Endogenous Nitroreductase Enzymes*. Current gene therapy, 2015. **15**(3): p. 277-288.
23. Prosser, G.A., et al., *Discovery and evaluation of Escherichia coli nitroreductases that activate the anti-cancer prodrug CB1954*. Biochem Pharmacol. **79**(5): p. 678-87.
24. Parker, W.B., et al., *In vivo gene therapy of cancer with E. coli purine nucleoside phosphorylase*. Hum Gene Ther, 1997. **8**(14): p. 1637-44.
25. Austin, E.A. and B.E. Huber, *A first step in the development of gene therapy for colorectal carcinoma: cloning, sequencing, and expression of Escherichia coli cytosine deaminase*. Mol Pharmacol, 1993. **43**(3): p. 380-7.

## **Chapter 5: Discussion and future work**

## Discussion and future work

The work outlined in this thesis provides proof-of-concept for the use of endogenous bacterial enzymes for activation of both fluorescent and luminescent imaging probes as well as the tumour-localised activation of one or more prodrugs. Genetic modification of bacteria, as is standard practice in almost all preclinical bacterial gene therapy and imaging studies, represents a major hurdle for clinical translation. As such, the data presented here describe the development of novel imaging and therapeutic strategies that rely solely on the use of the endogenous bacterial ‘enzymolome’. Native levels of unique bacterial enzymes were demonstrated to be sufficient for probe activation and prodrug conversion at levels adequate for the elicitation of imageable signal or therapeutic response *in vitro* and *in vivo*. This work, along with further studies in the use of non-engineered bacteria for imaging and disease treatment, contributes to the body of knowledge on progressing clinical use of bacteria as gene or protein delivery vehicles.

*Endogenous bacterial nitroreductases activate CytoCy5S*: The hypothesis that native levels of bacterial NTRs would be sufficient for the reduction of the quenched probe CytoCy5S to its fluorescent form was tested. Proof of principle and assay optimisation were achieved *in vitro* with a range of unengineered bacterial species before the system was tested *in vivo*. Probe activation by tissue localised bacteria was demonstrated in models of local *E. coli* muscle infection and systemic *Salmonella* infection. CytoCy5S was also shown to be amenable to use as an imaging probe for *in vivo* tumour imaging where tumour localised bacteria specifically activated the probe within the tumour site to produce a tumour localised fluorescent signal.

This highly versatile system successfully demonstrates the concept of NTR enzymes as a reporting strategy for wild-type bacteria using optical imaging and a fluorescent probe, but the concept may also be extended to NTR-specific ‘caged’ probes for use with other imaging modalities with more immediate clinical relevance, such as PET, MRI and SPECT [1, 2]. Overall, the ability to non-invasively monitor bacterial infection in a pre-clinical setting using relatively cheap and accessible optical imaging methods provides infection researchers with a valuable tool, which has the potential for clinical translation for both diagnostic and clinical trial uses.

Future work would involve the development of an assay that compares total NTR activity in a given bacterial strain with CytoCy5S fluorescence. Another development of the work described in this chapter would be the testing and optimisation of a quenched fluorophore with similar properties to CytoCy5S that is amenable for use in both optical and other imaging strategies. A nitroreductase activated fluorescent probe with an excitation wavelength of approximately 800 nm could be used to recapitulate the preclinical *in vitro* and *in vivo* experiments outlined in the CytoCy5S study but would also be suitable for an imaging modality with more clinical potential such as photoacoustic imaging [3]. The optical characteristics of this fluorescent probe would make it ideal for both preclinical and clinical use across imaging platforms and thus would represent an advancement of the work presented in this thesis. Future studies that utilise the CytoCy5S probe would focus on the *in vivo* detection of bacterial localisation in an extended number of models of infectious disease.

*Bacteria activate a novel caged luciferin probe:* The work presented in Chapter 3 builds on the data acquired from the CytoCy5S study and extends to demonstrate

bacterial-specific uncaging of a novel luminescent probe (NCL), thereby demonstrating the utility of bacterial enzymes as activating agents for bioluminescence imaging. Luminescence imaging of uncaged NCL was achieved *in vitro* and was successfully progressed to *in vivo* models of infection and cancer. Tumour localised BLI from bacterial colonised tumours was shown to be high. However, tumours that did not contain administered bacteria also showed relatively high levels of tumour localised luminescence. It is thought that this may be due to spontaneous colonisation of the tumour by naturally acquired bacteria. Other work in our lab has previously observed spontaneous colonisation of tumours by a range of bacteria [4] and could explain the activation of NCL in this murine model in the absence of administered bacteria. Although NCL was uncaged in untreated tumours, the level of probe uncaging was 10 X less than in mice that received IV *E. coli*. Of note is that the tumours examined in the NCL study were relatively large ( $\sim 1.15 \text{ mm}^3$ ), and therefore more likely to feature spontaneously colonising bacteria [5]. We did not examine CytoC5S with tumours this large.

Future work with the NCL probe could include the development of an *in vitro* screening assay for the accelerated detection of suitable prodrug activating agents. A screen based on quantification of light production following probe uncaging by NTR would facilitate large scale *in vitro* testing of an extended range of bacteria or NTR expressing viruses and engineered mammalian cells for the efficiency of probe uncaging and would thereby be used to identify the most efficient candidates for prodrug activation as the magnitude of the light signal produced would be directly proportional to the level of probe uncaging achieved. This novel reagent could significantly simplify screening of prodrugs *in vivo* and accelerate the

preclinical development of enzyme-activatable therapeutics for translation into the clinic.

*Endogenous bacterial enzymes can be exploited for tumour-targeted activation of prodrugs:* The data presented in Chapter 4 represent a novel addition to established GDEPT strategies. The use of wild type probiotic bacteria as delivery vehicles for endogenously expressed genes to a tumour site side-steps one of the major regulatory hurdles associated with the use of bacteria in cancer therapy namely, genetic modification. This work provides evidence that native bacterial enzymes are sufficient for the activation of various prodrugs and that the level of prodrug activation is sufficient to achieve a therapeutic response *in vivo*. The idea that a single strain of wild type bacteria can essentially be viewed as an “enzyme factory” capable of simultaneously activating a cocktail of prodrugs was also proffered. *In vivo* studies involving tumour colonising probiotic *E. coli* Nissle for the activation of individual prodrugs (CB1954 or 5-FC) were successful in significantly increasing the median survival of mice compared with drug free groups, while the combination of both prodrugs in a cocktail was observed to have an additive effect and also increased survival.

Future work for this chapter would include further investigation of the enzymatic capabilities of *E. coli* Nissle by testing a broader range of prodrugs for increased (or decreased) efficacy following exposure to endogenous *E. coli* Nissle enzymes. This may lead to the identification of a more efficacious *E.coli*-prodrug therapy system. A deeper analysis of the effect of various prodrug cocktails could also be carried out. Further tweaking of the CB1954/5-FC system described in this study may yield increased efficacy or an entirely novel and more effective prodrug cocktail may be identified. While the theranostic study involving *E. coli*

Nissle/CytoCy5S tracking of CB1954 therapy demonstrated that fluorescence imaging could be used to monitor bacterial levels within the tumour throughout the course of the therapy, it may be more interesting in future studies to employ this strategy using *E. coli* MG1655 instead of Nissle. *In vitro* data demonstrated that MG1655 was killed following incubation with CB1954. With this in mind, it can be assumed that a population of tumour colonising MG1655 would be affected by CB1954 treatment. In this case, CytoCy5S could be administered to mice each day and the re-colonisation of the tumour by MG1655 following CB1954 could be tracked by changes in fluorescence from bacterial-activated CytoCy5S. This would allow the researcher to choose the optimal day for subsequent CB1954 treatment as fluorescence levels would be used to indicate when the level of MG1655 tumour colonisation had returned to pre-CB1954 treatment levels.

## **Conclusion**

In conclusion, while modern research and treatments for cancer and infectious disease exclusively focus on the development of targeted therapies, it seems that wild type bacteria represent a highly novel and potentially useful tool for exploitation. Probiotic bacteria are currently an under-utilised source of native enzymatic activity, much of which is not found in mammalian cells. This fact, paired with their ability to target and grow within solid tumours, makes them highly attractive for improving the toxicity profile of therapeutic drug strategies, even beyond chemotherapy. Bacterial specific activation of imaging agents and drugs would also be of significant use in both the detection and treatment of bacterial infection.

At present, bacterial-mediated cancer therapy is under-developed but the versatility of bacteria as enzyme delivery agents, as well as the number of research fields to which this versatility could be applied makes it a certainty that the study and use of wild type bacteria as biological delivery vehicles will continue to grow and contribute significantly to a range of research areas.

## References

1. Tangney, M., *Editorial: in vivo imaging & gene therapy*. Curr Gene Ther, 2012. **12**(1): p. 1.
2. Collins, S.A., et al., *PET Imaging for Gene & Cell Therapy*. Curr Gene Ther, 2012. **12**(1): p. 20-32.
3. Galanzha, E.I., et al., *<italic>In Vivo</italic> Magnetic Enrichment, Photoacoustic Diagnosis, and Photothermal Purging of Infected Blood Using Multifunctional Gold and Magnetic Nanoparticles*. PLoS ONE, 2012. **7**(9): p. e45557.
4. Cronin, M., et al., *Orally administered bifidobacteria as vehicles for delivery of agents to systemic tumors*. Mol Ther, 2010. **18**(7): p. 1397-407.
5. Cummins, J. and M. Tangney, *Bacteria and tumours: causative agents or opportunistic inhabitants?* Infect Agent Cancer, 2013. **8**(1): p. 11.